DOE F 241.3
(2-01) p.1 of 2

UNITED STATES DEPARTMENT OF ENERGY (DOE)
Announcement of Scientific and Technical Information (STI)
(For Use By Financial Assistance Recipients and Non-M&O/M&I Contractors)

OMB CONTROL NO. 1910-1400

PART I: STI PRODUCT DESCRIPTION
(To be completed by Recipient/Contractor)

A. STI Product Identifiers

1. REPORT/PRODUCT NUMBER(s)
None

2. DOE AWARD/CONTRACT NUMBER(s)
DE-FC36-97ID13554

3. OTHER IDENTIFYING NUMBER(s)
None

B. Recipient/Contractor
Columbia University, Dept. of Earth & Environmental Engineering

C. STI Product Title
Integrating Steel Production with Mineral Carbon Sequestration

D. Author(s)
Klaus Lackner, Paul Duby, Tuncel Yegulalp, Samuel Krevor, Christopher Graves

E-mail Address(es):
kl2010@columbia.edu, sck69@columbia.edu

E. STI Product Issue Date/Date of Publication
05 (MM) 01 (DD) 2008 (YYYY)

F. STI Product Type (*Select only one*)

☒ 1. TECHNICAL REPORT
☒ *Final* ☐ *Other (specify)* _____

☐ 2. CONFERENCE PAPER/PROCEEDINGS

Conference Information (title, location, dates)

☐ 3. JOURNAL ARTICLE
a. TYPE: ☐ *Announcement Citation Only* ☐ *Preprint* ☐ *Postprint*
b. JOURNAL NAME
c. VOLUME _____ *d. ISSUE* _____
e. SERIAL IDENTIFIER (e.g. ISSN or CODEN)

☐ 4. OTHER, SPECIFY

G. STI Product Reporting Period
05 (MM) 06 (DD) 2005 (YYYY) Thru 05 (MM) 01 (DD) 2008 (YYYY)

H. Sponsoring DOE Program Office
Office of Industrial Technologies (OIT)(EE20)

I. Subject Categories (*list primary one first*)
32 Energy Conservation, Consumption and Utilization
Keywords: Steel, Carbon Sequestration, Mineral Sequestration

J. Description/Abstract
The objectives of the project were (i) to develop a combination iron oxide production and carbon sequestration plant that will use serpentine ores as the source of iron and the extraction tailings as the storage element for CO2 disposal, (ii) the identification of locations within the US where this process may be implemented and (iii) to create a standardized process to characterize the serpentine deposits in terms of carbon disposal capacity and iron and steel production capacity.

K. Intellectual Property/Distribution Limitations
(must select at least one; if uncertain contact your Contracting Officer (CO))

☒ 1. UNLIMITED ANNOUNCEMENT *(available to U.S. and non-U.S. public; the Government assumes no liability for disclosure of such data)*

☐ 2. COPYRIGHTED MATERIAL: *Are there any restrictions based on copyright?* ☐ *Yes* ☐ *No.*
If yes, list the restrictions as contained in your award document

☐ 3. PATENTABLE MATERIAL: THERE IS PATENTABLE MATERIAL IN THE DOCUMENT.
INENTION DISCLOSURE SUBMITTED TO DOE:
DOE Docket Number: S-
(Sections are marked as restricted distribution pursuant to 35 USC 205)

☐ 4. PROTECTED DATA: ☐ CRADA ☐ *Other, specify*
Release date (required) no more than 5 years from date listed in Part I.E. above ___ (MM) ___ (DD) ___ (YYYY)

☐ 5. SMALL BUSINESS INNOVATION RESEARCH (SBIR) DATA
Release date (required) no more than 4 years from date listed in Part I.E. above ___ (MM) ___ (DD) ___ (YYYY)

☐ 6. SMALL BUSINESS TECHNOLOGY TRANSFER RESEARCH (STTR) DATA
Release date (required) no more than 4 years from date listed in Part I.E. above ___ (MM) ___ (DD) ___ (YYYY)

☐ 7. OFFICE OF NUCLEAR ENERGY APPLICED TECHNOLOGY

L. Recipient/Contract Point of Contact *Contact for additional information (contact or organization name To be included in published citations and who would Receive any external questions about the content of the STI Product or the research contained herein)*

Dr. Klaus Lackner
Name and/or Position
KI2010@columbia.edu *(212) 854-0304*
E-mail *Phone*
Columbia University, Department of Earth and Environmental Engineering, 500 West 120th St., New York, NY 10027

DOE F 241.3
(2-01) p.2 of 2

UNITED STATES DEPARTMENT OF ENERGY (DOE)
Announcement of Scientific and Technical Information (STI)
(For Use By Financial Assistance Recipients and Non-M&O/M&I Contractors)

OMB CONTROL NO. 1910-1400

PART II: STI PRODUCT MEDIA/FORMAT and LOCATION/TRANSMISSION
(To be completed by Recipient/Contractor)

A. Media/Format Information:

1. MEDIUM OF STI PRODUCT IS:
   [X] Electronic Document [ ] Computer Medium
   [ ] Audiovisual Material [ ] Paper [ ] No Full-text
2. SIZE OF STI PRODUCT 75 Pages, 1914 KB
3. SPECIFY FILE FORMAT OF ELECTRONIC DOCUMENT BEING TRANSMITTED, INDICATE:
   [ ] SGML [ ] HTML [ ] XML [X] PDF Normal
   [ ] PDF Image [ ] TIFFG4
   [ ] WP-indicate Version (*5.0 or greater*) _____
   Platform/operation system _____
   [ ] MS-indicate Version (*5.0 or greater*) _____
   Platform/operation system _____
   [ ] Postscript _____
4. IF COMPUTER MEDIUM OR AUDIOVISUAL MATERIAL:
   a. Quantity/type (*specify*) _____
   b. Machine compatibility (*specify*) _____
   c. Other information about product format a user needs to know:
   _____

B. Transmission Information:

1. STI PRODUCT IS BEING TRANSMITTED:
   [X] a. Electronically via E-Link
   b. Via mail or shipment to address indicated in award document (*Paper product, CD-ROM, diskettes, video cassettes, etc.*)
   _____
2. INFORMATION PRODUCT FILE NAME
   [X] (*of transmitted electronic format*)
   TRP9957NonPropFinalReport

PART III: STI PRODUCT REVIEW/RELEASE INFORMATION
(To be completed by DOE)

A. STI Product Reporting Requirements Review.

[ ] 1. THIS DELIVERABLE COMPLETES ALL REQUIRED DELIVERABLES FOR THIS AWARD
[ ] 2. THIS DELIVERABLE FULFILLS A TECHNICAL INFORMATION REPORTING REQUIREMENT, BUT SHOULD NOT BE DISSEMINATED BEYOND DOE.

B. Award Office Is the Source of STI Product Availability

[ ] THE STI PRODUCT IS NOT AVAILABLE IN AN ELECTRONIC MEDIUM. THE AWARDING OFFICE WILL SERVE AS THE INTERIM SOURCE OF AVAILABILITY.

C. DOE Releasing Official

[ ] 1. I VERIFY THAT ALL NECESSARY REVIEWS HAVE BEEN COMPLETED AS DESCRIBED IN DOE G 241.1-1A, PART II, SECTION 3.0 AND THAT THE STI PRODUCT SHOULD BE RELEASED IN ACCORDANCE WITH THE INTELLECTUAL PROPERTY/DISTRIBUTION LIMITATION ABOVE.

Release by (*name*) _____

Date ___ ___ ____ (MM DD YYYY)

E-Mail _____

Phone _____

REPORT DOCUMENTATION PAGE

Title and Subtitle:

AISI/DOE Technology Roadmap Program for the Steel Industry
TRP 9957: Integrating Steel Production with Mineral Carbon Sequestration

Authors:

Klaus S. Lackner
Tuncel Yegulalp
Christopher Graves
Paul F. Duby
Samuel Krevor

Performing Organization

Columbia University
Department of Earth and Environmental Engineering
500 West 120th Street
New York, NY 10027

Abstract

Mineral sequestration, the disposal of carbon dioxide in the form of benign solid carbonate, provides a permanent and safe method of carbon dioxide disposal of virtually unlimited capacity. The objective of this project is to to develop a combination iron oxide production and carbon sequestration plant that will use serpentine ores as the source of iron and dispose of its own CO2. By using the same ore processing steps for carbon sequestration and iron ore production we increase the value of the carbon sequestration process and consequently reduce the cost of sequestration with this added value.

Particularly important for justifying the feasibility of a combined iron production and mineral carbonation process for the mitigation of CO_2 generated by the iron and steel industry is the identification of locations where this process may be implemented. This identification is dependent both on the physical and chemical characteristics of the deposits themselves, as well as the current land-ownership and use in their location and proximity to iron processing plants and/or large sources of CO_2. In this project we identify the locations of deposits, estimate the volume of mineral available, and summarize known geochemical data on major deposits as described in the geological literature.

In developing the chemical pathways for a hydrometallurgical process we will further the identification of potential solvents. Finally, we will create a standardized process through which to characterize serpentine deposits in terms of carbon disposal capacity and iron and steel production capacity.

Keywords: Steel, Mineral Sequestration, Carbon Dioxide

DOCUMENT AVAILABILITY

Reports are available free via the U.S. Department of Energy (DOE) Information Bridge:

Website: http://www.osti.gov/bridge

Reports are available to DOE employees, DOE contractors, Energy Technology Data Exchange (ETDE) representatives, and Informational Nuclear Information System (INIS) representatives from the following source:

Office of Scientific and Technical Information
P.O. Box 62
Oak Ridge, TN 37831
Tel: (865) 576-8401
Fax: (865) 576-5728
E-mail: reports@osti.gov
Website: http://www.osti.gov/contract.html

Acknowledgement: "This report is based upon work supported by the U.S. Department of Energy under Cooperative Agreement No. DE-FC36-97ID13554."

AISI/DOE Technology Roadmap Program

Final Report

TRP 9957 - Integrating Steel Production with Mineral Carbon Sequestration

By

Klaus S. Lackner, Paul F. Duby, Tuncel Yegulalp,
Samuel Krevor, Christopher Graves

May 2008

Work Performed under Cooperative Agreement
No. DE-FC36-97ID13554

Prepared for
U.S. Department of Energy

Prepared by
American Iron and Steel Institute
Technology Roadmap Program Office
Pittsburgh, PA 15222

Integrating Steel Production with Mineral Carbon Sequestration

Columbia University
Department of Earth and Environmental Engineering

Faculty Contributors:
Klaus S. Lackner
Paul F. Duby
Tuncel Yegulalp

Graduate Student Contributors:
Samuel Krevor
Christopher Graves

Table of Contents

Executive Summary	**3**
Introduction	**4**
Part I: The Mineral Resource Base For Mineral Carbon Sequestration In the United States	**5**
Part II: Mineral Processing for Mineral Carbon Dioxide Sequestration	**48**
Part III Mass Flow of Iron from Serpentine to Steel	**57**

Executive Summary

Here we propose to develop a combination iron oxide production and carbon sequestration plant that will use serpentine ores as the source of iron and dispose of its own CO_2 -- plus additional CO_2 from other sources -- in the mineral tailings that are left after iron is separated. By using the same ore processing steps for carbon sequestration and iron ore production we increase the value of the carbon sequestration process and consequently reduce the cost of sequestration with this added value.

1. Geographical information system (GIS) datasets describing surface geology were obtained for the majority of ultramafic-containing states and used to estimate surface area exposure of serpentinite and ultramafic resources. Regional and nationwide datasets filled in gaps where statewide data is not available. Various land use datasets were integrated to account for areas such as urban centers and designated wilderness to eliminate locations where it will not be politically feasible to operate a mineral sequestration plant. The east coast ultramafic resource surface area is approximately 1086.44 km^2. After filters for land-use are applied, there are 976.10 km^2 suitable reserves. The west coast resources are much greater, at 8,730 km^2 and reducing to 6677 km^2 after land use is taken into account. With depths of at least 500 m available for economic mining and using the density of serpentine (2.55 g/cm^2), reserves for the entire U.S. are estimated at 9,758,000 Mt.

- **Using an R(CO_2) value of 2.1 (100% conversion of serpentine) the sequestration potential of this mass of material is 4,647 Gt of CO_2 or more than 500 years of the United States' current production of CO_2.**

2. Magnetic iron oxide is nearly always present in serpentinite deposits as a result of the process by which serpentine is formed from the alteration of other magnesium silicates. A simple test has found that the liberation size of the magnetite is 53 micron, consistent with other determinations of the liberation size of magnetite. The chemical processing of silicate minerals for carbonation is a major barrier to the implementation of direct aqueous mineral carbonation as a viable carbon sequestration technology. A viable mineral carbon sequestration process utilizing serpentine has never been demonstrated due to slow reaction times with carbon dioxide in aqueous solutions. Experiments were performed exploring the catalytic effect that NaCl and NH_4Cl may have on serpentine dissolution, the rate limiting step in the overall carbonation process.

- **It was found that while initial dissolution rates appear to be enhanced by the presence of the salts, long-term dissolution rates remain unaffected and thus these salts will not contribute to lowering the costs of a mineral carbonation process. More research is needed to develop a viable carbon sequestration technology using serpentine or similar minerals.**

3. Process studies were undertaken to illustrate the relationship between silicate ore composition, iron oxide recovery, and sequestration potential. A computer model has been developed to investigate the impact of various system parameters (recoveries and efficiencies and capacities at different system components), serpentinite quality, as well as incorporation of CO_2 from external sources. Modules with user inputs include the mine, the mineral processing plant, the sequestration plant, the palletizing plant, and the steel plant. A simple cost model is used to illustrate limits on the cost of the various components.

- **A base case example is given showing that nearly 1/5 of the iron oxide required for a steel production process may be supplied by the serpentinite ore used to sequester 100% of the emissions created in the steel production.**

While sufficient serpentinite and ultramafic resources were identified in this project, mineral carbonation remains the critical process in demonstrating the viability of simultaneous production of iron oxides and carbon sequestration. This project was not successful in identifying a technique to accelerate direct aqueous mineral carbonation.

Introduction

In developing carbon dioxide disposal options, the steel industry will not be alone. Indeed, the power utilities provide far larger streams of carbon dioxide that need to be safely disposed of. Therefore it is unlikely that the steel industry will contribute much to the development of these options. The exception to this rule is the development of carbon dioxide disposal options that would be peculiar to the steel industry. There are several reasons to investigate and develop such options. In an industry specific disposal site the industry will not have to compete with a far larger utility industry which may consider sequestration as an in house operation not open to outsiders except at exorbitant fees. Secondly, the specifics of the industry could lead to a cheaper disposal option than is generally available. Finally, a carbon dioxide disposal option that exceeds the needs of the steel industry would offer an opportunity to sell carbon dioxide disposal credits to other industries. Such an option would become extremely valuable if across the economy the cost of carbon mitigation proves to be high. In that case, ownership in a good carbon sink would allow the steel industry to offset its own carbon costs by selling carbon credits. Thus mineral sequestration technology could act as insurance or a hedging strategy.

Mineral sequestration, the disposal of carbon dioxide in the form of benign solid carbonate, provides a permanent and safe method of carbon dioxide disposal of virtually unlimited capacity. This method of carbon dioxide disposal could greatly benefit from collaboration with the steel industry as the hydrometallurgical processing of the mineral ore (peridotite rock) results in the generation of virtually pure iron oxides.

The U.S. steel industry is accustomed to preprocessing iron ores prior to bringing them into the blast furnace. If the gangue materials could be used to chemically bind carbon dioxide than this would develop a niche market for the steel industry in which to dispose of its own carbon dioxide. For every ton of Fe produced at steel plants there is approximately a ton of carbon dioxide that will need to be sequestered as a result of iron reduction. Overall the steel making process is more carbon intensive and total CO2 production per ton of steel is approximately 1.7 tons.

Here we propose to develop a combination iron oxide production and carbon sequestration plant that will use serpentine ores as the source of iron and dispose of its own CO2 -- plus additional CO2 from other sources -- in the mineral tailings that are left after iron is separated. By using the same ore processing steps for carbon sequestration and iron ore production we increase the value of the carbon sequestration process and consequently reduce the cost of sequestration with this added value.

In developing the chemical pathways for a hydrometallurgical process we will further the identification of potential solvents for the minerals by building upon the studies of a handful of groups, all of which suggest that there remains a large parameter space within which to optimize. In addition, novel processes for recycling solvents in a hydrometallurgical scenario will be explored. Finally, we will create a standardized process through which to characterize serpentine deposits in terms of carbon disposal capacity and iron and steel production capacity.

Part I

The Mineral Resource Base For Mineral Carbon Sequestration In the United States

Contents

I) Introduction
    1) Report Overview and Purpose
    2) Underlying Process Assumptions
    3) Explanation of Indices
II) United States Ultramafic Geology Overview
    1) United States Map of Ultramafic Deposits
    2) Estimated Surface Exposure Area of Ultramafic Deposits
    3) Magnesium & Iron Content Distribution
III) Ultramafics of the Eastern United States
    1) Appalachian Belt
        A) Vermont
        B) Pennsylvania – Maryland – Washington, D.C. Region
        C) Western North Carolina
    2) Caribbean Belt
        A) Southwestern Puerto Rico
IV) Ultramafics of the Western United States
    1) Overview
    2) California and Oregon
        A) Overview and Geologic History
        B) Deposits of the Coast Ranges
        C) Deposits of the Sierra Nevada
        D) The Klamath-Trinity Region
        E) The Canyon Mountain Complex
    3) Washington State and the Twin Sisters Dunite
V) Conclusion and Ongoing Work
VI) References

Appendix A: Compositional data table of various ultramafic samples from each deposit

Appendix B: Geologic Vocabulary

Appendix C: Methodology for the Calculation of Ultramafic Mineral Resources in the United States

I. Introduction

I.1. Report Overview and Purpose

In the 2005 Intergovernmental Panel on Climate Change (IPCC) report on Carbon Dioxide Capture and Storage, it is identified that one of the most important areas of research to be performed for the development of an industrial scale mineral carbon sequestration process is the determination of "the fraction of the natural reserves of silicates, which greatly exceed the needs that can be effectively exploited for mineral carbonation." Particularly important for justifying the feasibility of a combined iron production and mineral carbonation process for the mitigation of CO_2 generated by the iron and steel industry is the identification of locations where this process may be implemented. This identification is dependent both on the physical and chemical characteristics of the deposits themselves, as well as the current land-ownership and use in their location and proximity to iron processing plants and/or large sources of CO_2. In this report we identify the locations of deposits, estimate the volume of mineral available, and summarize known geochemical data on major deposits as described in the geological literature.

In Section II generalizations are drawn about the deposits in the United States as a whole. Total surface area coverage of the deposits as well as total usable surface area is calculated from GIS datasets. A distribution of geochemical data from deposits around the country is created to show the variation in magnesium and iron content that we may expect to find among deposits.

In Section III, the ultramafics of the Eastern Coast and Puerto Rico are described. The ultramafics of the East Coast are categorized into three sections by their geography: Vermont, Pennsylvania-Maryland-Washington D.C. (PA-MD-DC), and Western North Carolina. Puerto Rico contains the largest deposits of serpentine of those in the East.

In Section IV, the ultramafics of the Western Coast (CA, OR, WA) are described. These deposits are large relative to those on the East Coast and those in the Klamath-Trinity region of the California-Oregon Border equal the size of the deposits in Puerto Rico.

I.2. Underlying Process Assumptions

It is assumed in this report that a mineral carbonation process will utilize ultramafic materials with high content serpentine and olivine minerals.

I.3. Explanation of Indices

$R(CO_2)$ – This value is the ratio of ore that must be mined to the amount of CO_2 that will be sequestered. It is the same statistic used by Goff et. al.[1]. $R(CO_2)$ for the 100% conversion of serpentine is 2.1 and that for olivine is 1.6.

Mass, CO_2 stored per 100 m depth- Many values are normalized to the utilization of ore material assuming the deposit is quarried to 100m. The minimum depth found for a deposit is 100m, and many of the deposits are well in excess of 500m in depth. Those on the East coast tend to have depths between 100 and 500 meters. It is expected that averaged over the entirety of ultramafic deposits, the average depth is well in excess of 500 meters, although normalizing to this value was not relevant for the shallow Eastern Coast deposits.

II. United States Ultramafic Geology Overview

The main source of ultramafic rocks is in continental exposures of oceanic lithosphere (ophiolite suites) along subduction zones and ancient continental margins. These exposures of ultramafic rocks are classified as "Alpine-Type" peridotites and are expressed in the United States in the Appalachian belt of the east coast and the Cordilleran belt in the west. There is also a belt in the Caribbean where the North American and Caribbean continental plates meet. Of particular interest in this region are the large deposits in Puerto Rico. The emplacement of these deposits can generally be associated with collision events that are also the major mountain building (orogenic) processes, which result in the mountainous regions associated with the deposits.

II.1. United States Map of Ultramafic Deposits

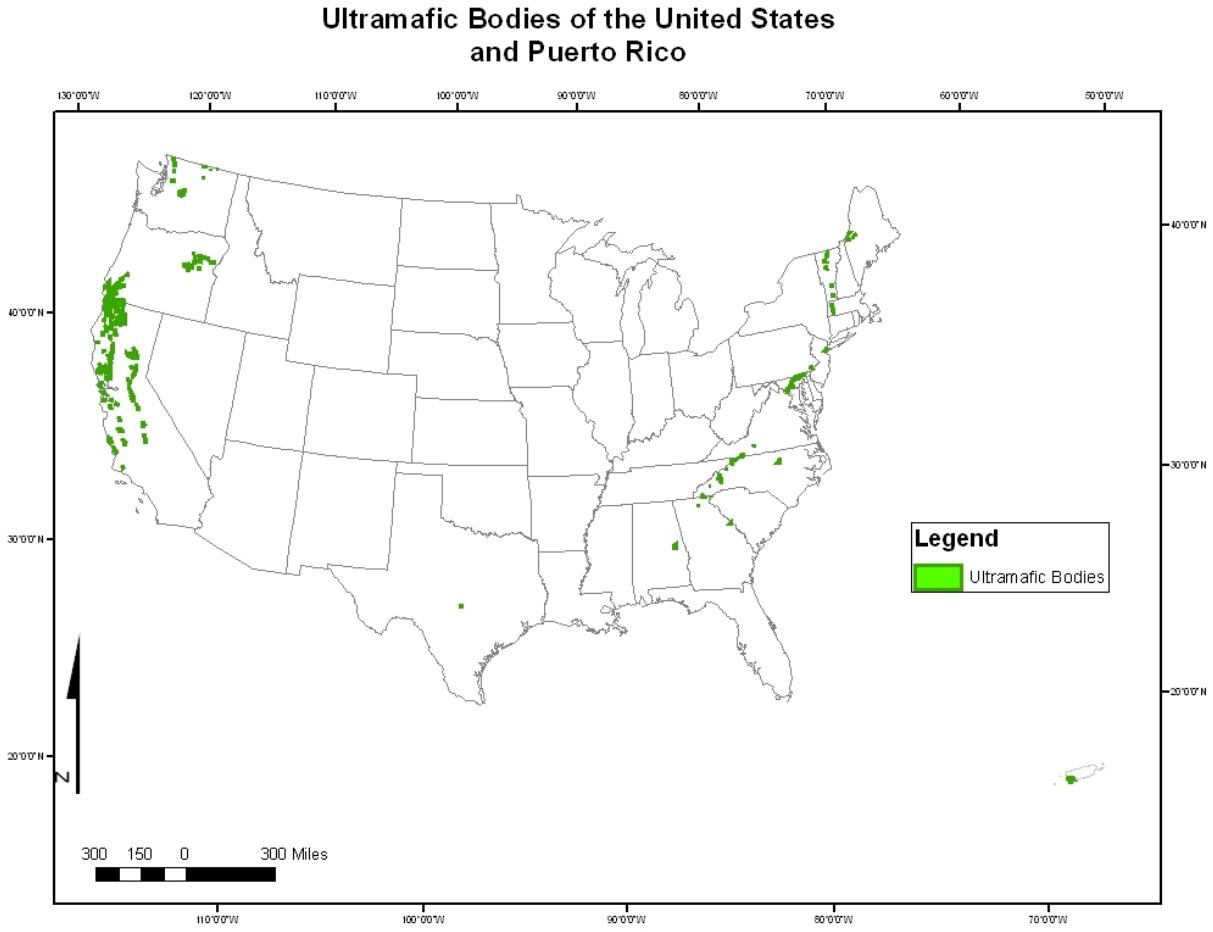

Figure 1. Ultramafic Bodies of the United States. Largest deposits occur along coasts near continental plate boundaries

II.2. Estimated Surface Exposure Area of Ultramafic Deposits

GIS datasets describing surface geology were obtained for the majority of ultramafic-containing states and used to estimate surface area exposure of serpentinite and ultramafic resources. Regional and nationwide datasets filled in gaps where statewide data is not available. Appendix C lists data sources for the digital datasets.

Various land use datasets were integrated to account for areas such as urban centers and designated wilderness to eliminate locations where it will not be politically feasible to operate a mineral sequestration plant. The methodology is described in detail in Appendix C.

The east coast ultramafic resource surface area is approximately 1086.44 km^2. After the filters are applied, there are 976.10 km^2 suitable reserves. The west coast resources are much greater, at 8,730 km^2 and reducing to 6677 km^2 after land use is taken into account. With depths of at least 500 m available for economic mining and using the density of serpentine (2.55 g/cm^2), reserves for the entire U.S. are estimated at 9,758,000 Mt. Using an $R(CO_2)$ value of 2.1 (100% conversion of serpentine) the sequestration potential of this mass of material is 4,647 Gt of CO_2 or more than half a millennium of the United States' current production of CO_2.

Region	Surface area (km^2)
Eastern USA	810.15
Western USA	6,677
Puerto Rico	165.95
Scattered igneous intrusions	11.20
Total	11941.61

Table 1. Estimated surface area of ultramafics by region [4]

II.3. Overall Magnesium & Iron Content Distribution

Two general characteristics that define the quality of the rock masses of interest are their potential for carbon sequestration and the amount of iron that may be recovered as a byproduct. The potential for carbon sequestration is represented by the $R(CO_2)$ value which is simply the ratio of the amount of rock mined to the amount of CO_2 that may be sequestered. This value is currently correlated directly to the percentage magnesium content of the material. Future tests may allow us to distinguish between ore of different mineralogical makeup as well. Thus for pure serpentine, or pure olivine, the $R(CO_2)$ values are:

$$\textbf{Theoretical min } R(CO_2)_{serpentine} = \text{MW Serp}/ 3*\text{MW } CO_2 = 2.099$$
$$\textbf{Theoretical min } R(CO_2)_{olivine} = \text{MW Oliv}/2 * \text{MW } CO_2 = 1.60$$

In considering the ability to rank the deposits in terms of these two characteristics, it is useful to compare the distribution of each of these characteristics among all deposits next to each other. If large distributions are observed among both characteristics, we can expect to be making tradeoffs between high iron content and high magnesium content (high sequestration potential).

Compositional analyses of 58 serpentine- and olivine-bearing ultramafic rock sample sets representing all of the major depositional areas in the United States (see Appendix A) yield the following boxplot distributions in terms of iron and magnesium content. Lower and upper bounds of the boxes represent boundaries below which exists 25% and 75% of the data. The central line indicates the median value for the distribution.

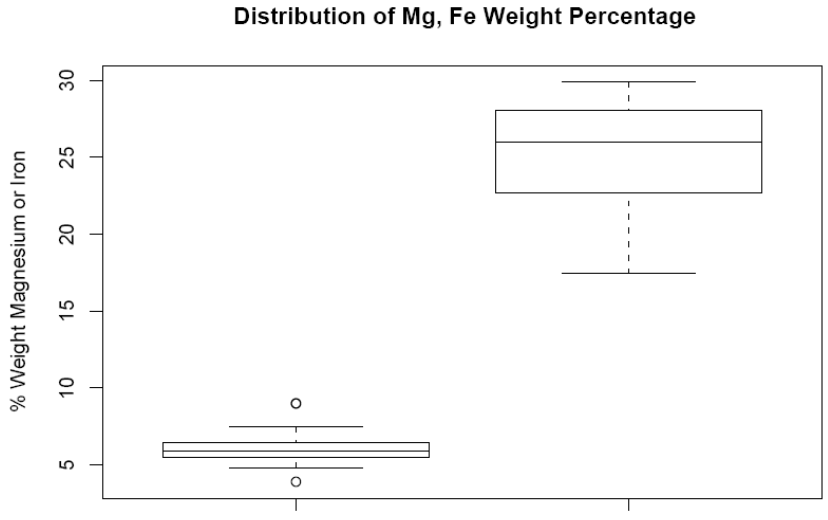

Figure 2. Boxplot of Magnesium and Iron Distribution in Ultramafic Deposits of the United States.

Figure 2 shows that the iron concentration of the various deposits is practically constant relative to the magnesium concentration. Thus, when optimizing, we can expect to rank deposits primarily on the basis of their $R(CO_2)$.

Overall, the studied serpentinite and peridotite rock deposits have R(CO_2) values ranging from 1.85 to 3.16. Taking into account their Fe contents, they have the potential to sequester 5 to 10 Gt of carbon dioxide per Gt of iron produced.

III. Ultramafics of the Eastern United States

State	Area (km^2)	%Total
AL	97.45	10.59%
CT	0.56	0.06%
GA	148.33	16.11%
MA	10.08	1.10%
MD*	212.63	23.10%
ME	177.79	19.31%
NC	86.47	9.39%
NJ	3.89	0.42%
NY	40.33	4.38%
PA	62.64	6.81%
VA*	52.71	5.73%
VT	27.6	3.00%
Total	920.48	100.00%

Table 2. Ultramafic Body Distribution Among States of the East Coast

III.1. Appalachian Belt

The Appalachian chain stretches from Alabama to Newfoundland. It is the result of uplift and deformation during early- to mid-Paleozoic subduction along the east coast of North America. Individual Appalachian ultramafic bodies are typically less than 1 km^3 in volume but can reach 7 km^3 [3].The surface area of ultramafics in the Appalachian chain is approximately 920 km^2 [Table 2].

The ultramafic bodies of the Appalachian belt can be categorized into 3 major sections. From north to south, they are: Vermont, Pennsylvania-Maryland-DC (PA-MD-DC), and Western North Carolina. Figure 3 shows a map of Appalachian ultramafic bodies.

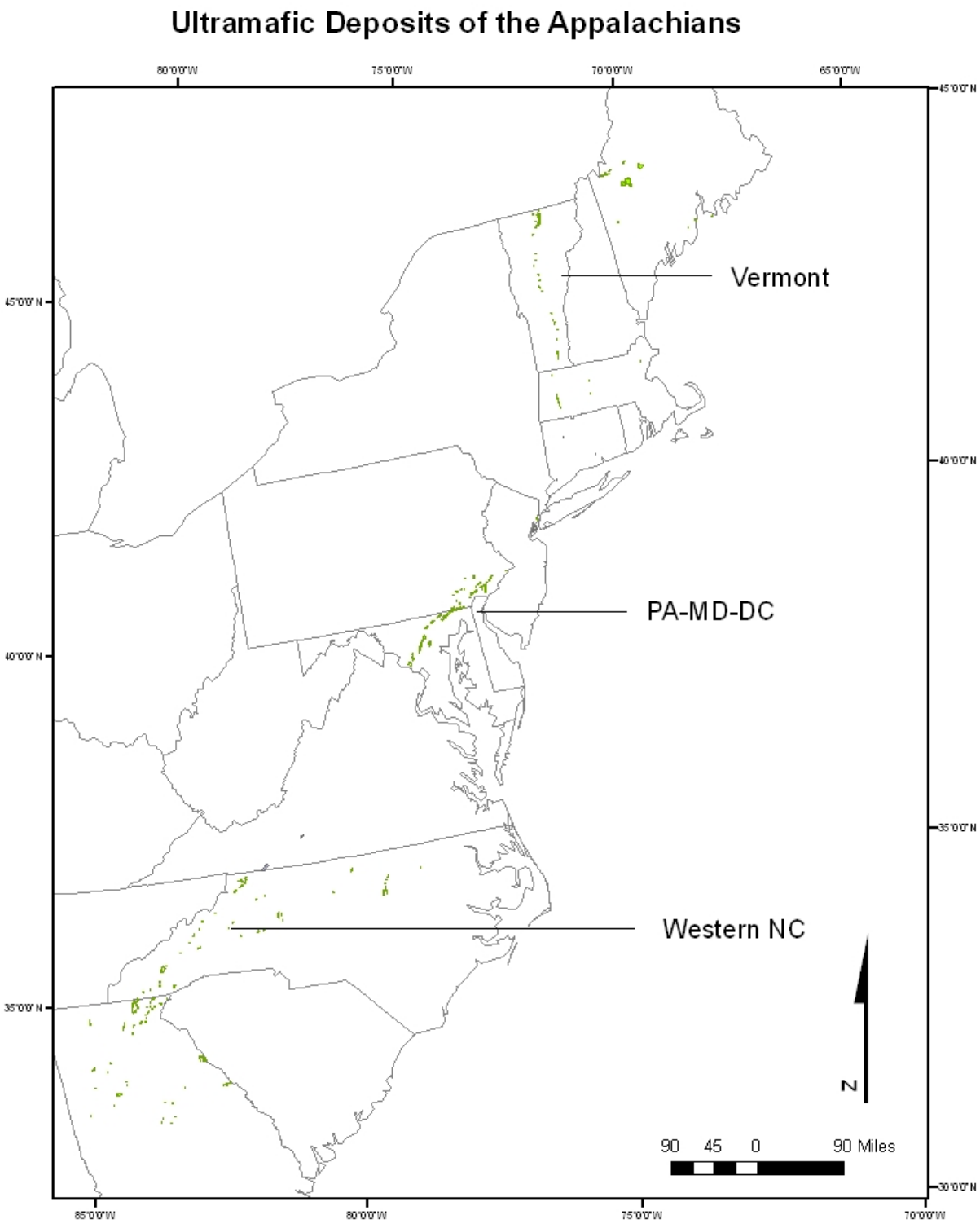

Figure 3. Ultramafic Bodies of the Appalachians

Amongst the studied Appalachian belt deposits, it can be seen that their mineralogy varies similarly to that of all studied United States deposits (Figure 4). As previously discussed, magnesium content varies considerably more than iron content. All variations are due to different levels of serpentinization amongst the deposits and different ultramafic purities of samples collected from the deposits.

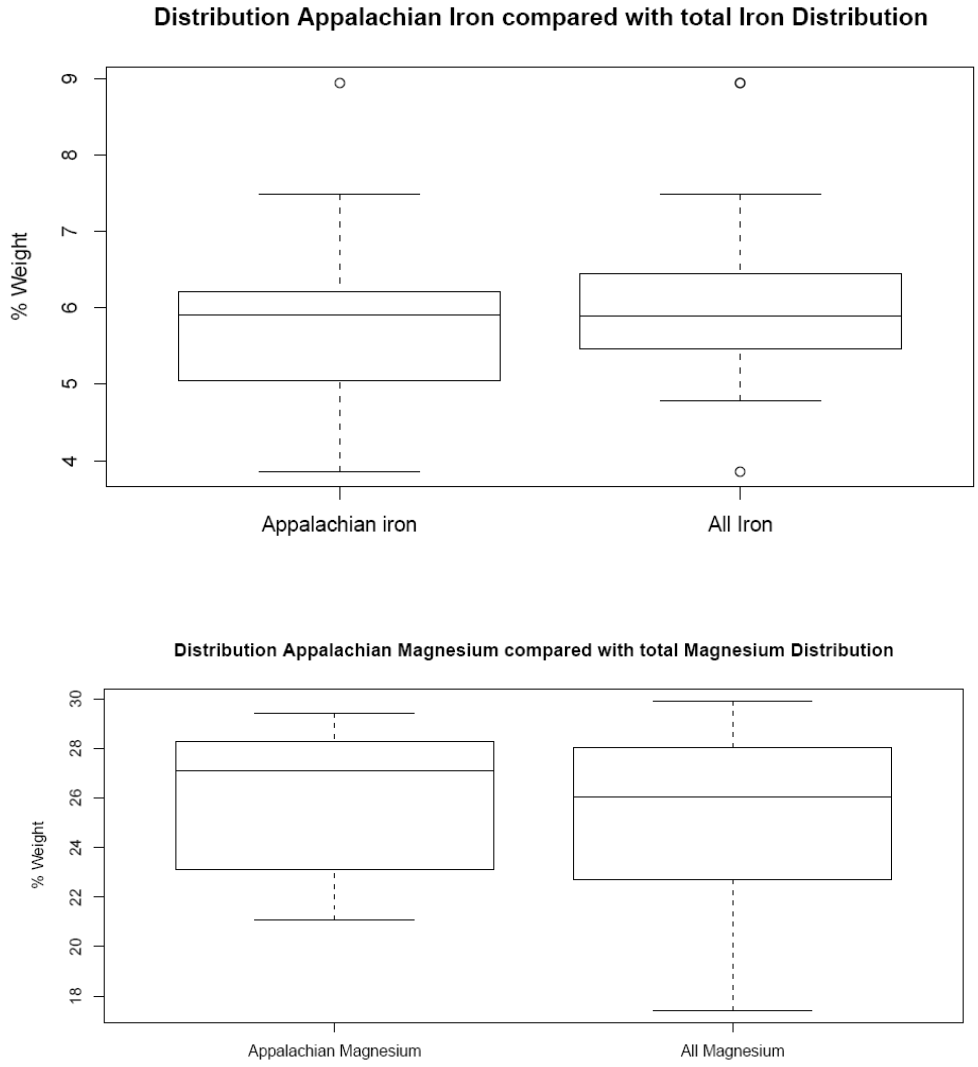

Figure 4. Distribution of iron and magnesium content among Appalachian deposits compared with overall USA contents.

III.1.A. Vermont

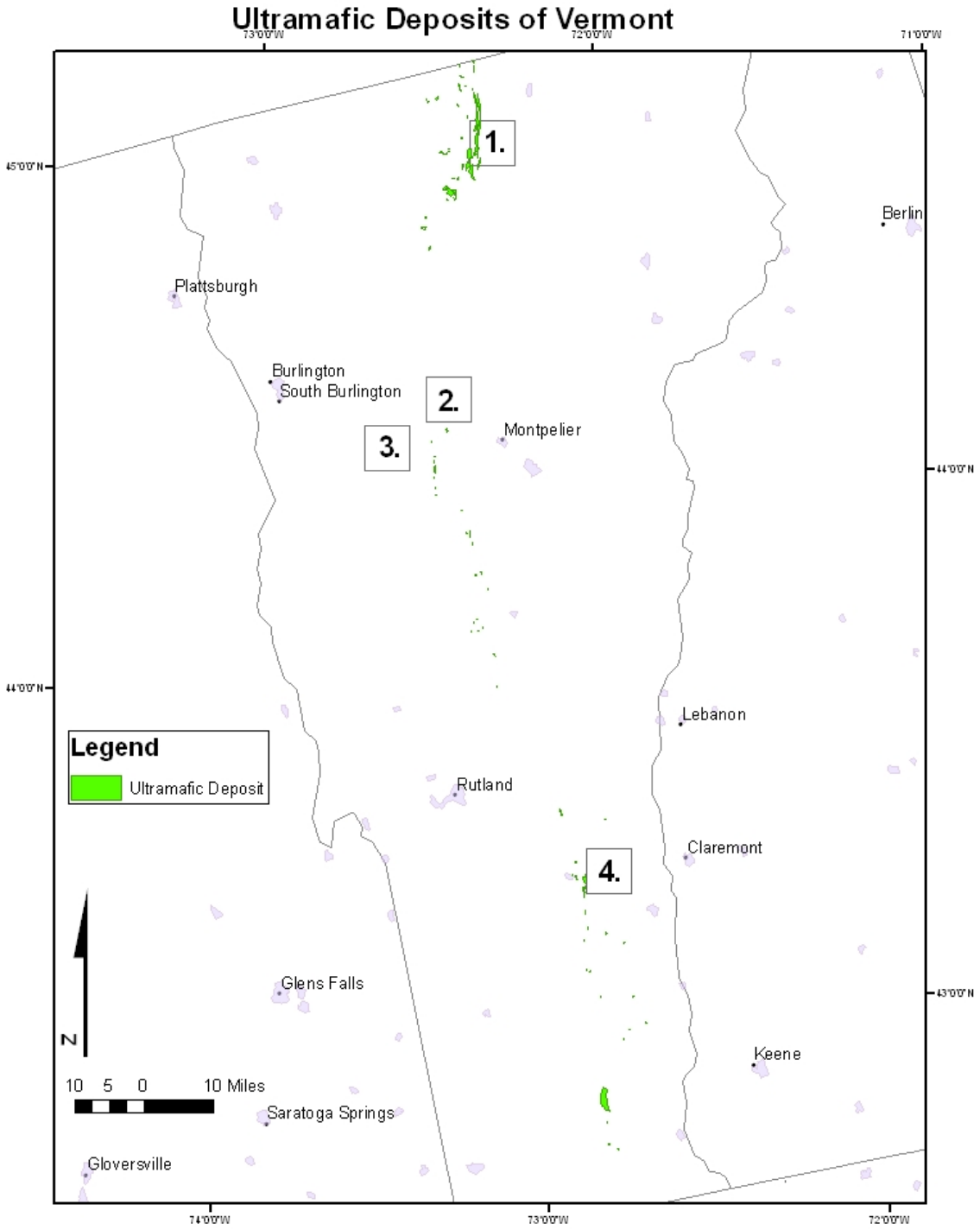

Figure 5. Ultramafic Deposits of Vermont 1. Belvidere Mountain 2. Barnes Hill Waterbury Mine 3. Mad River Talc Mine 4. East Dover

The major serpentinite deposits in Vermont studied for mineralogical and chemical composition are: Belvidere Mountain in the north; the north-central deposits of Barnes Hill, Mad River, and Waterbury; and East Dover in the south.

The Cambrian- and Ordovician-aged ultramafic rocks in Vermont can be found a narrow central region extending northward. [29] Serpentinized ultramafics consisting primarily of antigorite with minor chrysotile, lizardite, talc, carbonate, chlorite, tremolite, and magnetite are more common than unaltered dunites. Asbestos, talc, and ornamental serpentine have been mined from the various deposits over the last 150 years. [2] The Vermont region we have estimated to have a maximum surface area of 106.34 km^2 [4].

Of these deposits, Belvidere Mountain and East Dover are of the largest size. Table 3 and Figure 6 describe the size of each deposit. Belvidere Mountain has the greatest amount of iron via its high percentage iron content. These two largest deposits contain a large amount of unserpentinized peridotite rock, as pure as 80% by volume [2], evident in their higher density and higher magnesium content. Conversely, the three north-central deposits contain a larger amount of serpentinized rock. Table 4 is a summary of the compositional data, in which the average mineralogical composition for a variety of samples from each deposit has been assumed to describe the deposit as a whole. The complete non-extrapolated data set can be found in Appendix A.

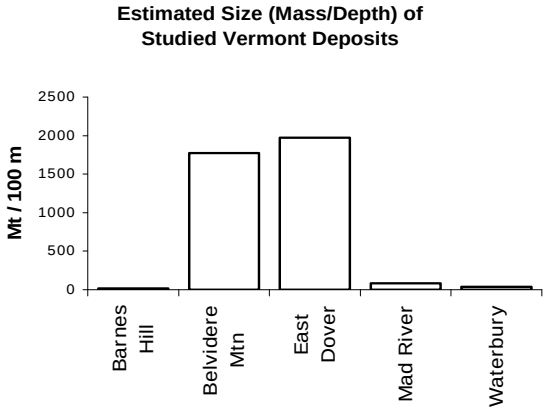

Figure 6

Ore Body	Surf. Area km^2	Density g/cm^3	Mass/depth Mt/100 m	Est. Depth km	Est. Vol. km^3	Est. Mass Mt
Barnes Hill	0.05	2.70	14.31	0.15	0.0080	21.465
Belvidere Mtn	6.12	2.90	1774.80	0.45	2.7540	7986.600
East Dover	6.80	2.90	1972.00	0.40	2.7200	7888.000
Mad River	0.31	2.68	81.74	0.20	0.0610	163.480
Waterbury	0.15	2.66	38.57	0.12	0.0174	46.284

Table 3. Vermont deposit sizes

Ore Body	Fe avg	Mg avg	Fe/depth	CO_2 seq/depth	R(CO_2)
	wt %	wt %	Mt/100 m	Mt/100 m	
Barnes Hill	5.897	23.099	0.844	5.984	2.39
Belvidere Mtn	8.939	26.024	158.651	836.091	2.12
East Dover	5.045	27.803	99.482	992.502	1.99
Mad River	5.947	21.082	4.861	31.194	2.62
Waterbury	4.806	22.399	1.854	15.639	2.47

Table 4. Vermont deposit compositions and carbon sequestration potential

It is clear that of the studied Vermont deposits, Belvidere Mountain and East Dover offer the greatest potential for carbon sequestration – greatest "CO_2 seq/depth" and lowest "R (CO2)" values – while also offering the greatest mass of potentially recoverable iron – "Fe/depth". This follows the fact that they are the largest of the studied deposits.

Following are detailed descriptions of each studied deposit.

Belvidere Mountain

The main Belvidere Mountain ultramafic deposit is composed of a central part of massive dunite and peridotite, transitioning outward into massive serpentinite and then surrounded by sheared serpentinite. It is made up of three large bodies at the surface: the Eden quarry, the Cortez Pond body (also known as C-area), and the Lowell quarry. This area has the largest known reserves of chrysotile asbestos in the eastern United States [30], comprising about 5% of rock quarried, and was actively mined for commercial asbestos until 1993. The Lowell deposit is a well-known mineral collecting area. [34] The total estimated mass of the Belvidere Mountain deposit is approximate 6.67 Gt [3] to 7.99 Gt [2].

Size estimations and compositional analyses of the Belvidere Mountain mine tailings have also been done [35, 36], accounting for approximately 0.057 Gt and similar Mg and Fe contents.

North-central deposits

The north-central ultramafic deposits consist of rock that has been almost entirely serpentinized and extensively steatized, most often encased in talc or talc-carbonate rock. The serpentinite is quite uniform in composition, and none in this area are known to contain unserpentinized peridotite. Probably more than 99 percent of the total serpentine in this area is antigorite. Mad River and Waterbury host idle talc mines, and Barnes Hill has been to a lesser extent mined for asbestos and talc. The mass of each ultramafic deposit has been estimated by various studies: Barnes Hill with 0.0215 Gt, Mad River with 0.163 Gt, and Waterbury with 0.0463 Gt. [29]

East Dover

The East Dover ultramafic deposit, located in south-central Vermont just northeast of the town of Wilmington, is comprised of one large body and two or three smaller bodies, all composed mainly of serpentinized dunites. Olivine and serpentine make up more than 90 percent of most samples. Present in some areas are also chrome spinel, magnetite, chlorite, carbonates, etc. The ultramafic rock is on the average 55% serpentinized, ranging from 5% to 100%. [30] The inner rock contains a substantial amount of olivine that has avoided serpentinization. The estimated mass is 7.89 Gt of ultramafic rock. [31]

III.1.B. Pennsylvania – Maryland – Washington, D.C. Region

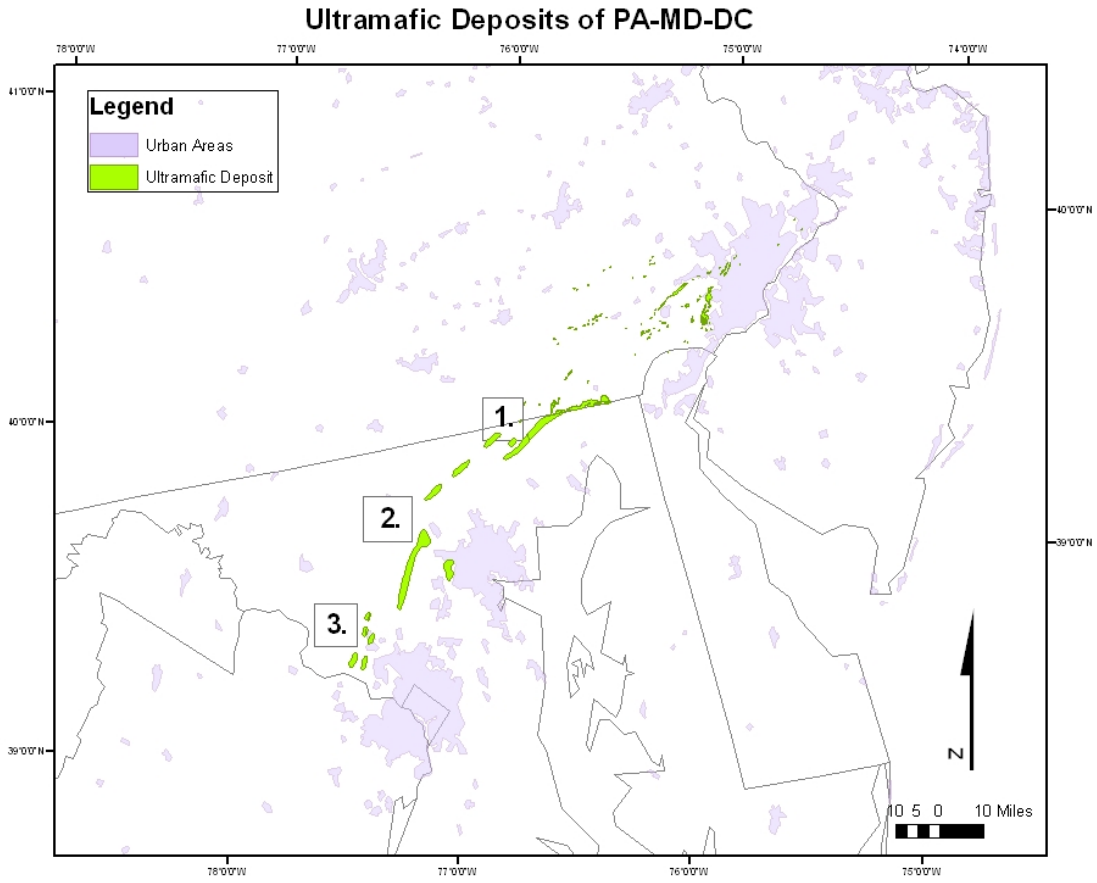

Figure 7 Ultramafic Deposits of the PA-MD-DC Area 1. Cedar Hills-Penn Mar 2. Chaote Mine- Soldier's Delight 3. Hunting Hill

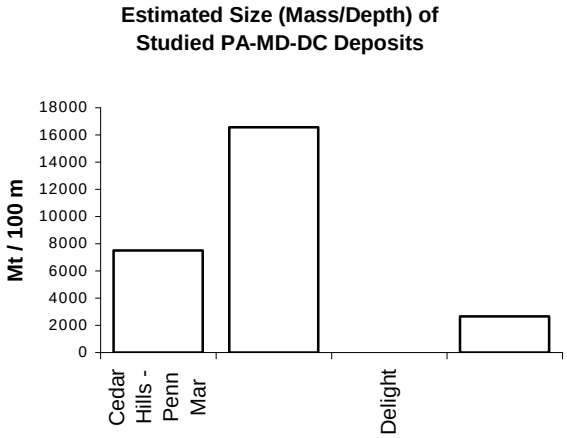

Figure 8. Size of Deposits in the PA-MD-DC Area

Hunting Hill The major serpentinite deposits in the PA-MD-DC region studied for mineralogical and chemical composition are from northeast to southwest: PA-MD state line deposits (Cedar Hills and Penn-Mar), the central deposits (including Delight and Choate Mine), and the Rockville area deposits (including Hunting Hill quarry).

This region of the Appalachian range hosts a belt that extends north-northeast about 150 km in length from southeast Pennsylvania through Maryland into central Virginia. This region is part of the Piedmont Upland, a north-east-trending belt reaching from Alabama to Trenton, NJ. [11] PA-MD-DC regions of this belt are known as the Baltimore Mafic Complex and the Liberty Complex. It is composed of a fragmented ophiolite sequence emplaced during early Paleozoic subduction. This ophiolite sequence is one of the largest in the Appalachian belt. The ultramafic rock in this region has in general undergone extensive serpentinization, and often further changed, or steatitized, to form deposits of soapstone and relatively pure talc. Much of it has been mined for chromite.

The PA-MD-DC region (within view in the Figure 7 map) we have estimated to have a maximum surface area of 313.13 km^2 [4]. The mass of serpentinite rock in the region has been estimated in literature as approximately 8 Gt [12].

Of the studied deposits, the state line and central deposits are of the largest size. Table 5 describes the size of each studied deposit. Note that the deposits are only a subset of the larger ultramafic belt area*. Table 6 is a summary of the compositional data, in which the average mineralogical composition for a variety of samples from each deposit has been assumed to describe the deposit as a whole. The complete non-extrapolated data set can be found in Appendix A.*

Ore Body	Surf. Area km^2	Density g/cm^3	Mass/depth Mt/100 m	Est. Depth km	Est. Vol. km^3	Est. Mass Mt
Cedar Hills - Penn Mar	30.00	2.50	7500.00	0.20	6.00	15.00
Chaote Mine - Soldier's Delight	69.00	2.40	16560.00	0.10	6.90	16.56
Delight	0.05	2.40	10.80	unknown	Unknown	Unknown
Hunting Hill - Rockville	10.62	2.50	2655.00	0.10	1.06	2.66

Table 5. PA-MD-DC deposit sizes

Ore Body	Fe avg wt %	Mg avg wt %	Fe/depth Mt/100 m	CO_2 seq/depth Mt/100 m	R(CO_2)
Cedar Hills - Penn Mar	5.054	24.335	379.016	3303.91	2.27
Chaote Mine - Soldier's Delight	5.561	23.159	920.954	6942.49	2.39
Delight	4.783	22.707	0.517	4.44	2.43
Hunting Hill - Rockville	5.510	22.737	146.301	1092.77	2.43

Table 6. PA-MD-DC deposit compositions and carbon sequestration potential

Magnesium content, iron content, and densities are quite constant across the various deposits studied. This corresponds to their being primarily composed of serpentinized rock. This is supported by Thomas regarding the PJM (Pennsylvania-New Jersey-Maryland) Piedmont region, another name for this area, in stating that it has a magnesium composition of 23-24% and is composed of ultramafics with high serpentinite content. [12]

It is clear that of the studied PA-MD-DC deposits, state line deposits Cedar Hills—Penn Mar and central deposits Chaote Mine—Soldier's Delight offer the greatest potential for carbon sequestration – greatest "CO_2 seq/depth" and lowest "R (CO2)" values – while also offering the greatest mass of potentially recoverable iron – "Fe/depth". This follows the fact that they are the largest of the studied deposits.

Following are more detailed descriptions of each studied deposit.

PA-MD-DC State Line Deposits

The Pennsylvania-Maryland state line hosts a large serpentinite body, located within southern Lancaster County, PA, and known locally as the State Line serpentinite. It is one of the largest of many ultramafic bodies in this area. Within this body there are deposits which have been mined, such as Cedar Hills and Penn Mar. It was mined for chromite during the early 19th century and contained the largest deposit of massive chromite ever found in the United States (the Wood deposit). The Wood deposit also hosts some of the more olivine-rich dunites of the PA-MD-DC region [11]. In general, the talc deposit associated with the State Line serpentinite is similar to talc deposits of Vermont and were derived from the same protolith. [10]

Central Deposits

The Chaote Mine--Soldier's Delight deposits are part of a central long, narrow belt of serpentine located in western Baltimore County, MD. Like the state line deposits, the central deposits are composed mainly of serpentinite. Like the rest of the Piedmont Upland, the serpentinites are generally considered unimportant for mineral mining, but once were mined for chromite, magnetite, rutile, talc, soapstone, amphibole asbestos, magnesite, feldspar, and corundum. Serpentinite rocks themselves have been of commercial value for building, decoration, and crushed stone. [11]

Rockville—Hunting Hill Area Deposits

The Hunting Hill quarry located in Montgomery County, MD, offers the best exposures of serpentinite in the Washington, DC area. It is composed of 80% to 90% serpentinite, the remainder rodingite. It has been mined mainly for crushed stone, used as asphalt filler, by such companies as Rockville Crushed Stone, Inc. [9]

III.1.C. Western North Carolina

The Western North Carolina region of the Appalachian ultramafics is composed of many scattered bodies. The studied deposits are evenly scattered across the belt from the northeast (Virginia) to the southwest (Georgia). This region is in the Blue Ridge belt of Appalachian ultramafics. Its ultramafic bodies differ in composition from the Piedmont Upland; they are comprised primarily of unserpentinized dunite. Dunite is the predominant variety of peridotite in North Carolina and Georgia. Much of the rock found here is nearly pure olivine and the rest is partly serpentinized dunite composed of 50% or more olivine. [2] Most of the larger dunite bodies in this belt are comprised of cores of relatively unaltered dunite surrounded by concentric levels of serpentinite.

The ultramafics of the Western North Carolina region has an estimated maximum surface area of 237.75 km^2 [4]. Total serpentinite mass in this region has been estimated at 3.3 Gt [2].

Of the studied deposits, Buck Creek is the largest dunite deposit in the region. Webster, a relatively more serpentinized body, is a close second in size. Table 7 describes the size of each studied deposit. Table 8 is a summary of the compositional data, in which the average mineralogical composition for a variety of samples from each deposit has been assumed to describe the deposit as a whole. The complete non-extrapolated data set can be found in Appendix A.

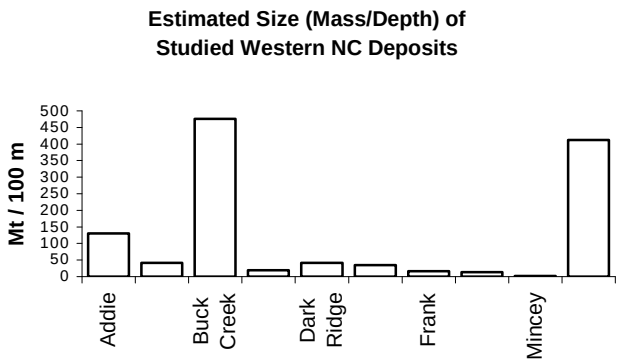

Figure 9.

Ore Body	Surf. Area km^2	Density g/cm^3	Mass/depth Mt/100 m	Est. Depth km	Est. Vol. km^3	Est. Mass Mt
Addie	0.41	3.17	129.97	0.15	0.0615	0.195
Balsam Gap	0.13	3.17	41.21	0.15	0.0195	0.062
Buck Creek	1.50	3.17	475.50	0.20	0.3000	0.951
Corundum Hill	0.06	3.17	19.02	0.13	0.0078	0.025
Dark Ridge	0.13	3.17	41.21	0.12	0.0156	0.049
Day Book	0.11	3.17	34.87	0.12	0.0132	0.042
Frank	0.05	3.17	16.48	0.13	0.0068	0.021
Micaville	0.04	3.17	13.95	0.10	0.0044	0.014
Mincey	0.01	3.17	2.22	0.05	0.0004	0.001
Webster	1.30	3.17	412.10	0.15	0.1950	0.618

Table 7. Western North Carolina deposit sizes

Ore Body	Fe avg	Mg avg	Fe/depth	CO_2 seq/depth	R(CO_2)
	wt %	wt %	Mt/100 m	Mt/100 m	
Addie	6.680	28.165	8.681	66.265	1.96
Balsam Gap	5.463	27.200	2.251	20.291	2.03
Buck Creek	7.484	28.044	35.586	241.394	1.97
Corundum Hill	5.679	28.828	1.080	9.926	1.92
Dark Ridge	6.868	28.286	2.830	21.101	1.95
Day Book	5.610	29.422	1.956	18.572	1.88
Frank	5.927	25.934	0.977	7.738	2.13
Micaville	3.861	27.562	0.539	6.959	2.00
Mincey	5.029	29.371	0.112	1.180	1.88
Webster	6.064	26.597	24.990	198.411	2.08

Table 8. Western North Carolina deposit compositions and carbon sequestration potential

Magnesium content, iron content, and densities are quite constant across the various deposits studied. The values correspond to their being primarily composed of unserpentinized dunite (most often less than 50% serpentinization). Some of these deposits are being mined currently for foundry olivine (Day Book) while others have been historically mined for vermiculite, corundum, and kaolin [2]. Talc and chromite are also often present alongside the dunite.

It is clear that of the studied deposits, Buck Creek and Webster offer the greatest potential for carbon sequestration – greatest "CO_2 seq/depth" and low "R (CO2)" values – while also offering the greatest mass of potentially recoverable iron – "Fe/depth". This follows the fact that they are the largest of the studied deposits.

III.2. Caribbean Belt

The geological boundary at which the North American and Caribbean plates meet is a source of abundant ultramafic rocks. The portion of the Caribbean belt belonging to the United States includes only the ultramafics of Puerto Rico.

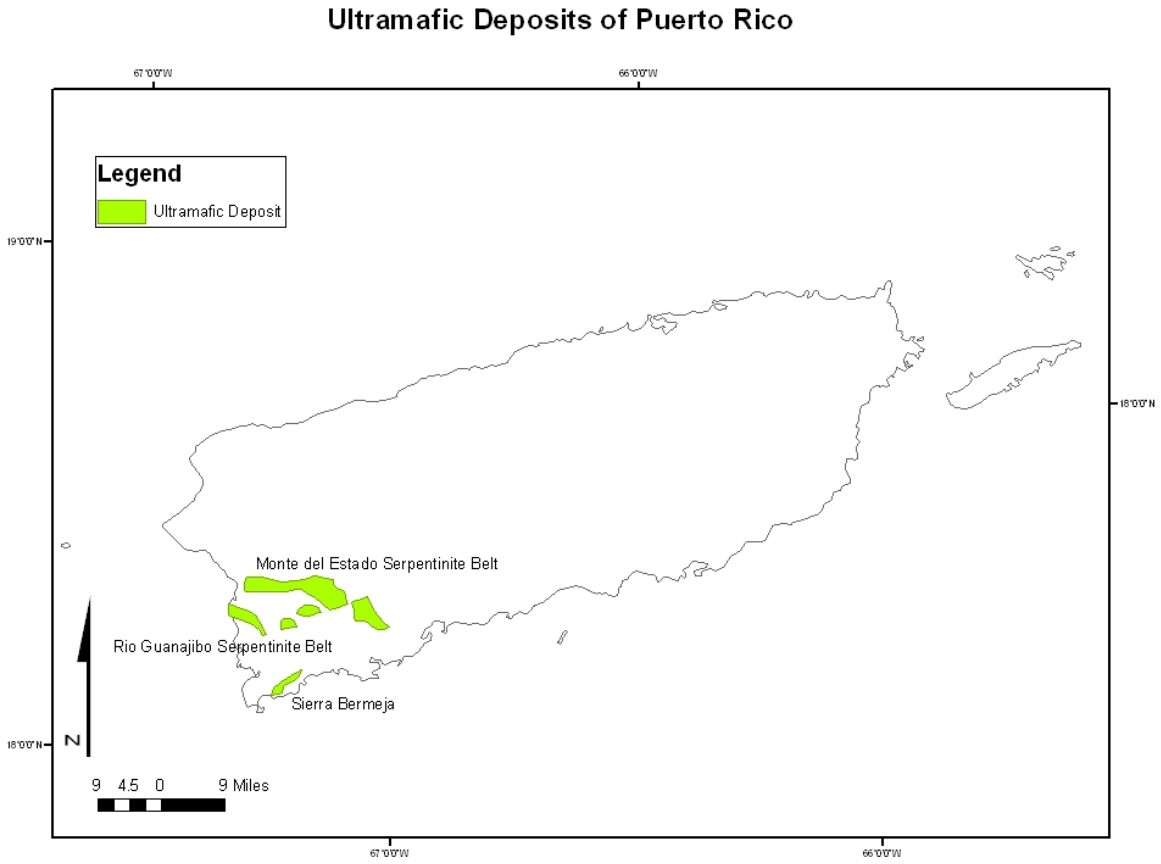

Figure 10. Ultramafic Deposits of Western Puerto Rico

III.2.A. Southwestern Puerto Rico

Puerto Rico is an island located on the boundaries of the North American and Caribbean plates, like Cuba, Haiti and the Dominican Republic. The disrupted ophiolite sequence has created subducted serpentinite in the southwest of the island, along with silicified volcanic rocks. [23] In 1961, the AMSOC core hole was drilled 305 meters deep and chemical and physical data obtained for a newly initiated deep-sea drilling program. The peridotites in Puerto Rico are highly serpentinized with less than 5% olivine by volume present. [2] The serpentinite is mainly of the lizardite-chrysotile type with no antigorite.

From a GIS geological dataset, we found the Puerto Rican ultramafics (within view in the Figure 12 map) to have an estimated maximum surface area of 165.95 km^2 [4]. The areas from literature of the three major deposits listed below sum to 109 km^2. Thus the GIS estimate is reasonable, taking into account the easternmost deposit and acknowledging that not all ultramafics will be suitable.

The Monte del Estado serpentinite belt is the largest body in Puerto Rico. Table 9 describes the size of each studied deposit. Table 10 is a summary of the compositional data, in which the average mineralogical composition for a variety of samples from each deposit has been assumed to describe the deposit as a whole. The complete non-extrapolated data set can be found in Appendix A.

Magnesium content, iron content, and densities are quite constant across the various deposits studied. The values correspond to their being primarily composed of serpentinized dunite (most often more than 95% serpentinized). These deposits are not known to have been mined.

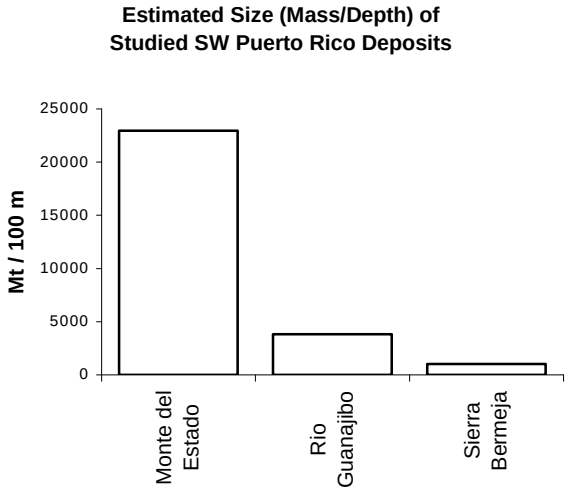

Figure 11

Ore Body	Surf. Area km^2	Density g/cm^3	Mass/depth Mt/100 m	Est. Depth km	Est. Vol. km^3	Est. Mass Mt
Monte del Estado	90.00	2.55	22950.00	1.5	135.00	344.250
Rio Guanajibo	15.00	2.55	3825.00	1.5	22.50	57.375
Sierra Bermeja	4.00	2.55	1020.00	0.2	0.80	2.040

Table 9. Southwestern Puerto Rico deposit sizes

Ore Body	Fe avg wt %	Mg avg wt %	Fe/depth Mt/100 m	CO_2 seq/depth Mt/100 m	R(CO_2)
Monte del Estado	5.423	22.194	1244.619	9220.490	2.49
Rio Guanajibo	5.424	21.772	207.466	1507.517	2.54
Sierra Bermeja	6.690	21.772	68.238	402.004	2.54

Table 10. Southwestern Puerto Rico deposit compositions and carbon sequestration potential

It is clear that the Monte del Estado belt offers the greatest potential for carbon sequestration – greatest "CO_2 seq/depth" and low "R (CO2)" values – while also offering the greatest mass of potentially recoverable iron – "Fe/depth". This follows the fact that it is the largest of the studied deposits.

IV. Ultramafics of the Western United States

IV.1 Overview

The ultramafic deposits of the western United States, comprising of the states of California, Oregon, and Washington hold the largest deposits of both olivine and serpentine in the United States. They have been mined extensively both for asbestos, as in the New Idria deposit in southern California, and olivine to be used as foundry sand, as in the quarries at Twin Sisters Washington.

Overwhelmingly, the Klamath-Trinity deposits of the Josephine Ophiolite and Trinity Ultramafic Sheet on the California-Oregon border provide the largest potential source of material, although they are located almost entirely within national forests and the ease of exploitation is uncertain. Other deposits mentioned are sufficiently large to take the output of a conventional steel or power plant for decades.

The expired asbestos mine in New Idria, CA (southern coastal ranges) is a particularly desirable location because of its past history of exploitation. Del Puerto may also be attractive due to its proximity to large sources of CO_2. The Twin Sisters Dunite deposit in Oregon may also be attractive due to its history of exploitation, as well as being a large and pure source of olivine, which is more easily reacted with CO_2 than serpentine.

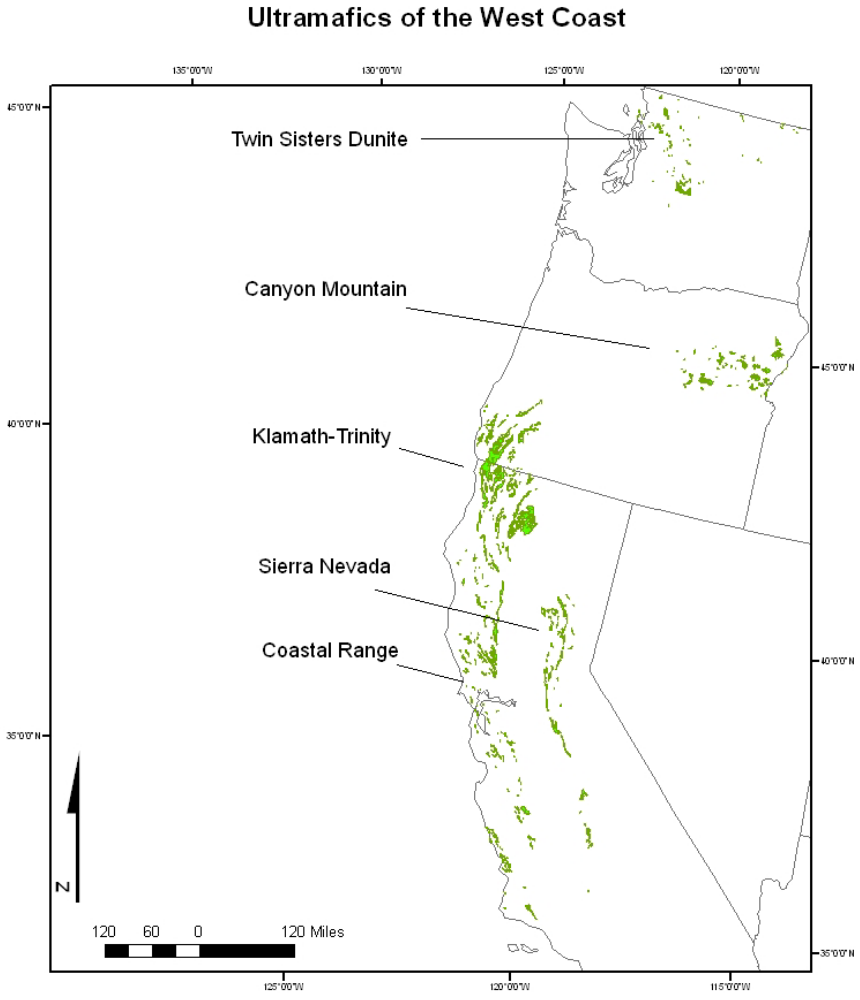

Figure 12. Ultramafic Deposits of the Western United States (Green)

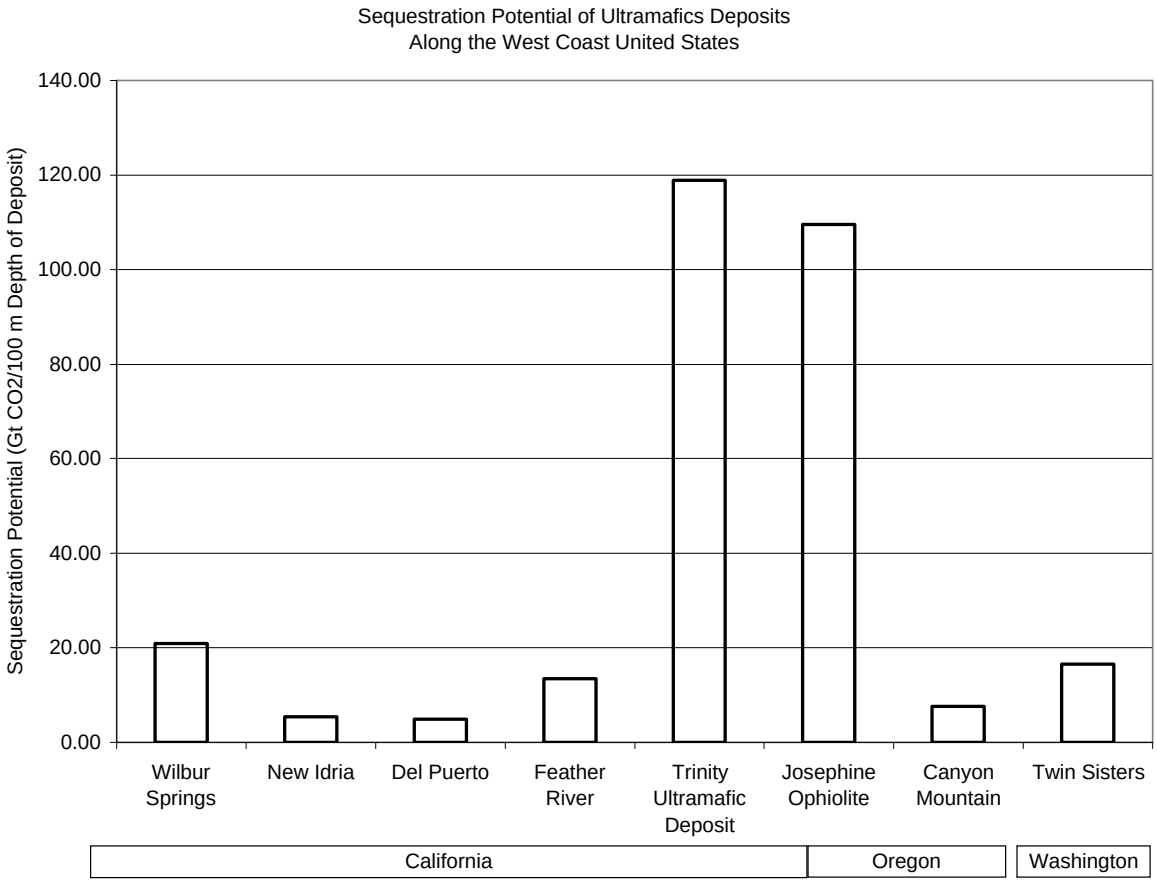

Figure 13. Sequestration potential of large ultramafic bodies in the Western United States ultramafics

IV.2 California and Oregon

IV.2.A Overview and Geologic History

The ultramafic deposits of California and Oregon are associated with ophiolite sequences deposited from the late Paleozoic to the upper Jurassic. The time periods over which the ophiolites were deposited can be separated into 4 sections- The Paleozoic, the Triassic, the lower or middle Jurassic, and the upper Jurassic [49]. The age of deposits trends from old to young as location runs from east to west. Thus, in many locations, the deposits may be described by their age alone. There are some locations, the Klammoth-Trinity region explicitly, in which the deposits of multiple time-periods are collected.

In terms of locality, the events that resulted in the deposit of the ophiolite sequences, created 4 mountainous geomorphic regions in which the deposits lie. The Sierra Nevada is the easternmost ultramafic belt in California, and likewise the deposits are the oldest. Here, the emplacement of most are estimated to have occurred during the lower to upper Paleozoic. The Canyon Mountain ophiolite in Eastern Oregon is of similar age. The Coast Ranges of California represents a large exposure of ophiolite ranging in age from the upper Jurassic to Cretaceous. The large deposits of ultramafics in the Klamath-Trinity area represent deposits spanning the entire time series from lower Paleozoic in the east (Trinity) to middle and upper Jurassic in the west (Josephine Peridotite).

IV.2.B Deposits of the Coast Ranges

The ultramafic deposits of the Coast Ranges are part of an assemblage of eugeosynclinal rocks deposited during the time period from the late Jurassic to the late Cretaceous. The largest masses are tabular parallel to the rock and were likely deposited as serpentine as indicated by high levels of shearing and little peripheral metamorphism. In the tabular masses, peridotite is generally completely serpentinized. Ultramafics in the southern examples of this assemblage exist as plug-like intrusions. These tend to have large quantities of dunite that are peripherally metamorphosed to serpentine. The most common variety of serpentine occurring in the coastal ranges is pervasively sheared, but another kind consists of interlocking tablets of true antigorite. This type is harder and tougher than most serpentinite. It is formed by the recrystallization of one of the other kinds of serpentine [40].

1. Wilbur Springs

The Northern Coast ranges is home of the largest ultramafic body. It is a sill-like mass running approximately 70 miles northwest to southeast along the western side of the Sacramento Valley. The mass ranges from less than a mile to 5 miles in width [40]. The Wilbur springs deposit is associated with this mass. With 200 km^2 of surface area [39] it is the largest body characterized below. The land occupied by the serpentinite belongs to the U.S. Bureau of Land Management and some cattle ranches [55].

2. Del Puerto

In the southern Coastal Ranges, dunite occurs in the central parts of the plug-like Cazadero, Burro Mountain, Red Mountain, and Del Puerto masses. These contain large amounts of unserpentinized peridotite and dunite (the Del Puerto deposit has greater around 25% unaltered dunite). The Del Puerto deposit has been mined for magnesite, cinnabar, pyrolusite, and chromite.

3. New Idria (Coalinga)

The larger New Idria plug consists of wholly serpentinized and generally sheared ultramafic rock. The deposit is located in Fresno and San Benito Counties, 25 miles northwest of Coalinga California. This location is notable not only in its size but for the fact that it has been heavily mined for quicksilver [41] and asbestos [42]. The Coalinga deposit has more than 50% asbestos content and was once responsible for 1/3 of the total U.S. production of asbestos. It has been reported that the Union Carbide Corporation was producing 75,000 tons of powdered asbestos per year before operations ceased in 1977. Tailings piles currently cover a 20 acre area [43].

The Major Ore Bodies are outlined below:

Ore Body	Surf. Area (km^2)	Density (g/cm3)	Mass/ depth (Gt/100m)	Depth (km)
Wilbur Springs	>200	2.65	53	.2-2
Del Puerto	40	2.73	12.5	.3
New Idria	50	2.5	10.9	>.6

Table 11. Coastal Range Deposit Sizes

Ore Body	Fe (wt %) avg	Mg (wt %) avg	Total Fe (Gt/100m depth)	CO2 seq (Gt /100m depth)	R (CO2)
Wilbur Springs	5.82	21.83	3.08	20.95	2.53
Del Puerto	6.12	24.91	.67	4.92	2.22
New Idria	5.46	24.1	.68	5.45	2.29

Table 12. Coastal Range Deposit Composition and Carbon Sequestration Potential

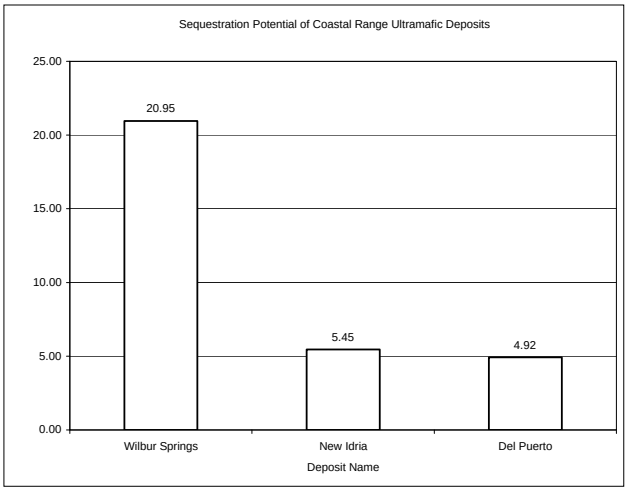

Figure 15. Sequestration potential of ultramafics in the Coastal Range, a subset of western California and Oregon ultramafics (directly proportional to surface area of the deposits due to their similar compositions)

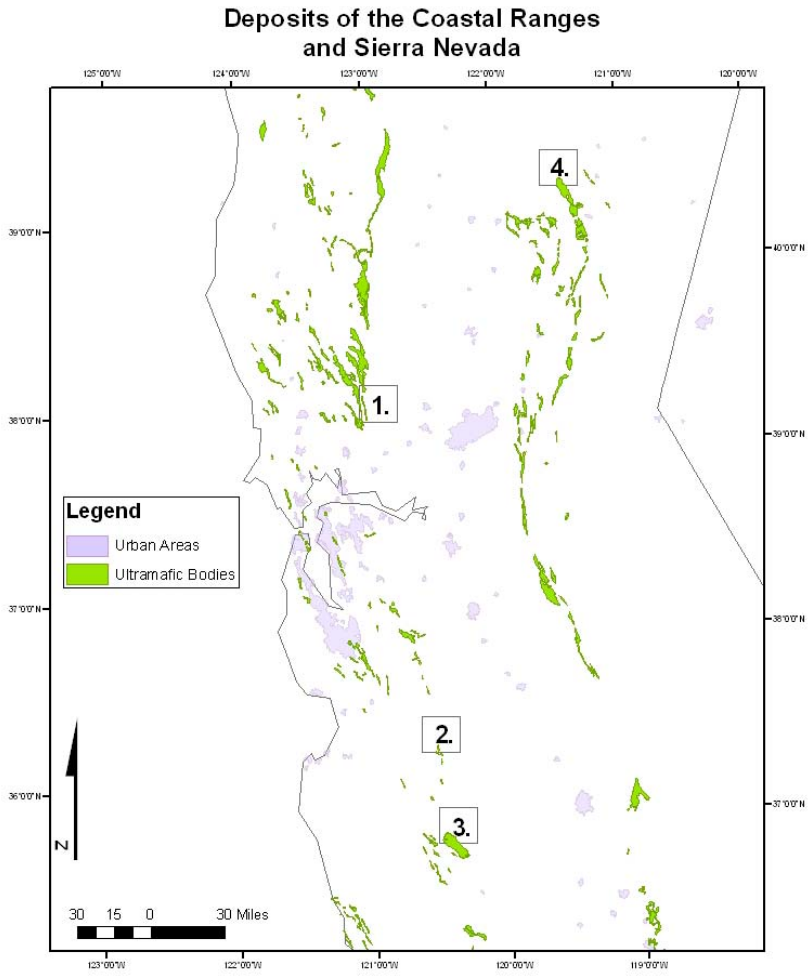

Figure 16. Ultramafic Deposits of the Coastal Ranges and Sierra Nevada 1. Wilbur Springs 2. Del Puerto 3. New Idria 4. Feather River

IV.2.C Deposits of the Sierra Nevada

It is generally thought that the emplacement of ultramafic bodies in the eastern Sierra Nevada took place sometime during the upper to lower Paleozoic (45). Relatively little research has been performed on the ultramafic bodies of the Sierra Nevada compared to their counterparts in the Klamath-Trinity region or the California Coastal Ranges. Nonetheless the major ultramafic deposit of the Sierra Nevada, the Feather River Ultramafic body of the Northern Sierra Nevada, could represent a large source of both olivine and serpentine.

4. Feather River

The Feather River ultramafic body is an elongate mass of metamorphosed dunite and harzburghite. The surface exposure ranges between 3 and 6 km wide and 54 km long. The deposit is located along the northernmost part of the Melones fault zone.

The ultramafic body is made of dunite and peridotite partly to completely altered to serpentine, tremolite, anthophylite, chlorite, and talc [46]. Because of the lack of geological and industrial study on the sites, there are no estimates as to the general mineralogical makeup of the body throughout its length. Ehrenberg [46] provides an analysis of the northernmost section of the deposit, which is approximately 25% dunite and 25% serpentinite. Taking these values as representative for the entire mass, we obtain the

tables describing the characteristics. This, however, can only be taken as a very loose approximation, and we simply hope to underscore that the size of the deposit warrants further investigation.

Ore Body	Surf. Area (km^2)	Density (g/cm3)[1]	Mass/ depth (Gt/100m)	Depth / th (km)
Feather River	100	2.5	25	unknown

Table 13. Sierra Nevada Deposit Sizes

Ore Body	Fe (wt %) avg	Mg (wt %) avg	Total Fe (Gt/500m depth)	CO2 seq (Gt /100m depth)	R (CO2)
Fearther River	7.29	29.86	1.8	13.5	1.85

Table 14. Sierra Nevada Deposit Composition and Carbon Sequestration Potential

IV.2.D The Klamath-Trinity Region

The Klamath Mountains of Northwestern California and southwestern Oregon, contain the largest concentrated deposits of ultramafic rocks in the country. The bulk of the rock here exists in two in two deposits- the Trinity Ultramafic Sheet of the Eastern Klamath Mountains and the Josephine Peridotite of the western Klamath mountains. Together, they cover over 1,500 km^2 of surface area.

The Trinity Ultramafic body is dated as Paleozoic in origin and correlated tectonically with the Feather River Ultramafic body of the Sierra Nevada [49]. The Josephine Ophiolite, being farther west, represents events from the late Jurassic. It is hypothesized that the Josephine ophiolite formed in a Late Jurassic back-arc basin [47]. The petrography of the Josephine ophiolite is very similar to that of the Wilbur Springs/Burro Mountain deposit in the northern coast ranges of California.

1. The Trinity Ultramafic Sheet

The Trinity Ultramafic Sheet is located in the Eastern Klamath Mountains and covers an area of roughly 40 by 50 km. The surface area of exposure is estimated at approximately 1,170 km^2 contained within a several massive deposit. Studies indicate that much of the area is highly serpentinized, but give no overall estimate as to the distribution of serpentine minerals within the deposit.

2. The Josephine Peridotite

The Josephine peridotite stretches more than 120km north-south across the western border of California and Oregon. The body ranges greatly from a few kilometers to upwards of 20 kilometers in thickness in the section closest to the border. It contains over 800 km^2 of surface area distributed among 5 deposits, each with areas greater than 50 km^2 [47, 49, 50].

The chemical and mineralogical characteristics come from a study performed in the Vulcan Peak area of the deposit [49]. Here it is asserted that primary minerals harzbhurgite and dunite are generally 30-50% serpentinized and that of the remaining, approximately 10% exists as dunite in concordant and discordant layers.

[1] Because the entirety of the deposit has not been characterized, a lower bound of 2.5 g/cc is taken i.e. assuming that the entire deposit has been serpentinized.

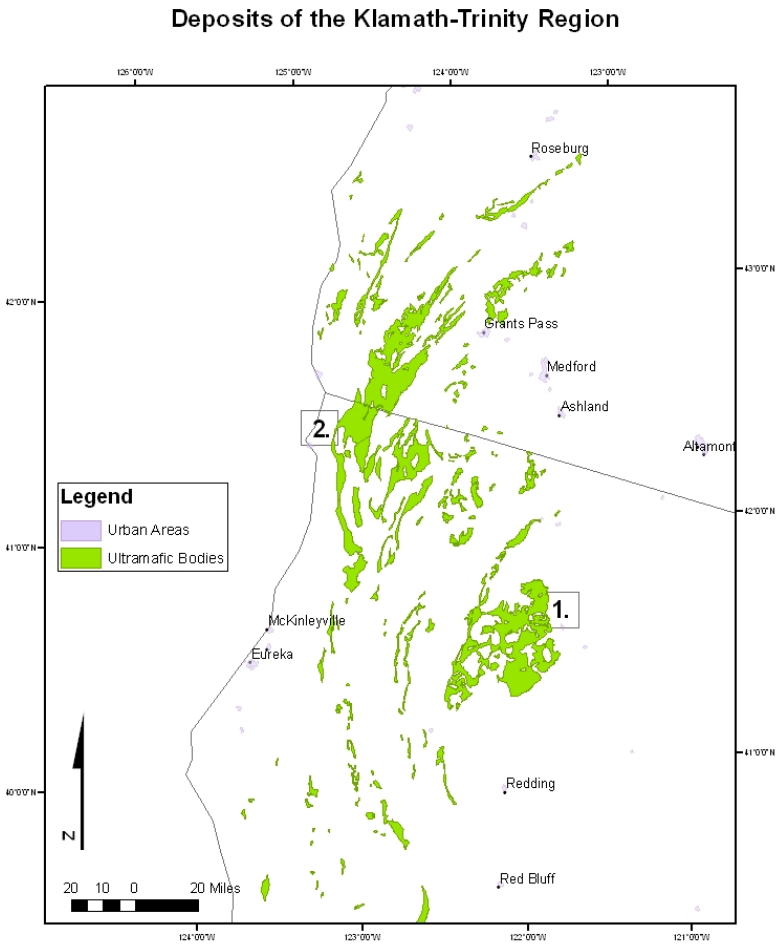

Figure 17. Ultramafic Deposits in the Klamath Trinity Region

Ore Body	Surf. Area (km^2)	Density (g/cm3)	Mass/ depth (Gt/100m)	Depth (km)
Josephine Ophiolite	800	2.9	1,160	Unknown
Trinity Ultramafic Deposit	1170	2.5	1,460	Unknown

Table 15. The Klamath-Trinity Region Deposit Sizes

Ore Body	Fe (wt %) avg	Mg (wt %) avg	Total Fe (Gt/100m depth)	CO2 seq (Gt /100m depth)	R (CO2)
Josephine Ophiolite	6.09	26.08	14.1	109.5	2.12
Trinity Ultramafic Deposit	4.56	22.46	13.3	118.92	2.46

Table 16. The Klamath-Trinity Region Composition and Carbon Sequestration Potential

IV.2.E The Canyon Mountain Complex

The Canyon Mountain complex lies in Eastern Oregon forming the western half of the Strawberry Range. The ultramafic section of the deposit covers an area of about 156 km^2. The olivine and serpentine rich section of the complex forms an east-west band in the northernmost section of the deposit covering approximately 50% of the real extent of the complex. This section, in turn consists 90% of rocks with high content olivine and serpentine.

Ore Body	Surf. Area (km^2)	Density (g/cm3)	Mass/ depth (Gt/100m)	Depth / th (km)
Canyon Mountain	156	2.5	19.5	Unknown

Table 17. The Canyon Mountain Complex Deposit Size

Ore Body	Fe (wt %) avg	Mg (wt %) avg	Total Fe (Gt/100m depth)	CO2 seq (Gt /100m depth)	R (CO2)
Canyon Mountain	5.46	21.46	1.06	7.58	2.57

Table 18. The Canyon Mountain Complex Composition and Carbon Sequestration Potential

IV.3 Washington State and the Twin Sisters Dunite

This deposit lies about 60 miles north of Seattle and 22 miles east of Bellingham. Its surface exposure is approximately 90 km^2 of material that is more than 90% dunite. The material has been extensively mined as a foundry sand [51].

Ore Body	Surf. Area (km^2)	Density (g/cm3)	Mass/ depth (Gt/100m)	Depth / th (km)
Twin Sisters	90	3.3	29.7	.6

Table 19. Twin Sisters Dunite, Washington State, Deposit Size

Ore Body	Fe (wt %) avg	Mg (wt %) avg	Total Fe (Gt/100m depth)	CO2 seq (Gt /100m depth)	R (CO2)
Twin Sisters	3.89	30.76	1.15	16.5	1.80

Table 20. Twin Sisters Dunite, Washington State, Composition and Carbon Sequestration Potential

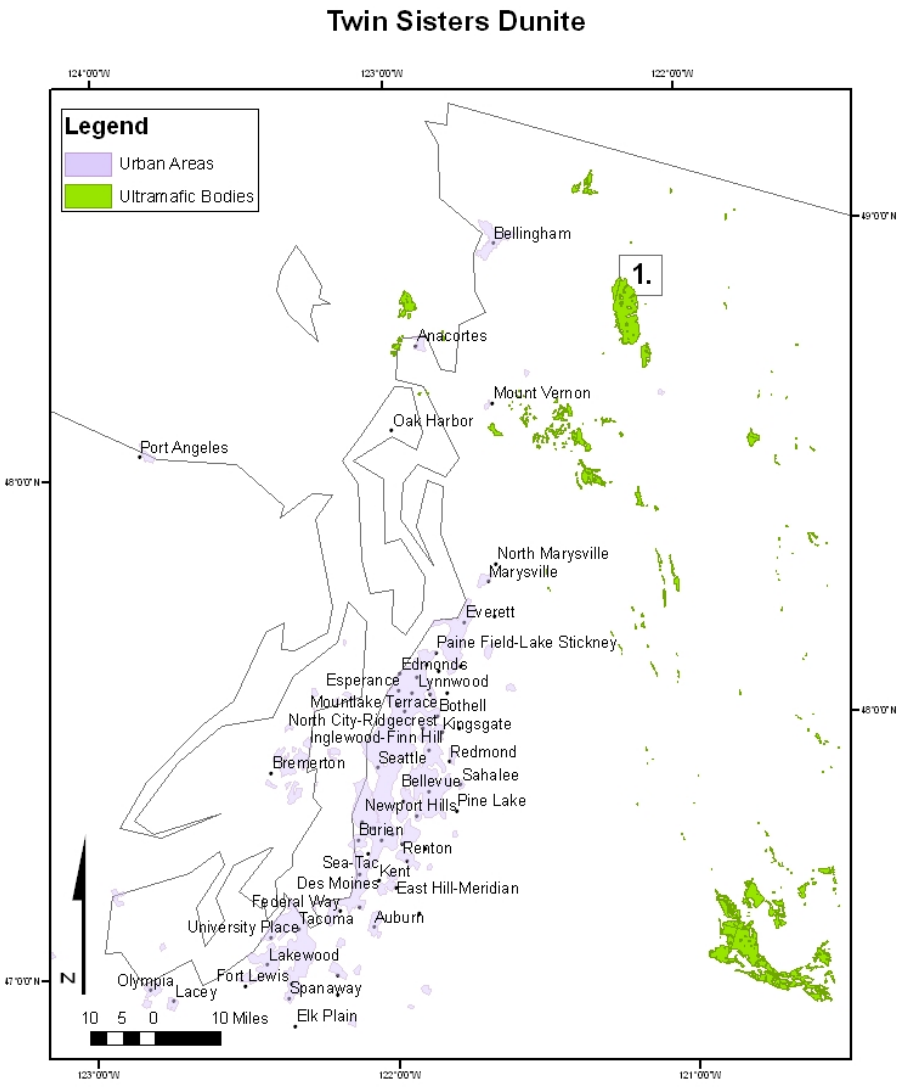

Figure 18. Location of the Twin Sisters Dunite Deposit

V. Conclusion and Ongoing Work

In this project it has been shown that the ultramafic coverage of the United States is sufficiently large to sequester century's worth of the CO_2 output of the United States.

That major land-use categorizations do not influence this conclusion is testament to the ubiquity of ultramafic material. Individual operations will be subject to the political and environmental conditions on the local level. In addition, any deposit that may be potentially used for an industrial scale operation must be surveyed via the standard techniques of ore body analysis used in the mining industry. Such feasibility studies and ore body estimations should be performed when the prospect of a pilot operation becomes likely. The geological studies referenced herein, however, provide a firm basis from which to target a particular location.

Ongoing work to augment this study will include expanding the dataset to cover the ultramafic distribution of the world. In addition to this, it will be useful to identify those locations, such as in New Idria, California and Belvidere Mountain, Vermont where the tailings piles of asbestos or metal mining operations are made of ultramafic material. These locations will most likely be the most appealing for an initial pilot operation as: no further mining will be necessary, the reactant mineral has already been ground, and the tailings piles are often seen as a hazardous waste if they contain chrysotile (asbestos). Finally, a database of CO_2 emissions from point sources in the United States has been obtained and can provide useful information about sources of CO_2. As expected, mineral resources is sufficient in the coastal regions to accommodate any fraction of CO_2 coming from these sources.

Appendix A

Compositional analyses of 56 serpentine- and olivine-bearing ultramafic rock sample sets representing all of the major depositional areas in the United States. Note: each sample set is comprised of numerous sample analyses.

State	Ore Body	Ore Type	# of analyses	Sample ID Number	FeO (wt %)	Fe_2O_3 (wt %)	Total Fe (wt %)	MgO (wt %)	Mg (wt %)	Ref
Montana	Stillwater	Hzbgite+Dunite	26	ST-AVE	6.54	2.94	7.14	29.00	17.49	3
California	Cazadero	Hzbgite		PCC-1 STD	5.06	2.72	5.84	43.43	26.19	3
California	Del Puerto	Dunite	1	UM96-19	4.68	4.72	6.94	46.43	28.00	3
California	Del Puerto	Dunite		66R22	5.00	2.80	5.84	46.10	27.80	3
California	Del Puerto	Hzbgite		66R20	7.00	0.80	6.00	43.00	25.93	3
California	Del Puerto	Serpentinized Perid.	8	DPS-AVE	4.74	3.23	5.94	42.50	25.63	3
California	Del Puerto	Serpentinite (Massive)	8	UM96-26	1.88	5.49	5.30	34.70	20.93	3
California	San Mateo	Serpentinite (Sheared)	15	FG96-312	0.00	8.92	6.24	33.06	19.94	1
California	Wilbur Springs	Serpentinite		um96-3	1.38	6.80	5.83	34.61	20.87	1
California	Wilbur Springs	Serpentinite		um96-13	3.53	4.58	5.95	36.85	22.22	1
California	Wilbur Springs	Serpentinite	4	WSS-AVE (Avg of 15 Samples)	2.94	5.06	5.82	36.20	21.83	1
Oregon	Canyon Mtn	Hzbgite	11	CM-AVE	4.69	2.49	5.39	35.60	21.47	3
Oregon	Vulcan Peak	Dunite+Hzbgite	13	VP-AVE	6.93	1.52	6.45	45.50	27.44	3
Oregon	Vulcan Peak	Hzbgite		1VP68	7.80	0.52	6.43	45.30	27.32	3
Oregon	Vulcan Peak	Dunite		19VP68	9.80	1.10	8.39	47.40	28.59	3
Washington	Twin Sisters	Dunite		Rock Std. (DTS-1 STD)	6.97	1.03	6.14	49.59	29.91	1
Washington	Twin Sisters	Dunite		UNIM	0.00	7.68	5.37	48.01	28.96	1
PA / MD / DC	Baltimore Cplx	Serpentinite	3	BCS-AVE	2.43	6.17	6.20	35.09	21.16	1
PA / MD / DC	Cedar Hills	Serpentinite	1	Brownish-green	0.38	6.77	5.03	38.70	23.34	2
PA / MD / DC	Cedar Hills	Serpentinite	1	Greenish-black	1.42	5.68	5.08	42.00	25.33	2
PA / MD / DC	Chaote Mine	Serpentinite	1	Greenish-gray	0.28	7.64	5.56	38.40	23.16	2
PA / MD / DC	Delight	Serpentinite	1	Mottled gray	1.36	6.00	5.25	38.60	23.28	2
PA / MD / DC	Delight	Serpentinite	1	Banded dolomite-bearing	3.27	2.53	4.31	36.70	22.13	2
PA / MD / DC	Penn-Mar	Serpentinite	1	Greenish-black	1.39	4.94	4.54	41.90	25.27	2
PA / MD / DC	Rockville	Serpentinite	104	Avg from all samples around quarry	2.50	5.10	5.51	37.70	22.74	2
PA / MD / DC	Rockville	Serpentinite	2	Avg of 2 analyses on dense, black serpentinite	2.16	5.53	5.55	39.10	23.58	2
Vermont	Barnes Hill	Serpentinite (Massive)	1	B-DDH-9B1-432	2.25	5.93	5.90	38.30	23.10	2
Vermont	Belvidere Mtn	Dunite	3	BM-AV	8.90	0.00	6.92	48.30	29.13	1
Vermont	Belvidere Mtn	Serpentinite	3	BMS-AVE	14.10	0.00	10.96	38.00	22.92	1
Vermont	Belvidere Mtn	Dunite	2	Average of 2 samples	3.50	2.30	4.33	48.50	29.25	2
Vermont	Belvidere Mtn	Serpentinite (bulk)	2	Average of 2 bulk samples	14.30	0.00	11.12	36.90	22.25	2

State	Ore Body	Ore Type	# of analyses	Sample ID Number	FeO (wt %)	Fe_2O_3 (wt %)	Total Fe (wt %)	MgO (wt %)	Mg (wt %)	Ref
Vermont	Belvidere Mtn	Serpentinite	9	Average of 9 samples	2.50	2.70	3.83	39.40	23.76	2
Vermont	Belvidere Mtn mine tailings	Serpentinite	1	TC1T (Krevor, Graves, Rappold, Matter; May 2005)	0.00	7.78	5.44	39.10	23.58	–
Vermont	East Dover	Assuming 55% olivine, 44% antigorite, 1% chromite		Zone 1	5.47	0.00	4.25	46.20	27.86	2
Vermont	East Dover	Assuming 80% olivine, 16% antigorite, 1% chromite, 3% magnetite		Zone 2	8.05	0.00	6.26	48.40	29.19	2
Vermont	East Dover	Assuming 30% olivine, 65% antigorite, 1% chromite, 4% magnetite		Zone 3	5.95	0.00	4.63	43.70	26.36	2
Vermont	East Dover	Dunite	18	average of 18 samples	7.57	0.00	5.88	51.78	31.23	36
Vermont	Ludlow	Dunite	6	average of 6 samples	7.51	0.00	5.84	51.40	31.00	36
Vermont	Mad River	Serpentinite (Schistose)	1	MR-103	4.46	3.85	6.16	37.11	22.38	2
Vermont	Mad River	Serpentinite (massive)	1	MR-13	0.00	8.20	5.74	32.80	19.78	2
Vermont	Waterbury	Serpentinite (massive)	1	W-DDH-13-65	5.22	1.07	4.81	37.14	22.40	2
North Carol.	Addie	Dunite	9	fresh & partly serpentinized	0.00	9.55	6.68	46.70	28.16	2
North Carol.	Balsam Gap	Dunite	6		0.00	7.81	5.46	45.10	27.20	2
North Carol.	Buck Creek	Dunite	1		0.00	10.70	7.48	46.50	28.04	2
North Carol.	Corundum Hill	Dunite	6		0.00	8.12	5.68	47.80	28.83	2
North Carol.	Dark Ridge	Dunite	2		0.00	9.82	6.87	46.90	28.29	2
North Carol.	Day Book	Dunite	5		0.00	7.60	5.32	48.80	29.43	2
North Carol.	Day Book	Dunite	1		6.56	1.15	5.90	48.77	29.41	2
North Carol.	Frank	Dunite	7		4.71	3.24	5.93	43.00	25.93	2
North Carol.	Micaville	Dunite	9		0.00	5.52	3.86	45.70	27.56	2
North Carol.	Mincey	Dunite	20		0.00	7.19	5.03	48.70	29.37	2
North Carol.	Webster	Dunite	3		0.00	8.67	6.06	44.10	26.60	2
SW Puerto Rico	Monte del Estado	Serpentinite	1	serpentinized harzburgite, 5% relict orthopyroxene and olivine	1.92	5.05	5.02	37.10	22.38	2
SW Puerto Rico	Monte del Estado	Serpentinite	6	average of 6 serpentinites	1.47	6.12	5.42	36.80	22.19	2
SW Puerto Rico	Rio Guanajibo	Serpentinite	2	average of 2 serpentinites	1.39	6.21	5.42	36.10	21.77	2
SW Puerto Rico	Sierra Bermeja	Serpentinite	1	single sample	1.94	6.69	6.19	36.10	21.77	2
SW Puerto Rico	AMSOC Hole	Serpentinite	13	normalized average	2.80	4.81	5.54	37.67	22.72	2
SW Puerto Rico	Monte del Estado	Serpentinite	1	sheared detrital serp	1.40	5.46	4.91	37.80	22.80	2

APPENDIX B- Geologic Vocabulary

Alpine- Mountain belts created as one continent moves under another. The top of the subducting continent is scraped off and forms the assemblage of the alpine belt.

Concordant Contact- The planar contact of an intrusion that follows the bedding of the country rock

Dike- A planar body of intrusive rock that has discordant contacts with the surrounding rock

Discordant Contact- A contact that cuts across bedding or foliation planes, such as the contact between a dike and country rock

Dunite- A rock that is > 90% by volume olivine.

Eugeosyncline- The oceanic part of a *geosyncline*, characterized by volcanism associated with clastic sedimentation

Geosyncline- A major downwarp in the Earth's rust, usually more than 100km in length, in which sediments accumulate to thicknesses of many kilometers. The sediments may eventually be deformed and metamorphosed during a mountain-building episode.

Harzburgite- A rock consisting of > 10 vol% orthopyroxene with the remainder mostly olivine.

Olivine- Name given to the orthosilicate with the chemical formula $(Mg,Fe)_2SiO_4$. Forsterite is the name given to a pure Mg_2SiO_4 mineral and Fayalite to a pure Fe_2SiO_4 mineral. There is a liquidus in composition between the two and the chemical composition of the mineral is generally given as Fo_x referring to Forsterite of X percentage Mg (or 1-X percentage iron substitution for Mg).

Ophiolite- A rock association consisting of ancient oceanic crust; usually exposed along subduction zones and ancient continental margins. A complete ophiolite sequence consists of a basal slab of mantle peridotite overlain by gabbroic intrusive bodies, basaltic dikes and lavas, pillow basalt, chert, argillaceous siltstone, and fine-grained oceanic sediment.

Peridotite- The name applied to rocks that contain both olivine and pyroxenite.

Serpentine- Generic name for the three Mg-rich, silicate minerals antigorite, chrysotile, and lizardite. Lizardite and chrysotile share the same ideal chemical formula, while that for antigorite differs slightly. The ideal formula is $(Mg,Fe)_3Si_2O_5(OH)_4$ and the mineralogy is a phylosilicate, or sheet silicate.

Serpentinite- Ultramafic rock that has undergone any amount of serpentinization.

Serpentinization- The process whereby primary mantle rocks such as dunite and harzburgite react chemically with water to form serpentine. This is also generally referred to as 'weathering'.

Sill- A horizontal tabular intrusion with concordant contact

Ultramafic Rocks- Igneous rocks with iron and magnesium content such that they are composed of <45% SiO_2. Ultramafic rocks are composed principally of one or more of the common magnesium-iron silicate minerals olivine, pyroxene, serpentine, and less commonly amphibole.

APPENDIX C- Methodology for Calculation of Ultramafic Resources and References to Digital Data

Ultramafic coverage was created by selecting from the geological datasets as described in the table C.1. Each separate dataset resulting from this operation was then re-projected into the projection North America Albers Equal Area Conic and geographic coordinate system GCS North American 1983. This re-projection was performed as well on the Federal Lands, Urban Lands, and Indian Lands datasets. Next, the clip operation was performed on Federal Lands, Urban Lands, and Indian Lands using the ultramafic coverage as the input shape (Figure 1).

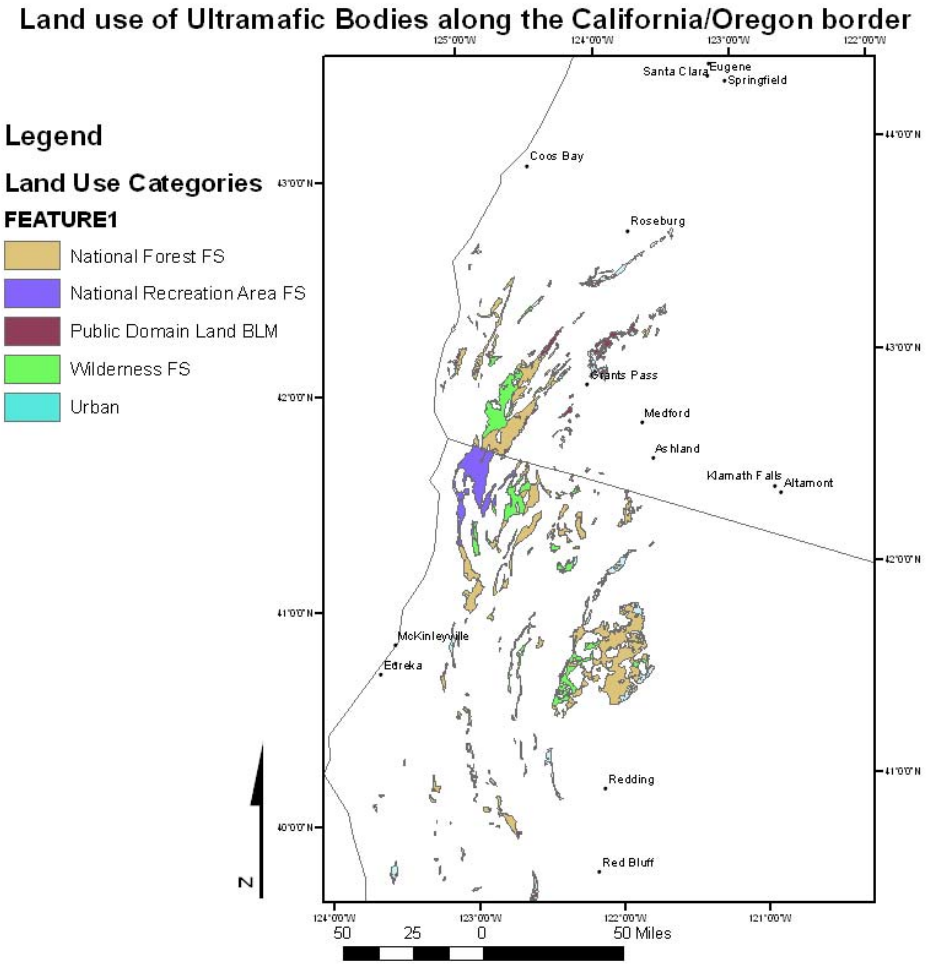

Figure 19. Map Showing various datasets clipped with the shape of the ultramafic deposits

All areas were calculated using ArcGIS functions.

Analysis Methodology- West Coast Example

Collectively, the ultramafic deposits of the west coast cover a surface area of over 8,500 km^2 and offer the potential to sequester centuries of the entire nation's output of CO_2.

State	Surface Area (km^2)
CA	5.79E+03
OR	2.57E+03
WA	3.73E+02
Total	8.73E+03

Overlaying Federal Lands, urban areas, and Indian Reservations datasets, one can account for 78% of the surface area of ultramafic lands. Furthermore, 5 categories of land jurisdiction make up nearly all of that coverage: Forest service National Forests, Forest Service Wilderness, Public Domain Land, National Recreation Areas and Null.

Land Jurisdiction	**Surface Area (km^2)**	**% Area of Total UM**
Air Force DOD	3.39E+00	0.04%
Army Corps of Engineers DOD	1.40E+00	0.02%
Army DOD	1.37E+01	0.16%
Bureau of Reclamation BOR	6.56E+00	0.08%
Indian Reservation	2.57E+01	0.29%
National Forest FS	3.61E+03	41.29%
National Monument BLM	4.01E-01	0.00%
National Park NPS	3.89E+00	0.04%
National Recreation Area FS	5.07E+02	5.81%
National Recreation Area NPS	4.86E+00	0.06%
National Scenic Area FS	2.30E+01	0.26%
Null	4.05E+02	4.63%
Public Domain Land BLM	8.16E+02	9.34%
Wilderness BLM	1.25E+01	0.14%
Wilderness FS	1.27E+03	14.49%
Wilderness NPS	4.27E-01	0.00%
Wilderness Study Area BLM	7.48E+01	0.86%
Urban	3.09E+01	0.35%
Total	**6.80E+03**	**77.87%**

Out of all of these categories, the following were deemed to be un-exploitable:

Land Jurisdiction	**km^2**	**% Area of um**
Air Force DOD	3.39E+00	0.04%
Army DOD	1.37E+01	0.16%
Indian Reservation	2.57E+01	0.29%
National Monument BLM	4.01E-01	0.00%
National Park NPS	3.89E+00	0.04%
National Recreation Area FS	5.07E+02	5.81%
National Recreation Area NPS	4.86E+00	0.06%
National Scenic Area FS	2.30E+01	0.26%
Wilderness BLM	1.25E+01	0.14%
Wilderness FS	1.27E+03	14.49%
Wilderness NPS	4.27E-01	0.00%
Wilderness Study Area BLM	7.48E+01	0.86%
Urban	3.09E+01	0.35%
Total	**1.97E+03**	**22.52%**

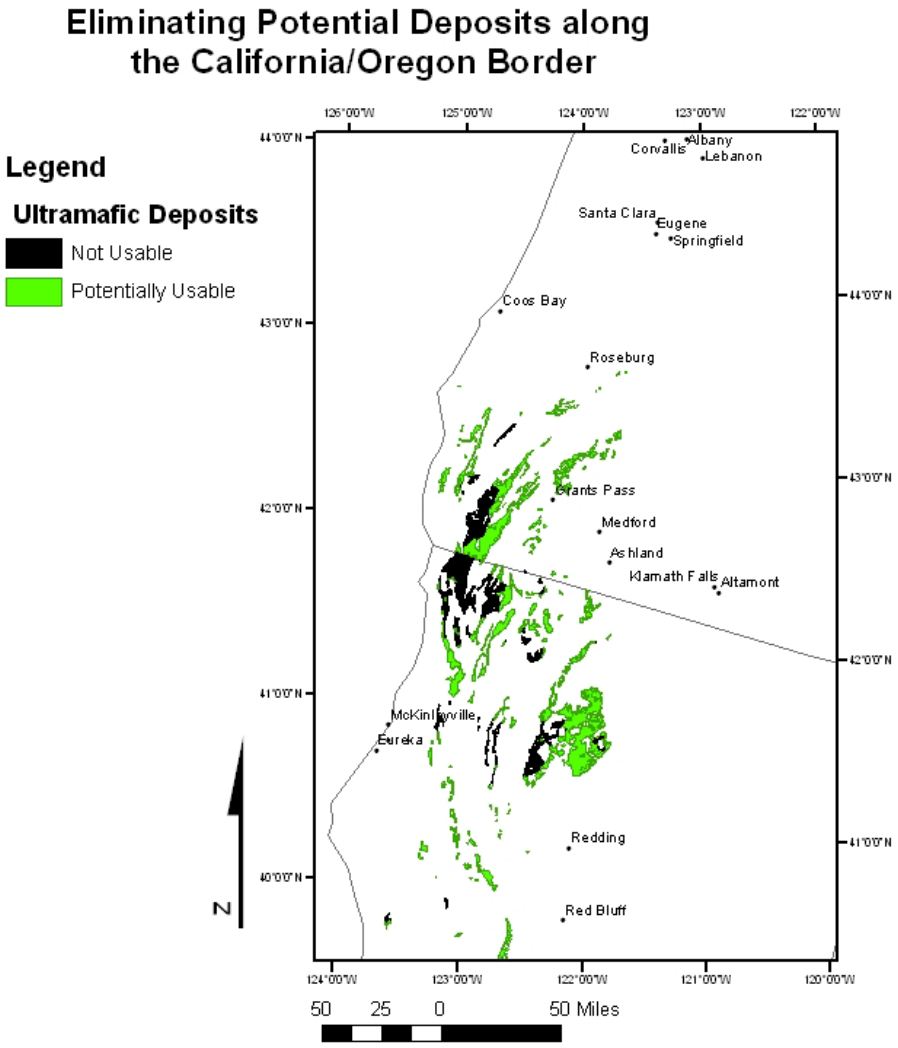

Figure 20. Potentially usable (green) and non-usable (black) land coverage of ultramafic deposits

A power plant producing 350 tons of CO_2 per hour will require 8.1 Mt of magnesium silicate annually. The minimum depth that was found ascribed to a particular mineral deposit was 50 meters (.05 km). If we require that a deposit of this depth be able to sequester this output of CO_2 for 15 years, then we can create a lower bound on the suitable surface exposure of a deposit at 1 square kilometer[2]

After eliminating all un-exploitable surface coverage as well as deposits smaller than 1 km^2 in surface exposure, the ultramafic distribution is:

STATE	area (km^2)	% Orig
CA	4.54E+03	78.42%
OR	1.92E+03	74.89%
WA	2.12E+02	56.73%
Total	**6676.6634**	**76.45%**

[2] [(120 Mt mineral)/(2,500 Mt/km^3)] / .05km = .96 km^2

Taking a mineral density of 2.5 g/cc and an $R(CO_2)$[3] value of 2.1, and an average depth of .5 km[4], we obtain values for mineral mass and CO_2 sequestration potential:

STATE	Total Mineral mass (Mt)	Sequestration Potential (Gt CO2)	Years US Output
CA	5.68E+06	2703.188639	443
OR	2.40E+06	1145.068314	187
WA	2.64E+05	125.9474527	20
Total	**8.35E+06**	**3974.204406**	**650**

[3] $R(CO_2)$ is the simply the ratio of mineral mass to CO_2 required to sequester the CO_2.
[4] While the minimum depth found was .05 km, many of the deposits were estimated to be well greater than 1 km in depth and it is estimated that .5km is below average depth.

Table C.1 Sources of Digital Data

State/ Region	Scale (1:…)	SQL command (SELECT * FROM … WHERE) used in ArcGIS to Extract Ultramafic data	Obtained from
Caribbean	2,500,000	"DESCRPTN" like '%ltramaf%'	http://greenwood.cr.usgs.gov/energy/WorldEnergy/OF97-470K/graphic/data.html
Coterminous U.S.	2,500,000	"ROCK" like '%ltramaf%'	http://pubs.usgs.gov/dds/dds11/
New England	100,000-500,00	"ROCK_GPB" = 'Ultramafic Rocks' *(re-represents Maine, Mass, Connecticut, Vermont)*	http://pubs.usgs.gov/of/2003/of03-225/
Alabama	250,000	"ROCK_TYPE" = 'Mafic-Ultramafic Rocks'	http://www.gsa.state.al.us/gsa/GIS/geologydetails.html http://www.gsa.state.al.us/gsa/GIS/DATA.html
Alaska	see above	"GEOLOGY" like '%ltramaf%' *in geol_regions/usa_noncoterm_AK-HI-PR-VI*	http://pubs.usgs.gov/atlas/geologic/
California	750,000	"PTYPE" = 'um'	Reference 5. Jennings
Connecticut	50,000	"DEFINITION" like '%ltramaf%' *…note: this is the same as using fields Litho1 or Litho2…*	http://dep.state.ct.us/gis/Data/data.asp
Delaware	Not Yet Constructed	Digital Dataset has not yet been constructed	http://www.udel.edu/dgs/dgsdata/GeoGIS.html
Georgia	500,000	"GEOLCODE" = 'mp3' OR "GEOLCODE"= 'um'	https://gis1.state.ga.us/index.asp?body=preview&dataId=13899
Maine	500,000	"UNIT" = 'CA9c' OR "UNIT" = 'S9c' OR "UNIT" = 'SZ9c' *note:* *"CA9c","Cambrian ultramafic rocks"* *"S9c","Silurian ultramafic rocks"* *"SZ9c","Silurian - Precambrian Z ultramafic rocks"* *(there are also gabbro/ultramafic areas, see units descriptions)*	

Maryland	2,500,000	See coterminous usa dataset	http://www.mgs.md.gov/indexdata.html
Mass	500,000-100,000	"ROCK_GPB" = 'Ultramafic Rocks' *…note: this is the same as* *"LITHO_CODE"= 50* *where 50 : "ultramafic rocks; includes serpentinites, dunites, peridotites, and tremolite-talc schists associated with other ultramafic rocks"*	http://www.mass.gov/mgis/ftpstate.htm via http://www.mass.gov/mgis/
Montana			Not Obtained
New Jersey	100,000	Preparation: fix projection by doing Define Projection: `NAD_1983_StatePlane_New_Jersey_FIPS_2900_Feet` via: *Projected Coord Systems > NAD 1983 (Feet) > NAD 1983 StatePlane New Jersey FIPS 2900 (Feet).prj* & then Project to North_America_Albers_Equal_Area_Conic "LITHOLOGY" like '%serp%'	http://www.state.nj.us/dep/njgs/pricelst/index.htm
North Carolina	250,000	GEO_NAME" = 'PzZu' …where PzZu = 'Meta-ultramafic Rock' from metadata	http://www.geology.enr.state.nc.us/
Oregon	500,000	"PTYPE" = 'ju' OR "PTYPE" = 'TRv' OR "PTYPE" = 'TRPzu'	http://geology.wr.usgs.gov/docs/geologic/or/oregon.html
Pennsylvania	250,000	"LITH1" = 'Serpentinite'	http://www.dcnr.state.pa.us/topogeo/map1/bedmap.aspx
Rhode Island	See Caribbean		http://www.edc.uri.edu/rigis-spf/Statewide/state.html#geology
South Carolina	See Coterminous U.S.		http://www.dnr.sc.gov/geology/DigitalMapping.htm
Texas	Not Obtained		Not Obtained

Vermont	250,000	“SUB_CATEGO” = 8	http://www.vcgi.org/dataware/?page=./search_tools/search_action.cfm&query=theme&theme_id=008-0005
Virginia	Not Obtained		
Washington	100,000	Multiple depending on quadrangle See metadata of the dataset	http://www.dnr.wa.gov/geology/dig100k.htm
West Virginia	No ultramafics		http://wvgis.wvu.edu/data/dataset.php?action=search&ID=197

VI. References

General ultramafic references:

1. Goff, F. and K. S. Lackner (1998). "Carbon dioxide sequestering using ultramafic rocks." Environmental Geosciences **5**(3): 89-101.
2. Goff, F., G. Guthrie, et al. (2000). "Evaluation of Ultramafic Deposits in the Eastern United States and Puerto Rico as Sources of Magnesium for Carbon Dioxide Sequestration." **LA-13694-MS**.
3. Lackner, K. S., D. P. Butt, et al. (1997). Carbon Dioxide Disposal in Mineral Form: Keeping Coal Competitive. Los Alamos, New Mexico, Los Alamos National Laboratory: 90.

GIS data sets:

4. Schruben, Paul G., Arndt, Raymond E., Bawiec, Walter J., King, Philip B., and Beikman, Helen M., 1994, *Geology of the Conterminous United States at 1:2,500,000 Scale -- A Digital Representation of the 1974 P.B. King and H.M. Beikman Map*: U.S. Geological Survey Digital Data Series DDS-11, U.S. Geological Survey, Reston, VA. http://pubs.usgs.gov/dds/dds11/
5. Saucedo, G.J., D.R. Bedford, G.L. Raines, R.J. Miller, C. M. Wentworth 2000 *GIS Data for the Geologic Map of California—A Digital Representation of the 1977 C.W. Jennings, R.J. Strand, and T.H. Rogers Map: Geologic Map of California,* California Department of Conservation Division of Mines and Geology
6. http://www.nationalatlas.gov
7. Walker, G.W., and N.S. MacLeod 1991 *Geologic Map of Oregon* U.S. Geological Survey- http://geopubs.wr.usgs.gov/docs/geologic/or/oregon.html
8. Harris, C.F.T, (1998) "1:100,000 Scale Digital Geology of Washington State" Washington State Department of Natural Resources Division of Geology and Earth Resources http://www.dnr.wa.gov/geology/dig100k.htm

PA-MD-DC Region:

9. Larrabee, D.M., 1969. Serpentinite and rodingite in the Hunting Hill quarry, Montgomery County, Maryland. U.S. Geol. Surv. Bull. 1283, 1–34.
10. Linder, D.E., Wylie, A.G., and Candela, P.A., 1992. Mineralogy and origin of the State Line talc deposit, Pennsylvania: Economic Geology 87:1607–1615.
11. Pearre, N.C., and Heyl, A.V., 1960. Chromite and other mineral deposits in serpentine rocks of the Piedmont Upland, Maryland, Pennsylvania, and Delaware: U.S. Geol. Surv. Bull. 1082-K, 707–833.
12. Thomas, L. M., Jr. and R. D. Doctor (200X). "Carbonate Sequestration And Co2 Pipeline Logistics For The Pjm Region."

Western North Carolina Region:

13. Astwood, P., Carpenter, J., and Sharp, W., 1972. A petrofabric study of the Dark Ridge and Balsam Gap dunites, Jackson County, North Carolina: Southeast. Geol., 14:183–194.
14. Carpenter, J.R., and Chen, H.S., 1978. Petrology and bulk rock chemistry of the Frank ultramafic body, Avery County, N.C., and associated other ultramafic rock bodies of the southern Appalachians: Southeast. Geol., 19:21–25.
15. Condie, K.C., and Madison, J.A., 1969. Compositional and volume changes accompanying progressive serpentinization of dunites from the Webster-Addie ultramafic body, North Carolina: American Mineralogist, 54:1173–1179.
16. Hahn, K.R., and Heimlich, R.A., 1977. Petrology of the dunite exposed at the Mincy Mine, Macon County, North Carolina: Southeast. Geol., 19:39–53.
17. Honeycutt, F.M., and Heimlich, R.A., 1979. Petrology of the Balsam Gap dunite, Jackson County, North Carolina: Southeast. Geol., 21:251–260.

18. Kingsbury, R.H., and Heimlich, R.A., 1978. Petrology of an ultramafic body near Micaville, Yancey County, North Carolina: Southeast. Geol., 20:33–46.
19. Kulp, J.L., and Brobst, D.A., 1954. Notes on the dunite and the geochemistry of vermiculite at the Day Book dunite deposit, Yancey County, North Carolina: Economic Geology, 49:211–220.
20. Miller, R., 1953. The Webster-Addie ultramafic ring, Jackson County, North Carolina: American Mineralogist, 38:947–958.
21. Yurkovich, S.P., 1977. The Corundum Hill dunite, Macon County, North Carolina: Southeast. Geol., 19:55–68.
22. Lipin, B.R., 1984. Chromite from the Blue Ridge province of North Carolina: Am. J. Sci., 284:507–529.

Puerto Rico:
23. Peter Humphrey Mattson - Geology of the Mayagueez area, Puerto Rico - Geological Society of America Bulletin (1960), 71(3):319-361
24. Field Trip: Recent Tectonics and Paleoseismology in Western Puerto Rico / May 3-4, 2003 / Seismological Society of America
25. Burk, C.A. (ed.), 1964. A study of serpentinite: the AMSOC core hole near Mayagüez, Puerto Rico: Nat. Res. Counc., Washington, D.C., Publication No. 1188, 175 pp.

Southeastern USA Region (N. Carolina and Georgia):
26. Carpenter, J.R., and Phyfer, D.W., 1975. Olivine compositions from southern Appalachian ultramafics: Southeast. Geol., 16:169–172.
27. Misra, K.C., and Keller, F.B., 1978. Ultramafic bodies in the southern Appalachians: A review: Am. J. Sci., 278:389–418.

Vermont & New England:
28. Chidester, A.H., 1961. Economic geology of the Belvidere Mountain asbestos area: New Eng. Intercoll. Geol. Congr., 1961 Field Trip Guide, Trip B-1, 3 pp. with map.
29. Chidester, A.H., 1962. Petrology and geochemistry of selected talc-bearing ultramafic rocks and adjacent country rocks in north-central Vermont: U.S. Geol. Surv. Prof. Pap. 345, 207 pp. with maps.
30. Chidester, A.H., Albee, A.L., and Cady, W.M., 1978. Petrology, structure, and genesis of the asbestos-bearing ultramafic rocks of the Belvidere Mountain area in Vermont: U.S. Geol. Surv. Prof. Pap. 1016, 95 pp. with maps
31. Hoffman, M.A., and Walker, D., 1978. Textural and chemical variations of olivine and chrome spinel in the East Dover ultramafic bodies, south-central Vermont: Geological Society of America Bulletin, 89:699–710.
32. Laird, J., Lanphere, M.A., and Albee, A.L., 1984. Distribution of Ordovician and Devonian metamorphism in mafic and pelitic schists from northern Vermont. American Journal of Science (May 1984), 284(4-5):376-413
33. Stanley, R.S., and Ratcliffe, N.M., 1985. Tectonic synthesis of the Taconian orogeny in western New England: Geol. Soc. Am. Bull., 96:1227–1250.
34. Baalen, M. R. V., C. A. Francis, et al. (1999). Mineralogy, Petrology, and Health Issues at the Ultramafic Complex, Belvidere Mt., Vermont, USA. Guidebook to Field Trips in Vermont and Adjacent Regions of New Hampshire and New York. S. F. Wright, Department of Geology - University of Vermont.
35. Kim, J. Magnesium Extraction from Asbestos Mine Tailings: A Report.
36. Doria, L. R. (2005). Belvidere Asbestos Mine: Site Suitability For CO2 Sequestration Through Mineral Carbonation. Department of Geology. Middlebury, Vermont, Middlebury College.
37. Coish, R.A. and Gardner, P., 2004. Suprasubduction-zone peridotite in the northern USA Appalachians: Evidence from mineral composition (Geology Department, Middlebury College): Mineralogical Magazine, v 68, n 4, August, 2004, p 699-708

California Coastal Ranges:
38. Himmelberg, G.R., and Coleman, R.G. Chemistry of Primary Minerals and Rocks from the Red Mountain-Del Puerto Ultramafic Mass, California: U.S. Geol. Surv. Prof. Paper 600-C., p. C18-C26, 1968 GEOLOGY LIBRARY-Obtained
39. McLaughlin, R.J., Ohlin, H.N., Thormahlen, D.J., Jones, D.L., Miller, J.W., and Blome, C.D., Geologic map and structure sections of the little Indian valley-wilbur springs geothermal area, northern coast ranges California: U.S> Geol. Survey Misc. Invest. Map I-1706, 1:24,000 Scale, 2 Sheets (color) -Obtained
40. Bailey, E.H., W.P. Irwin, D.L. Jones Franciscan and Related Rocks and Their Significance in the Geology of Western California, California Division of Mines and Geology, Bulletin 183 pp 177
41. Eckel, E.B, and W.B. Myers Quicksilver Deposits of the New Idria District San Benito and Fresno Counties, California in California Journal of Mines and Geology Vol. 42, January 1946
42. Mumpton, F.A., Thompson, C.S. (1975), Mineralogy and Origin of the Coalinga Asbestos Deposit in Clays and Clay Minerals Vol 23, pp. 131-143
43. Coalinga Asbestos Mine EPA #CAD9808172117 http://yosemite.epa.gov/r9/sfund/overview.nsf/0/9f395c6abcc33f428825660b007ee643?OpenDocument#descr

California- Transverse, and Sierra Ranges:
44. Paige, N.J., Serpentinization at Burro Mountain Contrib. Mineral Petrol., 14, 321, 1967
45. Saleeby, J.B (1982) Polygenetic Ophiolite Belt of the California Sierra Nevada: Geochronological and Tectonostratigraphic Development J. Geophys Res, 87, 1803-1824
46. Ehrenberg, S.N., (1975) Feather River Ultramafic Body, Northern Sierra Nevada, California Geological Society of America Bulletin, v. 86, p. 1235-1243

California-Oregon:
47. Harper, G.D., The Josephine Ophiolite, Northwestern California Geol. Soc. Amer. Bull. 95, 1009, 1984
48. Thayer, T.P., The Canyon Mountain Complex, Oregon, and some Problems of Ophiolites in (R.G. Coleman and W.P. Irwin, eds) North American Ophiolites: Oregon Dept. Geol. Mineral. Indus., Bull 95 p. 93, 1977 http://www.oregongeology.com/pub%26data/pub%26data.htm
49. Irwin, W.P. (1977) Ophiolitic Terranes of California, Oregon, and Nevada in (R.G. Coleman and W.P. Irwin, eds) North American Ophiolites: Oregon Dept. Geol. Mineral. Indus., Bull 95 p. 93, 1977
50. Himmelberg, G.R., and Loney, R.A., Petrology of the Vulcan Peak Alpine-type Peridotite, Southwestern Oregon: Geol. Soc. Amer. Bull., 84, 1585, 1973

Washington, Montana, Texas:
51. Onyeagocha, A. (1978) Twin Sisters Dunite: Petrology and Mineral Chemistry Geological Society of America Bulletin, v. 89, p. 1459-1474
52. Ragan, D.M. (1963) Emplacement of the Twin Sisters Dunite, Washington. Am J Sci, 261, 549-565
53. Czamanske, G.K., and Zientek, M.L., The Stillwater Complex, Montana: Geology and Guide: Montana Bureau of Mines and Geology, Spec. Pub. 92, Butte, MT, 395 p., 1985
54. Barnes, V. E., Shock, D. A., and Cunningham, W. A. (1950). Utilization of Texas serpentine (pp. 5-52). Austin TX: University of Texas, Publication, n 5020, Oct 15, 1950, 52p

Part II

Mineral Processing for Mineral Carbon Dioxide Sequestration

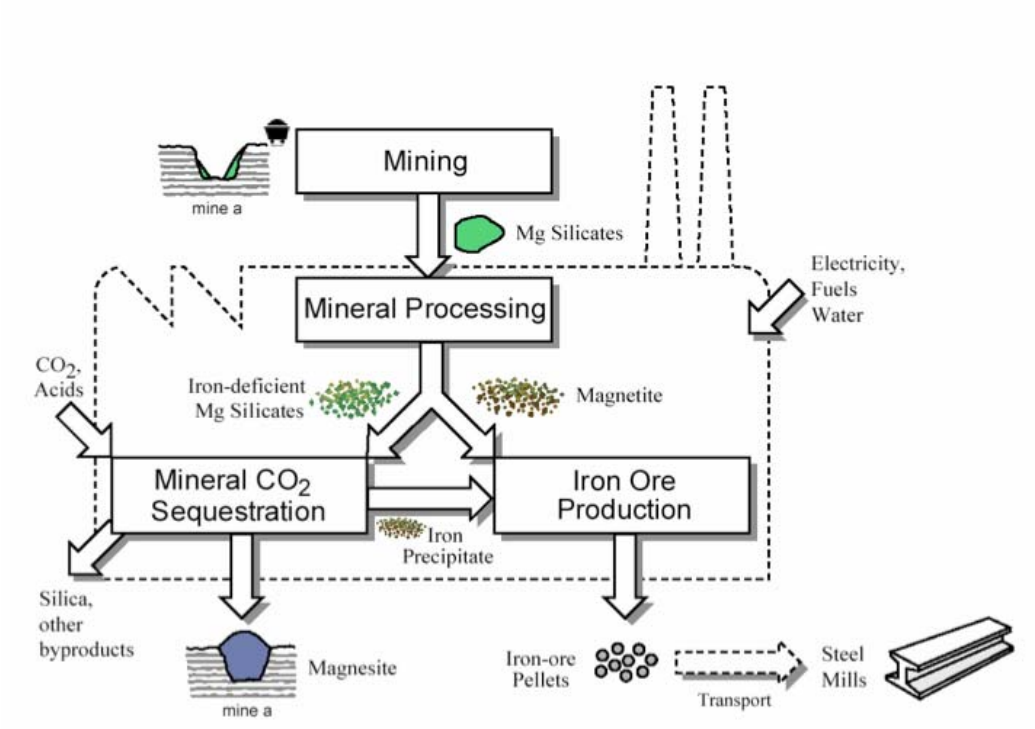

Figure 21. General schematic for a combined iron production mineral carbon sequestration process

Introduction

With this project it was proposed to develop ideas around an iron production and carbon sequestration plant that will use serpentine ores as the source of iron and dispose of its own CO_2 – plus additional CO_2 from other sources -- in the mineral tailings that are left at the end of the iron recovery process (Figure 21). By using the same ore processing steps for carbon sequestration and iron ore production we increase the value of the carbon sequestration process and consequently reduce the cost of sequestration with this added value.

Researchers have identified the magnesium silicate mineral serpentine as a potential substrate for a mineral carbon dioxide sequestration process. While iron often substitutes for magnesium in silicate minerals such as olivine (pure iron silicate olivine is known as fayalite and there is a solid solution between fayalite and forsterite, the pure magnesium silicate olivine mineral), iron is almost always found in associated oxide minerals, such as the spinel magnetite, when occurring with serpentine. This is because when magnesium silicate minerals are hydrothermally altered to produce the serpentine, the iron no longer fits in the serpentine mineral structure and must reform as an iron oxide. The presence of water in the alteration results in some oxidation of the iron from the ferric iron of the olivine to ferrous iron. As a result, almost all of the iron found in serpentine exists as magnetic iron oxide and can be easily removed once the material has been ground to the liberation size of the magnetite. Thus serpentine, both useful for a mineral carbon sequestration process, and containing relatively high concentrations of easily separable iron oxide is the mineral input of choice for this project.

The chemical processing of silicate minerals has been identified as the major barrier to the implementation of mineral carbonation as a viable carbon sequestration technology. In particular, a viable mineral carbon sequestration process utilizing serpentine has never been demonstrated due to low reaction times with carbon dioxide in aqueous solutions. Thus, in addition to a brief demonstration of the possibility of magnetically separating iron oxides from ground serpentine, this project has focused on catalyzing the process kinetics for carbonating the magnesium from ground serpentinite in aqueous media.

Magnetic Separation of Iron from Serpentinite

This research project used raw serpentine ore from the asbestos mine site at Belvidere Mountain in Essex and Lowell Counties in Vermont. The oxide composition of the material is given in table 21 below. This serpentine has a relatively high iron content for serpentinite deposits, with iron given as Fe_2O_3 constituting 7.8% by weight of the serpentine ore. SGS Mineral Services of Canada performed liberation size analysis. It was found that all of the iron is recoverable as iron oxide via grinding followed by magnetic separation if the minerals are ground to a grain size of less than 53 μm, or -270 mesh. This is in line with reported values of the liberation size of magnetite of 43 μm, or -325 mesh.

In general, the finer the input mineral is ground, the faster the overall process kinetics and as such, a requirement to grind the minerals to -270 mesh size to recover the iron oxide will only contribute to an enhancement in the subsequent CO_2 disposal process.

Thermodynamic Motivation for the Carbonation of Silicate Minerals

Magnesium and calcium carbonate minerals represent the most stable form of molecular carbon at temperature and CO_2 pressure conditions seen in the earth's crust. In other words, given a system of metal oxides and CO_2, equilibrium favors the formation of metal carbonate minerals.

$$MgO + CO_2 \rightarrow MgCO_3 + 179 \text{ kJ/mole}$$
$$CaO + CO_2 \rightarrow CaCO_3 + 118 \text{ kJ/mole}$$

In practice, calcium and magnesium oxide minerals are not readily found in nature, and the cations are far more prevalent in silicate minerals. Taking into account considerations of mineral availability, cation concentration, and reactivity, the focus of mineral carbonation research has been on rocks rich in the minerals olivine, serpentine, magnesium silicates, or wollastonite, a calcium silicate. Using the ideal formulas for these minerals, the overall carbonation reactions are at 25ºC:

$$1/3Mg_3Si_2O_5(OH)_4 + CO_2 \rightarrow MgCO_3 + 2/3SiO_2 + 2/3H_2O + 64 \text{ kJ/mole}$$
$$1/2Mg_2SiO_4 + CO_2 \rightarrow MgCO_3 + 1/2SiO_2 + 95 \text{ kJ/mole}$$
$$CaSiO_4 + CO_2 \rightarrow CaCO_3 + SiO_2 + 87 \text{ kJ/mole}$$

Several types of reactions could be considered for mineral carbonation; gas-solid, gas-melt, reaction of solids with dissolved CO2 in aqueous media, reactions of dissolved cations with dissolved CO_2 in aqueous media, reactions in media other than water, and more. As of yet, gas-solid and reactions in aqueous media have been studied on an experimental level. Rigorous theory has been developed for a process utilizing a salt melt as a reaction medium but no experimentation has been done. This research project has focused on the development of processes using an aqueous reaction medium.

Aqueous Mineral Carbonation

Processing in aqueous media has received the most attention from researchers. It has been theorized that the aqueous carbonation process follows two steps: (1) Dissolution of cations into solution followed by

(2) nucleation and growth of carbonate precipitate (Huijgen 2006, Chizmeshya 2003, Tier 2007, Guthrie 2001). Most of the evidence for the theory comes from SEM images showing the formation of magnesite and calcite crystals independent of the silicate minerals. At least one study has observed with imaging and EDS analysis that carbonate nanoparticles can form within the silicate mineral, but they do not make up a significant amount of the precipitated carbonate (Chizmeshya 2003).

As discussed below, the nucleation and growth of carbonate minerals is pH dependent as the acidity of a solution strongly controls the concentration of carbonate ion in solution. Because acidity will decrease the concentration of carbonate ion in solution, it is not possible to precipitate carbonate minerals from acidic systems i.e. solutions will always be undersaturated with respect to magnesium carbonates in acidic solutions (Figure 22).

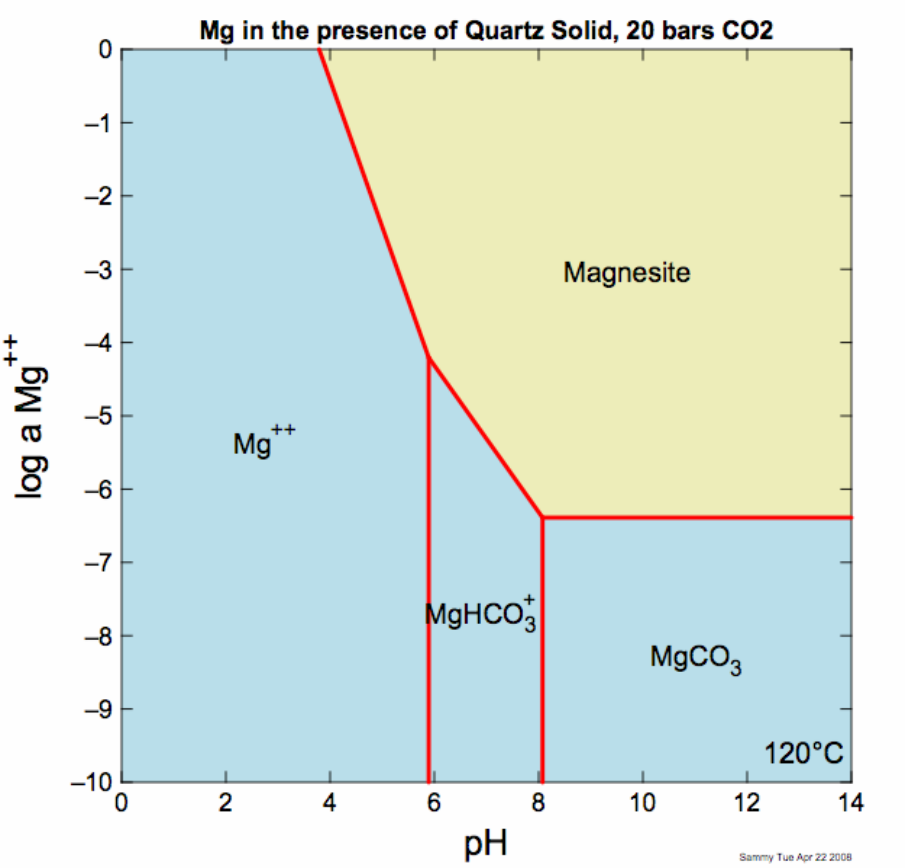

Figure 22. Solubility of $MgCO_3$ (magnesite) as a function of pH and Mg^{2+} activity in a solution at 120ºC and 20 bars of CO_2. All fields show major magnesium species; Blue indicates a species in solution and tan indicates a solid. Note, below pH 4, there is no stability field for magnesite. Diagrams produced with the Geochemist's Workbench® software package

The situation is different with regards to dissolution. Solution equilibrium will favor the dissolution of magnesium or calcium silicate minerals until the pH is strongly basic, or high concentrations of magnesium and calcium cations exist in solution (Figure 23). Thus it is possible to dissolve silicate minerals in solutions across a wide range of acid strengths, while the precipitation of carbonate minerals is only possible in neutral to basic conditions. It is generally thought that mineral dissolution kinetics (and not unfavorable equilibrium conditions) is the limiting factor in the carbonation process. Given these considerations, it is logical to search for an aqueous reaction medium that promotes the rapid dissolution of the silicate minerals under acid strengths in which solid carbonate phases are stable.

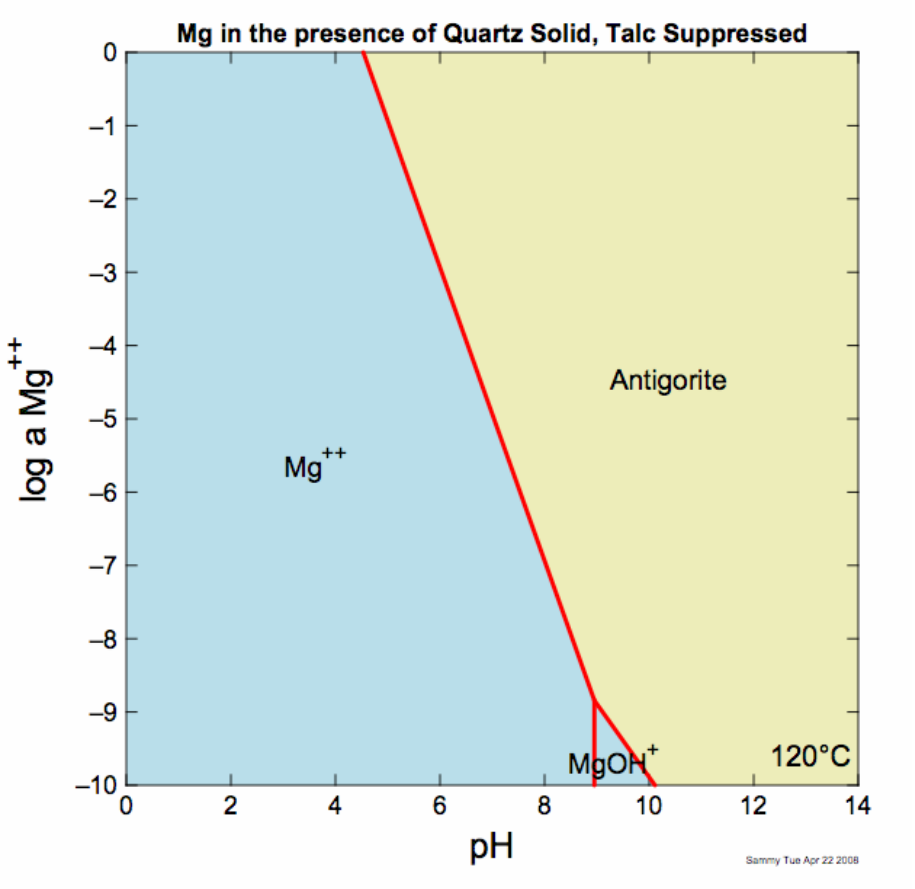

Figure 23. Solubility diagram for antigorite serpentine at 120°C as a function of pH and Mg^{2+} activity in solution. All fields show major magnesium species; Blue indicates a species in solution and tan indicates a solid. Solution is supersaturated with respect to silica. Diagram produced with the Geochemist's Workbench® software package

Aqueous Carbonation Processes Previously Developed

Direct Carbonation in Aqueous Media

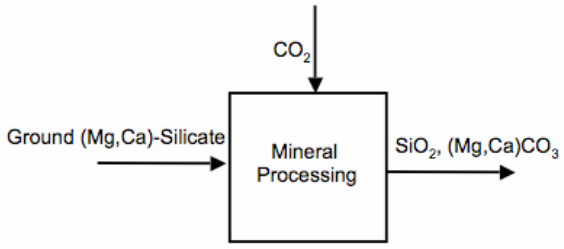

Figure 24. General schematic for the aqueous direct carbonation process

The Albany Research (NETL) - Gerdemann, O'Connor and other scientists at the Albany Research Center (now NETL) have performed the most comprehensive study of a mineral carbon sequestration pathway (Gerdemann 2007, O'Connor 2005). Performing experiments since 1998, they have focused entirely on the direct carbonation of silicate minerals in an aqueous medium. In particular they have performed over

700 tests in which a batch autoclave is filled with the slurry of mineral and reacting solution, purged with CO_2, heated to the desired temperature, and pressurized with CO_2 using a gas booster pump. Their tests were performed with serpentine, olivine, and wollastonite at a range of temperatures and CO_2 pressures. They also varied the solution composition with the addition of sodium chloride and sodium bicarbonate.

The Energy Research Center of the Netherlands (ECN) - Mineral carbonation studies at the Energy Research Centre of the Netherlands (ECN) have produced numerous studies on the carbonation of steel slag and wollastonite (Huijgen 2006). Their studies on the carbonation of wollastonite augment the work done by O'Connor et. al and demonstrate that high carbonation efficiencies can be achieved at relatively large mineral grain sizes and lower pressures of CO_2 than were achieved by the team at ARC. Specifically they are able to achieve conversion yields of 70 percent at 200 C and 20 bar CO_2 with particle sizes of less than 38μm.

Kakizawa et. Al - Kakizawa et. al, have demonstrated the use of a 2-stage process utilizing the mineral wollastonite (Kakizawa 2001). In the first stage of the process, the mineral silicate is digested by the weak acid, acetic acid. In the second stage, high pressures of CO_2 is introduced which results in the precipitation of calcium carbonate. While their reaction yields are reportedly lower than those achieved by both O'Connor and Huijgen, the reaction conditions of 60 C, atmospheric pressure, are far milder. No direct comparison has been performed on the potential for enhancing reaction yields over the conventional direct carbonation process by using such a 2-stage process.

Strong Acid pH Swing

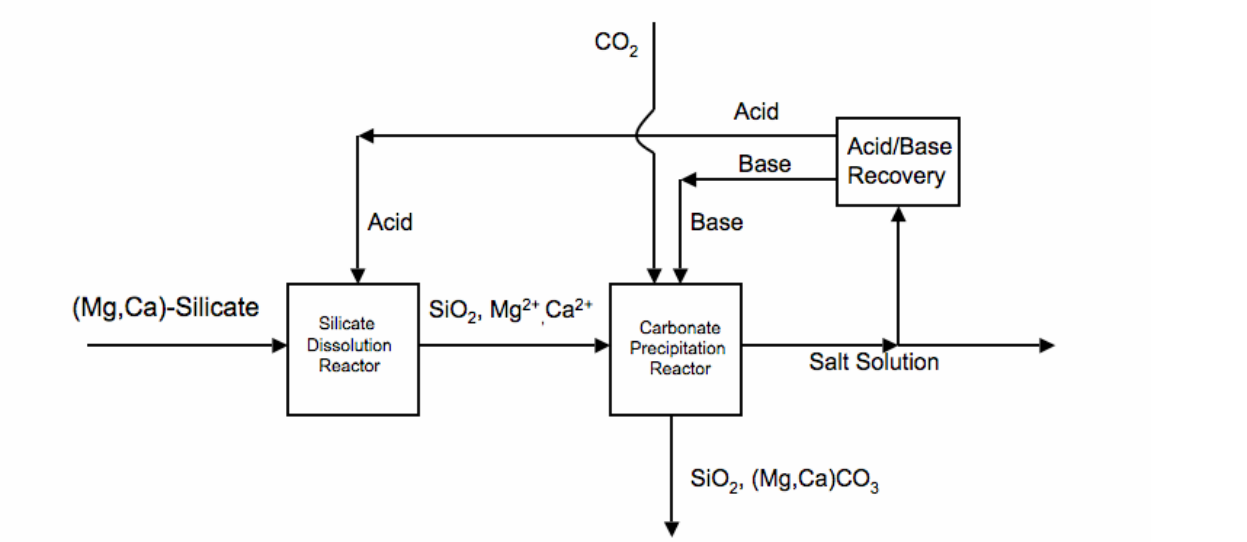

Figure 25. General schematic for an aqueous carbonation process utilizing a pH change between process steps

Pundsack et. Al - In a 1967 Patent filed by Frederick Pundsack and the Johns-Manville Corporation of New York, a process was developed for the recovery of silica gel, and magnesium oxide or magnesium carbonate from serpentine (Pundsack 1967). In the first stage the serpentine is digested using ammonium bisulfate, a strong acid, to form magnesium sulfate and ammonium sulfate. In a second stage, ammonia gas is introduced to neutralize any remaining acid, at which point CO_2 is introduced to form magnesium carbonate. The remaining ammonium sulfate brine is dehydrated to produce ammonium sulfate salt. This salt may be heated to drive off ammonia gas for recycle into the acid-neutralization step, leaving ammonium bisulfate, also for recycle into the serpentine digestion step.

Park et. Al - Following the process proposed by Pundsack et. al, Park and others at Ohio State University studied the use of a 2-stage process (Park 2004). In the first step, serpentine is dissolved in an acidic solution, as in the Pundsack process although a more effective solvent was identified. In the second stage, the pH is raised through the addition of ammonium hydroxide resulting in the precipitation of magnesium hydroxide for carbonation. No recovery method is proposed to recover the acid and base used in the process.

Maroto-Valer - Maroto-Valer and others at Pennsylvania State University have studied a process analagous to that proposed by Pundsack (Maroto-Valer 2005). In their research, they studied the use of sulfuric acid to leach magnesium from magnesium silicates. After the dissolution of the mineral, the pH of the system is raised by the addition of NaOH at which point magnesium hydroxide precipitates. They do not suggest mechanisms for the recovery of the acid and base used in the process.

Enhancing Process Kinetics for Mineral Carbonation

Because of the inherent costs associated with solvent recovery and complex multi-stage processes, this research has focused on the potential for an improvements to the direct carbonation system. Improvements were sought such that a direct carbonation process could be made functional with serpentine as a mineral input.

In a direct carbonation process, reaction solution conditions must meet requirements of being both undersaturated with respect to serpentine and supersaturated with respect to magnesium carbonate. These requirements define conditions with respect to magnesium concentration, pH, and CO_2 pressure. Figure 26 shows an example area defined by these conditions at 20 bars of CO_2 in a solution supersaturated with respect to silica.

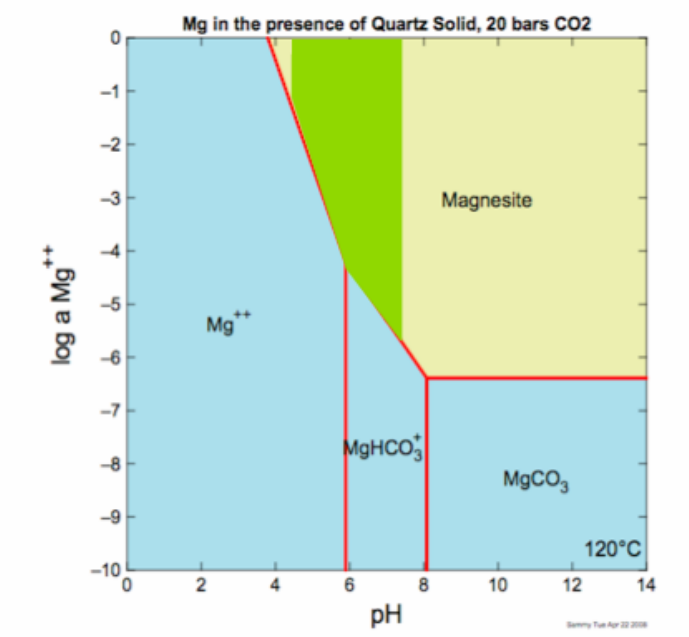

Figure 26. Solubility diagram for magnesite with green field showing example conditions in which an aqueous carbonation process could take place. Solubility of $MgCO_3$ (magnesite) as a function of pH and Mg^{2+} activity in a solution at 120°C and 20 bars of CO_2. All fields show major magnesium species; Blue indicates a species in solution and tan indicates a solid. Note, below pH 4, there is no stability field for magnesite. Diagrams produced with the Geochemist's Workbench® software package

With the pH and magnesium concentration conditions defined by the constraints of saturation levels with respect to serpentine and carbonate minerals, the acid-promoted dissolution rate of serpentine will be orders of magnitude lower than the precipitation rate of carbonate. Thus, the dissolution of the silicate minerals in weakly acidic to basic solutions can be considered the rate limiting step in the direct aqueous mineral carbonation process. As such, finding catalysts to enhance the dissolution of serpentine under these conditions was the focus of our attempts to enhance the overall process kinetics of system.

Methods and Materials

Starting material was raw antigorite serpentine ground to 90% below 75 microns in diameter, or -200 mesh. Surface area was determined using the nitrogen BET adsorption method, and was found to be 8.02 m^2/g. Analysis for major oxide content was performed by SGS Mineral Services using X-ray fluorescence and is given in Table 21.

Metal Oxide	SiO_2	Al_2O_3	CaO	MgO	Na_2O	K_2O	Fe_2O_3	MnO	TiO_2	P_2O_5	Cr_2O_3
Weight Content [%]	37.9	1.02	0.53	39.1	0.05	0.01	7.78	0.11	0.02	<0.01	0.39

Table 21. Major oxide composition of serpentinite used in experiments

About 3 grams of ground serpentine is reacted in 1 liter of fluid with dissolved NaCl, NH_4Cl, or plain distilled water in a Parr 4520 batch autoclave with temperature, pressure, and stirring control. All experiments have been performed at 120 C and under 20 bars of pressure, with either a nitrogen or carbon dioxide atmosphere. Salts are dissolved fully in solution, after which time the serpentine sample is added and the clock started. The reactor is closed and pressurized with either CO_2 or N_2.Experiments last from 6 to 24 hours and samples are drawn periodically during the experiment through a dip tube with a stainless steel 2 micron filter on the submerged end. Each sample results in a solution loss of about 5 grams and no more than 10% of the solution is drawn throughout any given experiment. Samples are analyzed for magnesium content using a Buck Instruments AA flame spectrophotometer, and results are given below.

Results

In experiments with no salts in solution, but 20 bars of CO_2 pressure, there is an initial rapid dissolution of about 6% of the material, followed by a linear dissolution rate. In experiments with NaCl, or NH_4Cl, and under a CO_2 atmosphere, there is a rapid initial phase of dissolution followed by a dissolution rate too slow for detection with our experimental procedure (Figure). The extent of the initial rapid phase of dissolution is dependent on the salt being used, with NH_4Cl leading to more dissolution than NaCl, but it is not clear that the rate itself is affected. There is no detectable difference in dissolution rate after the initial rapid dissolution stage. These results mirror results obtained by Bales and Morgan (Bales), although in their study serpentine is dissolved for hundreds of hours so that a dissolution rate in the latter slow dissolution stage can be observed.

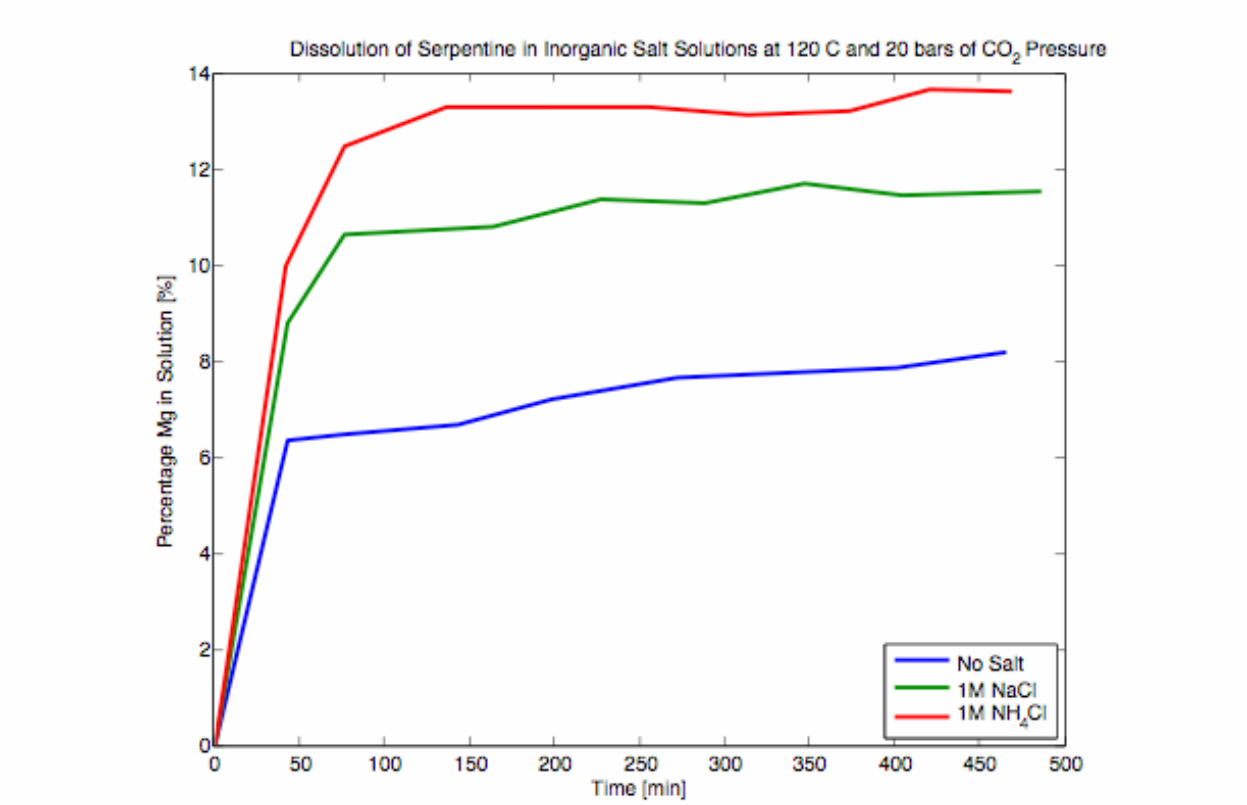

Figure 27. Results of serpentine dissolution experiments at 120°C under 20 bars of CO_2 pressure and varying salt solutions. Each experiment is characterized by a rapid initial dissolution stage followed by neglible amounts of dissolution over 6 to 8 hours

Conclusion

<u>This project was not successful in identifying a technique to accelerate direct aqueous mineral carbonation.</u>

While it is clear from the dissolution experiments in inorganic salt solutions that the presence of inorganic salts have an effect on the initial stage of dissolution, the cause of the effect is not clear. At the high concentrations of salts being used, the pH of the solutions is affected, and may in turn be affecting the initial dissolution. In any case, because of low overall dissolution yields resulting from an inability to affect the latter slow stage of dissolution, dissolution of serpentine in these systems is of little interest for an industrial scale mineral carbon sequestration process.

It is clear that a catalytic solvent must be found for the use of serpentine in a direct aqueous carbonation process. It does not appear, however, that sodium chloride or ammonium chloride solutions provide a sufficient dissolution rate enhancement to significantly alter the cost of a process utilizing serpentine.

References

Chizmeshya, A.V.G. and M. J. McKelvy and G. H. Wolf and R. W. Carpenter and D. A. Gormley *Enhancing the Atomic-Level understanding of CO2 mineral sequestration mechanisms via advanced computational modeling* Technical Report Arizona State University Center for Solid State Science

Gerdemann S.J., W.K. O'Connor, D.C. Dahlin, L.R. Penner, H.Rush 2007 *Ex Situ Mineral Carbonation* Environmental Science and Technology 41:2587-2593

Guthrie, G.D., J.W. Carey, D. Bergfeld, S. Chipera, H. Ziock, K. Lackner 2007 *Geochemical Aspects of the Carbonation of Magnesium Silicates in Aqueous Medium* Technical Report Los Alamos National Laboratory

Huijgen, W.J.J., G. Witkamp, R.N.J. Comans 2006 *Mechanisms of aqueous wollastonite carbonation as a possible CO2 sequestration process* Chemical Engineering Science 61:4242-4251

Kakizawa, M., A. Yamasaki, Y. Yanagisawa 2001 *A New CO_2 Disposal Process Via Artificial Weathering of Calcium Silicate Accelerated by Acetic Acid* Energy 26:341-354

Maroto-Valer, M.M., D.J. Fauth, M.E. Kuchta, Y. Zhang, J.M. Andresenn 2005 *Activation of Magnesium Rich Minerals as Carbonation Feedstock Materials for CO_2 Sequestration* Fuel Processing Technology 86:1627-1645

O'Connor, W.K., D.C. Dahlin, G.E. Rush, S.J. Gerdemann, L.R. Penner 2005 *Aqueous Mineral Carbonation Final Report* Technical Report Albany Research Center

Park, A.A., L. Fan 2004 *CO_2 Mineral Sequestration: Physically Activated Dissolution of Serpentine and pH Swing Process* Chemical Engineering Science 59:5241-5247

Pundsack, F.L. 1967 *Recovery of Silica, Iron Oxide and Magnesium Carbonate from the Treatment of Serpentine with Ammonium Bisulfate* U.S. Patent 3,338,667

Teir, S., H. Revitzer, S. Eloneva, C. Goelholm, R. Zevenhoven 2007 *Dissolution of Natural Serpentinite in Mineral and Organic Acids* International Journal of Mineral Processing 83:36-46

Part III

Mass Flow of Iron from Serpentine to Steel

1. Introduction

An advantage of mineral sequestration of CO_2 using serpentinite rock is the potential use of iron minerals present in the rock. Chemical processing of serpentine in the rock will create magnesite, $MgCO_3$, by conversion of Mg silicates in serpentine. During this process other minerals that do not accept CO_2 are expected to remain and eventually be disposed along with magnesite. The past and present studies show that serpentinite rocks contain iron minerals mostly in the form of magnetite, Fe_3O_4, and hematite Fe_2O_3. In addition to iron minerals, some serpentinite rocks contain chromites as well, which may be significant if they are also recoverable with iron minerals. As a byproduct of the sequestration process these iron minerals can be used in the steel making process. Of particular interest to this study is the recovery of iron values prior to chemical processing of rock for CO_2 acceptance. Magnetite is easily recoverable by means of magnetic separation methods without any chemical pretreatment. The only prerequisite is that magnetite mineral particles are separated from non-magnetic minerals by crushing and grinding. In this study we assume that the sequestration plant is located at the mine site to avoid transportation of large tonnages of rock, and return of waste back to the mine, as opposed to pipeline transport of CO_2 from the steel plant and other sources to the mine site. Transportation of serpentine rock may also be problematic due to its possible asbestos content. In the model we provide options for user inputs for distances and unit transportation costs regarding the location of the steel plant and external CO2 source so as to allow for exploration of various specific alternatives in this regard. We assume that the processing and sequestration plants are at the mine site. The following is a brief discussion of the processes involved in recovery of iron values and its potential impact on the operation of a steel plant.

2. System Structure

The entire system of steel making and CO_2 sequestration can be considered an integrated entity which sequesters its own emissions of CO_2, and utilizes some of the solid waste as input to the process. There are four major components: Steel plant, Serpentinite mine, Sequestration plant and iron recovery (processing) plant (Figure 28). We consider the steel plant as a “black box” in which steel making takes place. The inputs are iron ore or pellets, and coal, and outputs are steel products and concentrated CO_2 stream, and solid waste. The mine is typically a surface mine similar to a rock quarry at which the serpentinite rock is mined and sent to the sequestration plant. The mine will have the facility to accept the solid waste from the sequestration plant for permanent and safe disposal. The iron recovery plant (magnetic separation and pelletizing processes) receives the run-of-mine (ROM) rock (ORE) and separates the magnetic iron minerals by magnetic separation. It may also receive some amount of iron precipitate from the sequestration plant to mix with the magnetite recovered from ROM rock. This mixture is pelletized and sent to the steel plant. In the computer model we separate these functions by considering a processing plant where crushing, grinding and magnetic separation takes place. We refer to this plant as the processing plant. The concentrate containing magnetite and iron precipitate from the sequestration plant are sent to the pelletizing plant. The sequestration plant processes the serpentinite rock to produce magnesium carbonates by reacting CO_2 from the steel plant and the serpentine. The plant may also produce some quantity of iron precipitates to be sent to the iron recovery plant.

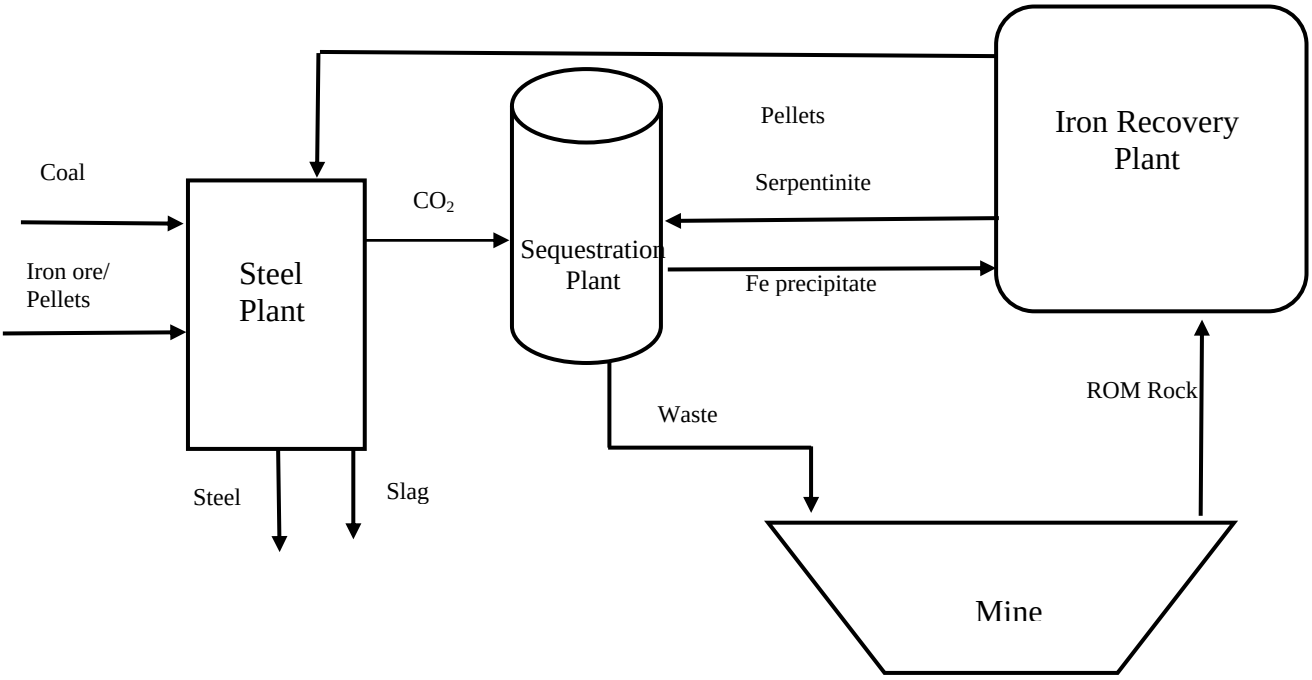

Figure 28. General System Layout

2.1. The Mine

Figure 29. General view of a strip mine

The mine will be located at one of suitable serpentinite deposits. Initially, it will work in a fashion similar to some open pit mines or rock quarries. In the long run however, it is likely that the mining activity may go underground when the surface mine depth exceeds the economic limit, or it may be closed entirely due to the same reason. Because of this reason, availability of reserves needs to be expressed as a function of depth from the surface. Since each deposit is unique in its specific geology and rock quality, it is not possible to make more specific statements regarding the mining method or depth at this stage. It is important to keep in mind, however that a well designed underground mine may be successfully operated at a cost competitive with surface mines.

Furthermore, an underground mine makes waste disposal easier by simply backfilling the mined out areas. At a surface mine, backfilling is not always feasible before the mining is completed, except in the case of shallow, flat deposits similar to some coal beds. In that case, a method similar to strip mining (Figure 29) can be utilized allowing immediate disposal of waste following the removal of ore.

Table 22. Cost estimation summary (initial estimate) Source: USBM Cost Estimation System

	Operating Cost ($/day)	Capital Cost	Preproduction Cost
Drill & blast	6,665	2,453,479	199,928
Electric shovels and trucks	25,515	13,164,362	765,439
Conveyors	8,172	9,806,289	
Crushers - in pit (Movable)	4,376	4,931,108	
Communications system		43,011	
Electrical system (Mine non-electric)		12,685	
Electrical system (Mine Electric)		184,250	
Fueling system		31,214	
TOTAL	44,728	30,626,398	965,367
Capacity(TPD) = 17,000			
Working days = 250/year			
Mine life = 15 years			
Capital cost recovery ($/ton)(straight line depreciation over 15 years)	0.50	Preproduction costs are capitalized	
Operating Cost $/ton	2.63		
Total ($/ton)	3.13		

Mining cost is a function of mining capacity. A steel plant producing 5000 tons/day pig iron also produces 6650 tons of CO_2 per day. In order to sequester this CO_2 by mineral carbonation process a serpentine mine with 40% usable MgO content needs to supply approximately 17,000 tons of rock per day (See the simplified example below). In mining terms, this is a small mine and costs will be

comparable to large stone quarries. We have estimated initially that for small operations like this example the surface mining cost will be about $3.13/ton[5], excluding the added cost of backfilling of waste. In the more detailed version of the cost analysis we also included the added cost of waste handling as backfill. It is assumed that the unit cost of mining and backfill are essentially the same. The total cost associated with this is calculated by taking into account the amount of generated waste after processing. The mineral sequestration system, including the mine, processing and sequestration plants may be designed to accept additional CO_2 from external sources, taking advantage of economies of scale as well as, by means of additional iron recovery, reduce the iron ore input to the steel plant from external sources. We will investigate this later in this report using the model developed for this purpose.

2.2. The Iron Recovery Plant

This plant will be at or very near the mine site to minimize transportation costs. The purpose is to recover iron values from serpentinite rock before and after the sequestration process. The ROM serpentinite rock will be crushed and ground to appropriate liberation size for magnetite mineral present in the serpentinite. The concentrate will be sent to a local pelletizing section. The tails will then be conveyed to the sequestration plant. This facility can also receive iron oxide precipitate from the sequestration plant to

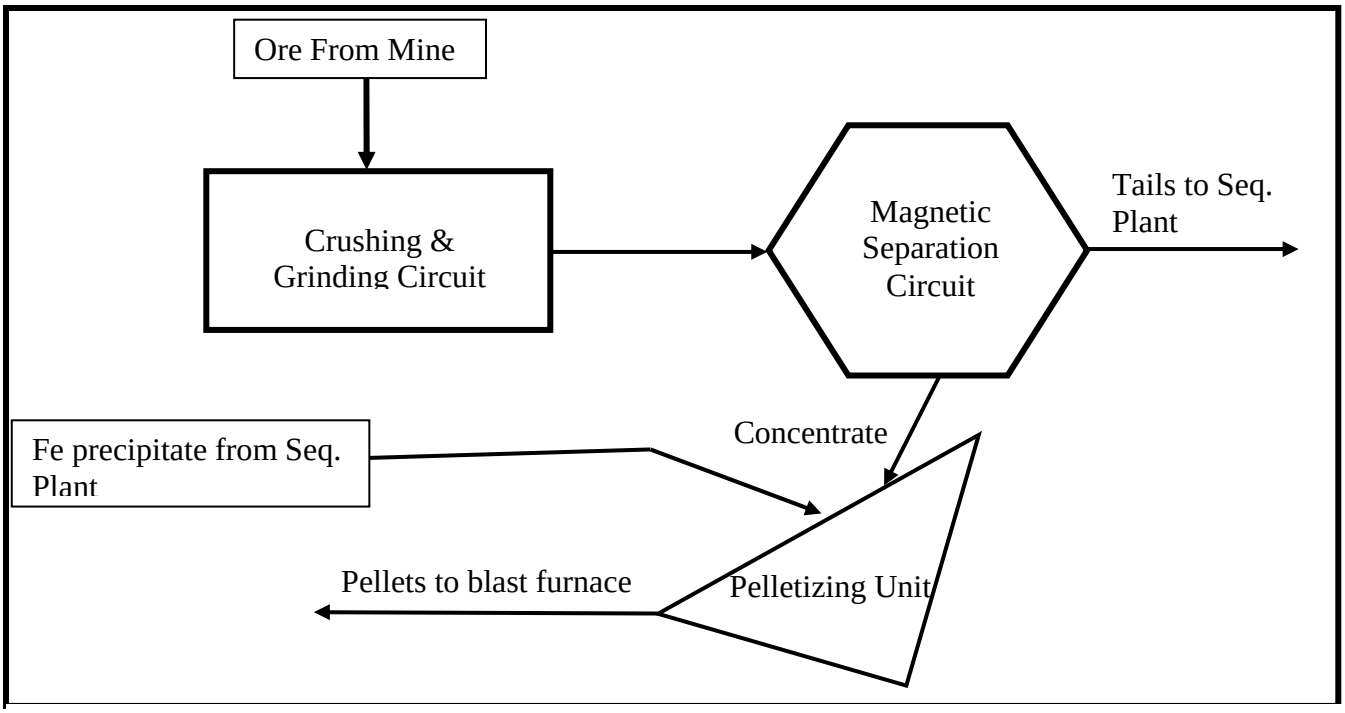

Figure 30. Basic flowchart for the iron recovery plant

recover the non-magnetic iron from the serpentinite. This will be blended with the magnetite before pelletizing operation. The specific design and contents of this plant will strongly depend on the mineralogy and the chemical composition of the mine output. An example flowchart is shown in Figure 30.

[5] This estimate is based on USBM Cost Estimation System formulation for open pit mining. The 1994 costs were inflated by 10% to reach 2005 values as a first approximation.

2.3. Sequestration Plant

This plant receives serpentinite from the tailings stream of the magnetic separation process. Depending on the liberation size of magnetite and the most effective grain size for leaching of serpentine to get Mg into solution, there may be an additional grinding circuit as part of this plant. It is likely that the material will be subject to a pretreatment for various reasons, including pH adjustment. The next step is reaction of CO_2 with the solution and selective precipitation of $MgCO_3$, in order to recover remaining iron values. (Recovery of iron at this stage is heavily dependent on the process used to produce $MgCO_3$. It may turn out that iron recovery may not be economically feasible due to additional processing requirements). This would be followed by a dewatering, filtering and drying steps to generate two main streams (iron and waste) of materials. The waste consisting mostly of silica and $MgCO_3$ will be sent to a disposal site (most likely to the mine site) and the iron concentrate will be returned to the iron recovery plant for blending with magnetite before pelletizing step (Figure 31). At this stage of our project the details of the steps and specific requirements are not known. We will be able to make better assessment of the technical and economic feasibility of the entire system as we gain some experimental experience and define the chemical processes that can be implemented at industrial scales.

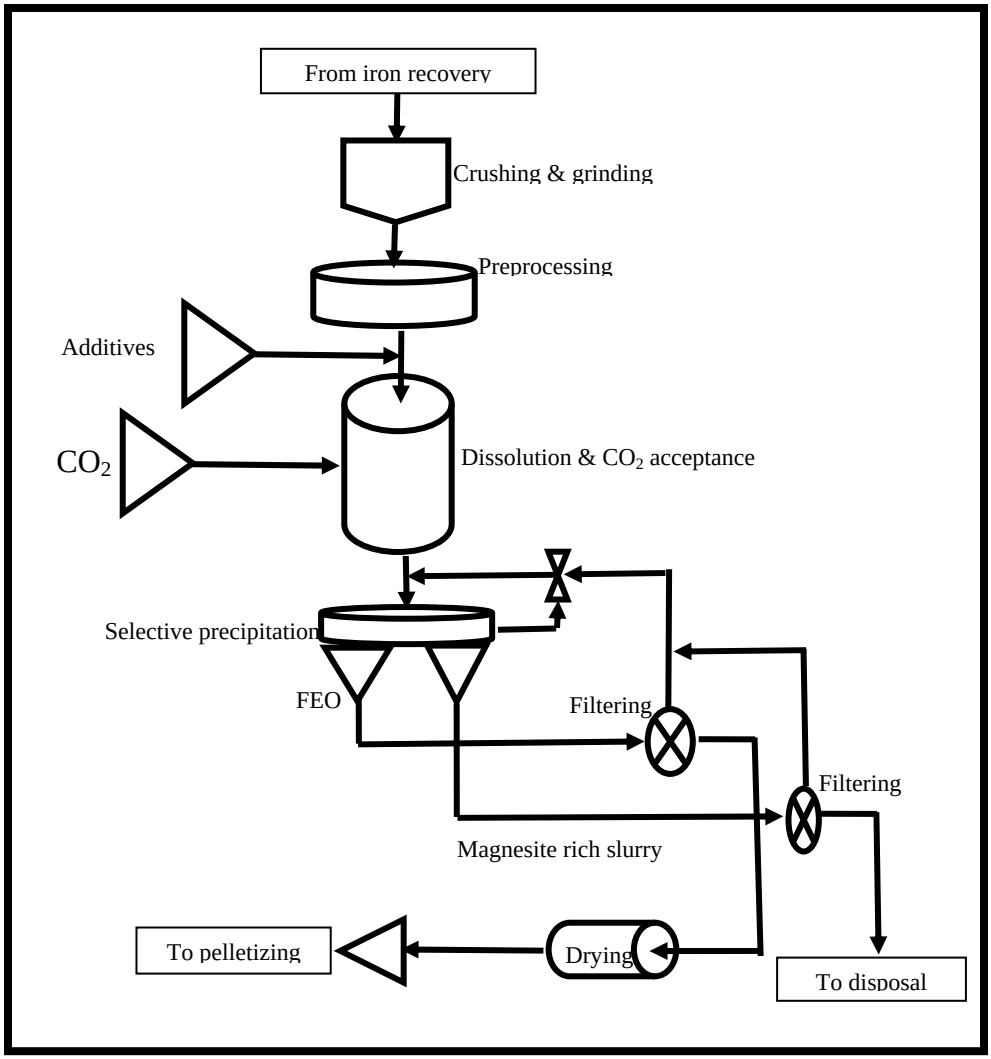

Figure 31. Basic Flowchart of the Sequestration Plant

3. An Example

A typical large US steel plant produces about 2 -3 MT of steel per year. This corresponds to a pig iron production of 5,000 – 8,000 tons per day. In order to illustrate how CO2 sequestration with iron recovery may impact the entire system, let us consider a steel plant with 5000 tons/day pig iron capacity producing a concentrated stream of 6650 tons of CO2 per day (1/1.33 ratio is used based on data reported in 1 and 2)[6]. This will require approximately 6045 tons of pure MgO to convert all CO_2 to $MgCO_3$. Considering a plant efficiency of 90%, we need approximately 6717 tons of MgO content in the ore coming into the sequestration plant. This feed is the tails after the iron recovery by magnetic separation. Considering a magnetic separation system with a magnetic separation efficiency of 90% producing a concentrate of magnetite with 90% magnetite content, 6717 tons of MgO will be contained in 16157 tons of tails. This translates to mining of 17007 tons per day of a serpentinite ore containing 40% MgO, 5% Fe_3O_4, 5% Fe_2O_3, 45% SiO_2, and 5% other material. With the above data we also estimate that about 17 % of steel plant input would come from the sequestration process.

Table 23. Example

Serpentinite assay		**Steel Mill**		**Mine**		**Pelletizing Plant**	
	grade	Inputs	Tons/day	Serpentinite Ore	Tons/day	Inputs	Tons/day
MgO	0.4	Fe Ore (52%)	8,007	ROM ore to concentrator	17,007	Fe3O4 Conc.	850
Fe_2O_3	0.05	Fe_3O_4				FeO	285
Fe_3O_4	0.05	Fe2O3					
SiO_2	0.45	Pellets from Seq.	1,609				
Other	0.05	Contribution	0.17	**Concentrator**		Outputs	
				Magnetite Concentrate	850	Pellets (52% Fe)	1,609
		Outputs		FeO precipitate	285		
		Steel (Pig Iron content Fe)	5,000	Serpentinite Conc. (Dry)	16157		
Total	1	CO_2	6,650				

4. Discussion

In the simplified example above we considered pellets containing magnetite, hematite and other iron oxides with a binder of clay assaying approximately 52% Fe. Pellets are priced on the basis of Fe content. On the basis of $54/t per iron content (USGS) the 52% Fe pellets would have a value of approximately $28/ton.(USGS, 2005) This would correspond to approximately $45,181/day savings ($6.79/day per ton of CO_2 sequestered). Additional savings would be realized if there is a tax levied on CO_2 emissions in the future. At $30/t tax for CO_2 emissions savings will be approximately $199,500/day. These savings need to offset the costs associated with mining and processing of serpentinite rocks. We can safely assume that for a small mine mining cost will not be above $4/t, i.e., $68,028/day. The difference of $176,653/day ($10.38/ton of ore) would be the upper bound for processing serpentinite and disposal of the waste. We

[6] This ratio is, based on EPA report of 53.8 MT CO_2 from pig iron production and USGS report of 40.6 MT pig iron production in US in 2003.

have modified these initial estimates as shown later in this report. Additional cost or benefits can be included considering the options for transport of CO_2 to mine site where the sequestration plant is located against the alternative of transporting the serpentine ore to the sequestration plant located elsewhere and return of waste back to the mine site for disposal.

Due to the economies of scale mining and processing costs can be reduced if the throughputs are higher. This would require several steel plants pooling their CO_2 output for sequestration at a single site.

5. Model Study

A computer model has been developed to investigate the impact of various system parameters (recoveries and efficiencies and capacities at different system components), serpentinite quality, as well as incorporation of CO_2 from external sources. In the following we present a base case similar to the initial study presented above, and discuss the impact of a number of deviations from the base case.

5.1. General system layout

The system consists of a steel plant, a mine to produce desired quantities of serpentinite rock (ore), a processing plat to recover magnetite from the ore, a sequestration plant processing CO_2 from the steel plant, a pelletizing plant producing iron pellets using the recovered magnetite at the processing plant and iron precipitate recovered at the sequestration plant.

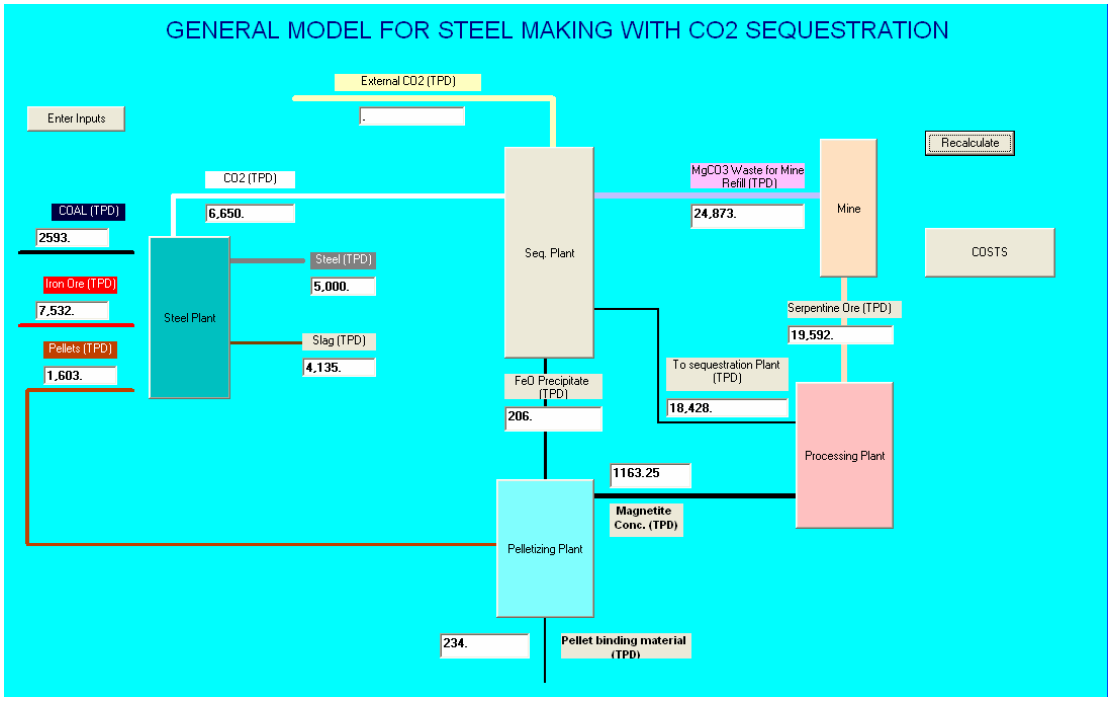

Figure 32. Front Page of the General Evaluation Model

5.2. User inputs

The model accepts user inputs defining the properties of serpentine rock, and operating parameters of the plants in the system as shown below. User supplied data includes a complete ore assay, basic parameters for the steel plant, the processing plant, the mine, the pelletizing plant, and the sequestration plant. Plant life and working days/year, and parameters for the cost curves are included so as to allow unit cost calculations by the cost model.

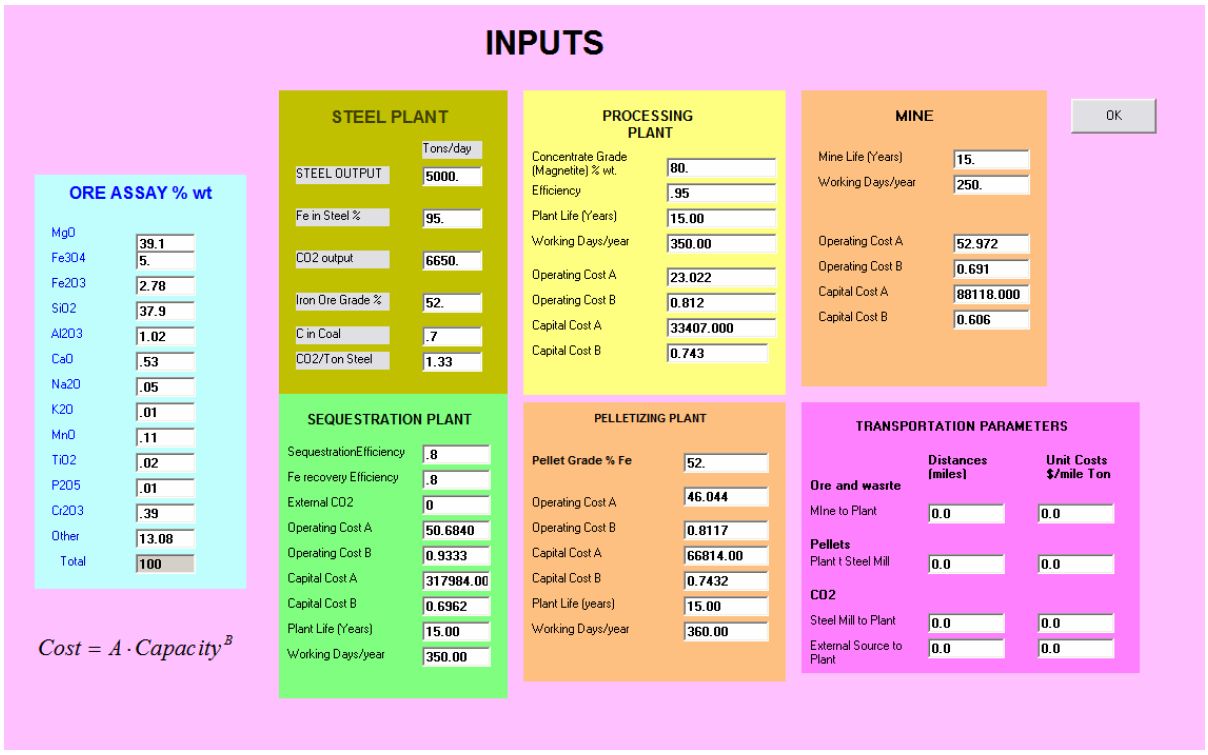

Figure 33. Input page for mineral carbonation process model

5.3. Serpentinite

We consider a serpentinite rock described by its chemical analysis as shown in the inputs page above. The critical components are The MgO, Fe_2O_3 and Fe_3O_4 . One can investigate the impact of higher and lower iron values, as well as a range of MgO concentration on the overall system behavior.

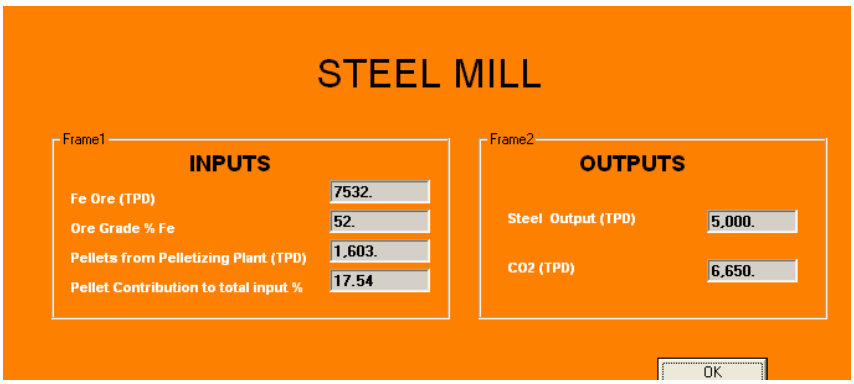

Figure 34. Steel Mill options page

5.4. Steel Plant

We initially considered a steel plant designed to produce 5000 TPD steel. Iron ore (or iron pellets) (52% Fe) is supplemented by locally produced pellets (52%) from the pelletizing plant producing pellets from recovered iron values in the serpentine ore. The quantities are a function of recovery efficiencies for associated system components.

User definable inputs are the desired steel output Fe concentration in steel, Fe concentration of the iron ore, coal quality expressed only as it carbon content, and approximate CO_2 output per ton of steel produced. The iron content of the iron ore and pellets are also user definable parameters

5.5. The Processing Plant

The input for the processing plant is received from the mine by truck or conveyor belt after a primary crushing process at the mine. The ore is crushed and ground to a size sufficient to liberate magnetite minerals from the gangue material. The concentrate grade is predetermined by user input (in this case is 80% Fe_3O_4). Concentrate assay values calculated on the basis of a used defined efficiency (95% in this case). Tailings containing other iron values ($Fe2O_3$) and the bulk of Mg containing silicates is sent to the sequestration plant. The Figure 35 below shows the detailed assays of both concentrate and tailings.

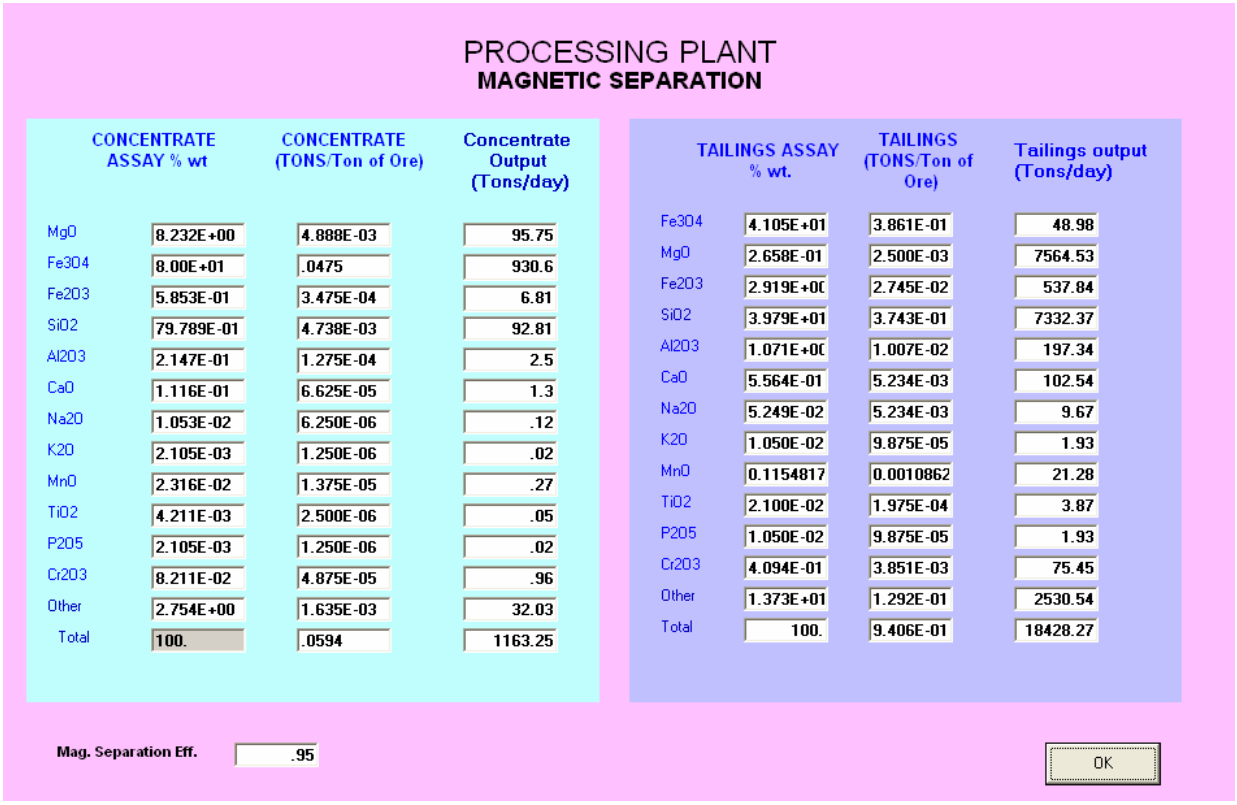

Figure 35. Magnetic Separation page

5.6. The Pelletizing Plant

This plant is dedicated to the production of pellets from the recovered iron minerals in the processing plant and sequestration plants. The model calculates the amount of pellets that can be produced at a particular grade, selected by the user (52% in this case), from the input material as well as the needed binding material quantity as shown below (Figure 36). No cost data for pellet plants were available at the time of completion of this model. A cost structure, however is incorporated in the model for the pelletizing plant with user selectable parameters. The default parameters supplied are similar to that of the magnetic separation plant.

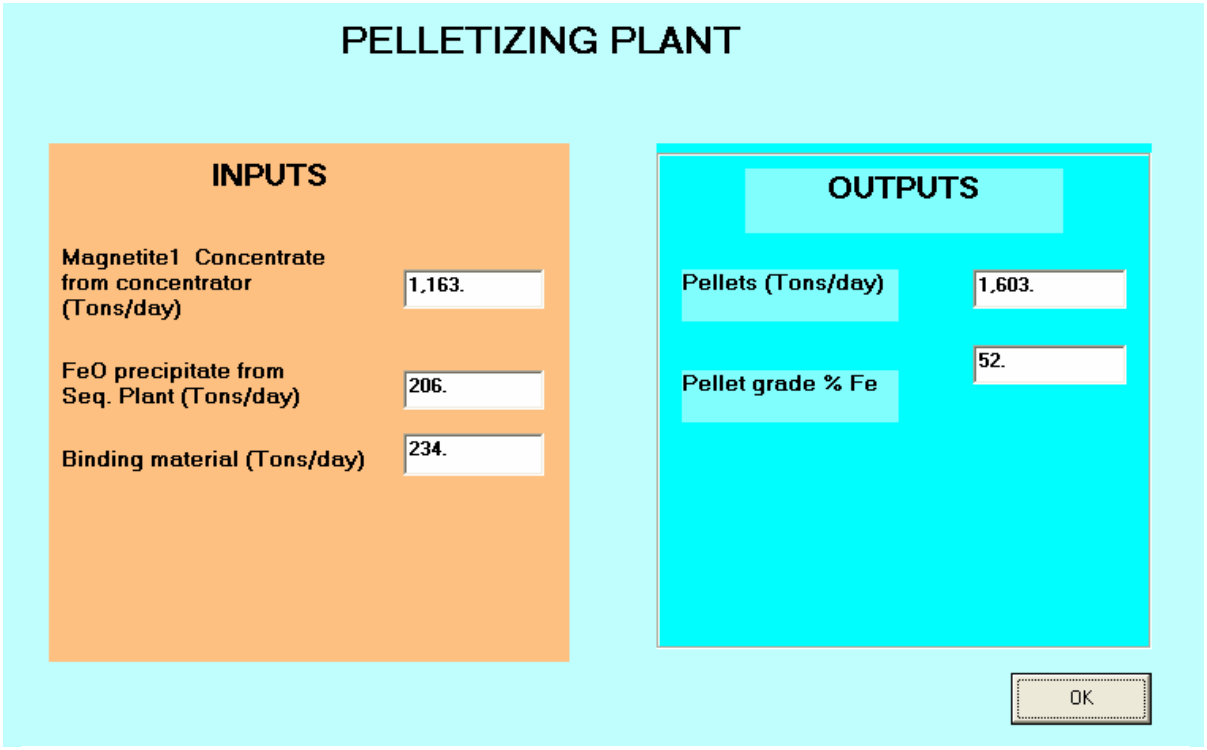

Figure 36. Pelletizing Plant Page

5.7. The Sequestration Plant

Based on the user defined sequestration efficiency (% of MgO utilized to produce $MgCO_3$ from all CO_2 input), and Fe recovery efficiency, quantities of output material (MgCO3 , FeO and total backfill to be sent for disposal at the mine) are calculated as shown in figure 37.

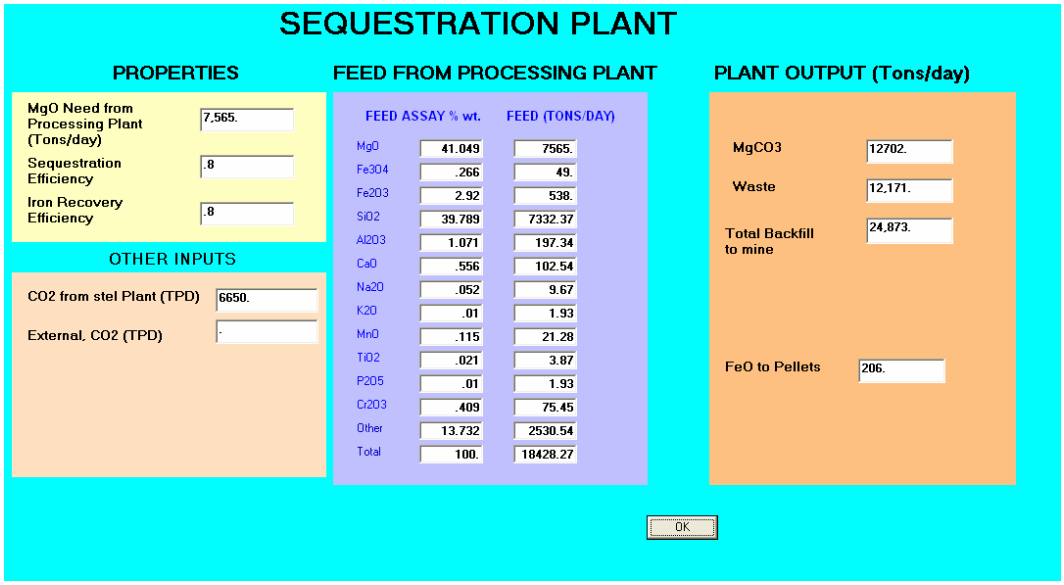

Figure 37 Sequestration plant page

5.8. The Mine

The production rate at the mine is determined by the MgO demand at the sequestration plant. Mine output (ROM ore) is sent to the processing plant after initial primary crushing (if necessary) at the mine. If trucks are used, there will be no need for a primary crusher at the mine. This will be incorporated to the processing plant design. In case of belt haulage to the processing plant, a primary crusher is needed to be installed at the mine. The model uses cost data based on the use of in pit crusher and belt haulage to the processing plant. It is very important to note that the waste disposal tonnage at the mine will always exceed the ore output tonnage. One also needs to consider the volumetric expansion of the processed waste material. This issue needs to be addressed at the mine site or an additional disposal site with a sufficient capacity needs to be established nearby. It is expected that the waste consisting mostly carbonates, oxides and silicates will not create an environmental hazard, but its environmental impact with respect to the land use needs to be addressed.

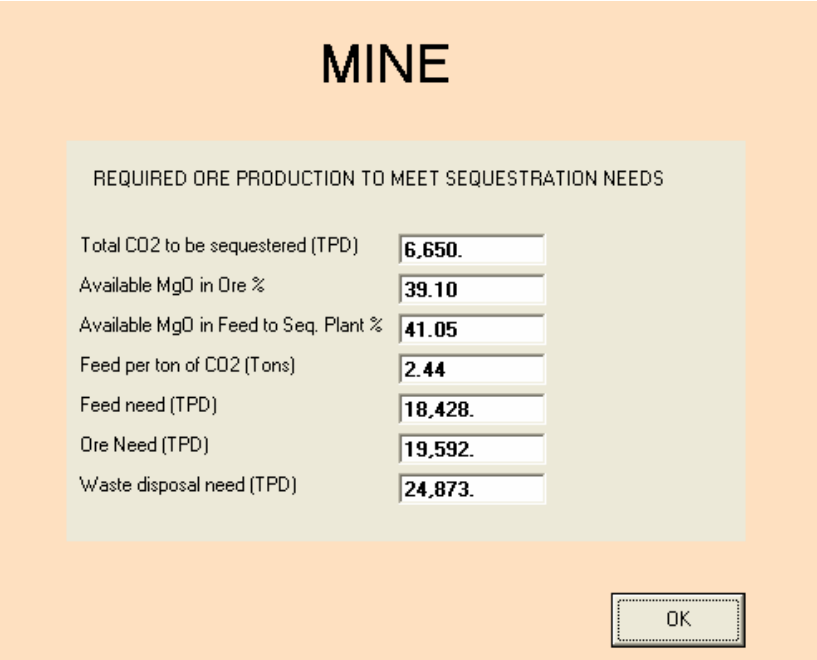

Figure 38. The Mine Page

5.9. The Cost Model

The cost model incorporates the capital and operating cost estimates for the mine, processing plant and the sequestration plant on the basis of a general cost estimation model developed originally by the US Bureau of Mines. The model is modified so as to reflect the cost structure as of 2005. The operating and capital cost are calculated by means of power curves developed by using USBM cost estimation program for a range of capacities. In addition to calculating capital, operating and unit costs ($/ton), the total cost per ton of CO_2 sequestered is also calculated and reported. The base case scenario displayed here shows that the cost of sequestering CO_2 produced at the steel plant is estimated as $ 42.55/ton. Capital and operating costs are calculated using the power relationship

Where X represents the plant capacity (TPD throughput). The parameters a and b are user definable

$$y = aX^{b}$$

values and can be modified in the cost page of the model as shown in figure 39.

Table 25 shows the default values of a and b used for estimating costs for the mine, processing sequestration and pelletizing plants. We do not have reliable cost data to estimate the capital and operating costs of pelletizing plants available. For the sake of completeness we assumed that the capital and operating cost parameters (a) are twice the values used for the processing plant. The power parameters were kept the same as those of the processing plant. The cost data for a future sequestration plant is also not available. In this analysis we used the cost curves developed for alumina production plant using Bayer process, considering the complexity of that similar to that of a future sequestration plant. In

case of the sequestration plant cost functions, the variable X is the MgO content (TPD) of the plant output as $MgCO_3$.

Table 24. Default Cost Parameters

	Operating Cost ($/day)		Capital Cost ($)	
	a	b	a	b
Mine	**52.972**	**0.6912**	**88,118**	**0.6061**
Processing Plant	**23.022**	**0.8117**	**33,407**	**0.7432**
Sequestration Plant	**50684**	**0.9333**	**317,984**	**0.6962**
Pelletizing Plant	**46.044**	**0.8117**	**66,814**	**0.7432**

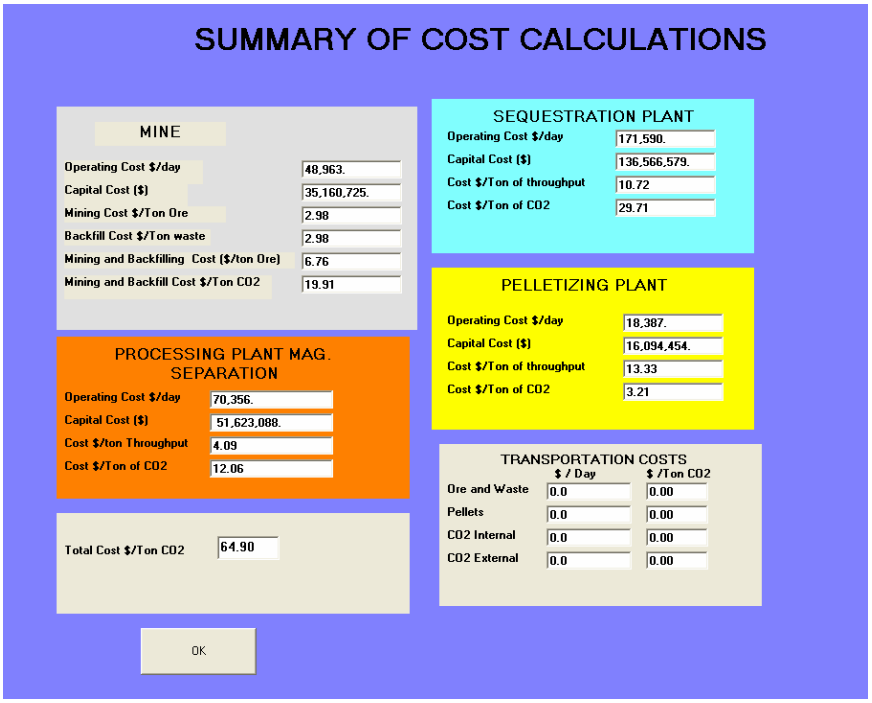

Figure 39. Cost Output Page

6. The Base Case:

The base case for the analysis is the same as what we presented in the initial cost analysis. The system is based on the needs of a 5000 Ton/day steel plant producing 6650 tons of CO_2. Table 26 shows the input/output values and Table 27 shows the estimated costs for the entire system. Within the framework of above stated assumptions and limitations, cost per ton of sequestered CO_2 is calculated as $ 48.64. With the benefit expected from recovery of iron values this is modified as $41.87 as shown in Table 26.

Table 25. Base Case

Base Case Input Parameters	
Steel Production(TPD)	5000
CO2/Ton Steel	1.33
C in Coal	0.7
Iron Ore Grade, % wt.	52
Processing Plant	
Mag. Conc. Grade, % wt.	80
Plant efficiency	0.95
Pellet Plant	
Pellet Grade, % Fe	52
Seq. Plant	
Sequestration Eff.	0.8
Fe Recovery eff.	0.8
External CO2 input	0
Total CO2	6650
Ore (Serp.) Assay % wt	
MgO	39.1
Fe3O4	5
Fe2O3	2.78
SiO2	37.9
Al2O3	1.02
CaO	0.53
Na2O	0.05
K2O	0.01
MnO	0.11
TiO2	0.02
P2O5	0.01
Cr2O3	0.39
Other	13.08
Total	100

SIMULATION OUTPUTS	
Steel Plant	
Inputs:	
Iron Ore (TPD)	7532.1
Pellets (TPD)	1602.51
Coal (TPD)	2592.75
CO2 (TPD)	6650
Outputs:	
Steel (TPD)	5000
Slag (TPD)	4134.62
Pellet contribution to total input %	17.54
Mine	
Ore (Serpentinite) Production (TPD)	19591.51
Waste disposal (TPD)	24872.53
Available MgO in Ore % wt.	39.1
Processing Plant	
Concentrate Output (TPD)	1163.25
MgO	95.75
Fe3O4	930.6
Fe2O3	6.81
SiO2	92.81
Al2O3	2.5
CaO	1.3
Na2O	0.12
K2O	0.02
MnO	0.27
TiO2	0.05
P2O5	0.02
Cr2O3	0.96
Other	32.03
Tailings (Feed to seq. plant)(TPD)	18428.27
MgO	7564.53
Fe3O4	48.98
Fe2O3	537.84
SiO2	7332.37
Al2O3	197.34
CaO	102.54
Na2O	9.67
K2O	1.93
MnO	21.28
TiO2	3.87
P2O5	1.93
Cr2O3	75.45
Other	2530.54

Sequestration Plant	
Output (TPD)	
MgCO3	12701.62
Waste	12170.91
Total backfill to mine	24872.53
FeO to pellet plant	205.74
Pellet Plant	
Inputs (TPD)	
Fe3O4 Concentrate	1163.25
FeO from Seq. Plant	205.74
Binding material	233.53
Output	
Pellets (TPD)	1602.51
Pellet grade(% Fe)	52

Table 26. Cost Estimates

COSTS (Base Case)	
Mine	
Op. Cost/day	$ 48,963
Cap. Cost	$ 35,160,725
Mining Cost/ton	$ 2.98
Backfill cost/ton	$ 2.98
Mng+backfill Cost/Ton ore	$ 6.76
Mng+backfill Cost/Ton CO2	$ 19.91
Processing Plant	
Operating cost/day	$ 70,356
Capital. Cost	$ 51,623,088
Cost/Ton Throughput	$ 4.09
Cost/Ton CO_2	$ 12.06
SEQ. Plant	
Operating Cost/day	$ 171,590
Capital Cost	$ 136,566.579
Cost /Ton Throughput	$ 10.72
Cost / Ton CO_2	$ 29.71
Pellet Plant	
Operating Cost/day	$ 18,387
Capital Cost	$ 16,094,454
Cost /Ton throughput	$ 13.33
Cost /Ton CO_2	$ 3.21
Totals	
Operating Cost/day	$ 309,296
Capital Cost	$ 239,444,847
Cost /Ton CO_2	$ 64.89
Pellet Value/day	$ 44,998
Pellet Unit Price ($/unit Fe)	$ 54
Minus Pellet Value/ton CO_2	$ 6.77
Total Cost CO_2/Ton	$ 58.12

7. The impact of sequestering additional CO_2

The impact of sequestering additional CO_2 from external sources is studied by simply specifying external CO_2 from 1,000 TPD to 10,000 TPD in the model. This clearly affects the capacities of the mine, processing plant, pelletizing plant as well as the sequestration plant.

Table 27. Impact of sequestering additional CO_2 from external sources

Impact of External CO2											
Ext. CO2	0	1000	2000	3000	4000	5000	6000	7000	8000	9000	10000
Pellet production (TPD)	1603	1843	2084	2325	2566	2807	3048	3289	3530	3771	4012
Pellet Cost $/ton CO2	3.21	3.13	3.05	2.99	2.93	2.88	2.83	2.79	2.75	2.71	2.68
Mine output (TPD)	19592	22538	25484	28430	29513	34322	37268	40214	43160	46106	49052
Mining & Backfilling Cost ($/ton CO2)	19.91	19.03	18.29	17.66	17.11	16.62	16.18	15.79	15.44	15.11	14.81
Processing Plant Throughput (TPD)	19592	22538	25484	28430	29513	34322	37268	40214	43160	46106	49052
Processing Plant Cost ($/Ton CO2)	12.06	11.73	11.45	11.21	10.99	10.80	10.63	10.47	10.33	10.19	10.07
Sequestration Plant Throughput (TPD)	24873	28613	32353	36093	39833	43574	47314	51054	54794	58535	62275
Sequestration Plant Cost ($/Ton CO2)	29.71	29.31	28.97	28.66	28.40	28.15	27.94	27.74	27.56	27.39	27.23
Savings from pellet contribution ($/Ton CO2)	6.77	6.77	6.77	6.77	6.77	6.77	6.77	6.89	6.77	6.89	6.77
Total Cost $/Ton CO2)	58.12	56.43	54.99	53.75	52.66	51.68	50.81	49.90	49.31	48.51	48.02

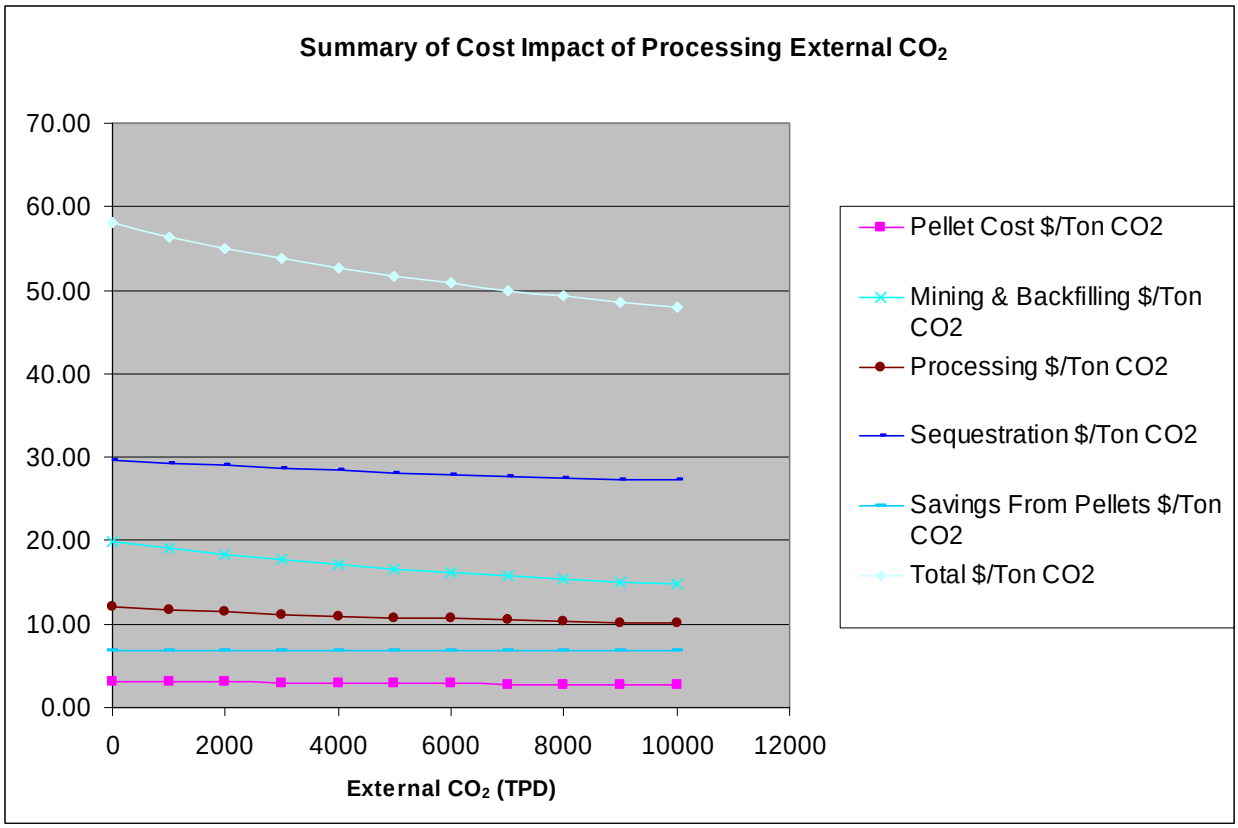

Figure 40. Costs associated with processing external CO_2

References

1. Mineral Commodity summaries , 2005, Iron and Steel, USGS
2. Inventory of US Greenhouse Gas Emissions and Sinks 1990-2003, April, 15, 2005, EPA 430-R-05-003
3. U.S. Bureau of Mines. Bureau of Mines Cost Estimating System Handbook, (in two parts), 1. Surface and Underground Mining. USBM IC 9142, 1987, 631 pp.